RECEIVER AND PARAMETER ESTIMATION TECHNIQUES FOR QUASI-SYNCHRONOUS REVERSE LINK MULTICARRIER CDMA SYSTEM

Mr. Suwich Kunaruttanapruk

A Dissertation Submitted in Partial Fulfillment of the Requirements
for the Degree of Doctor of Philosophy in Electrical Engineering
Department of Electrical Engineering
Faculty of Engineering
Chulalongkorn University
Academic Year 2004

ISBN 974-17-6561-4

เครื่องรับและเทคนิคการประมาณพารามิเตอร์สำหรับการเชื่อมโยงขากลับแบบควอไซซิงโครนัสของระบบมัลติแคเรียร์ซีดีเอ็มเอ

นายสุวิชช์ คุณารัตนพฤกษ์

วิทยานิพนธ์นี้เป็นส่วนหนึ่งของการศึกษาตามหลักสูตรปริญญาวิศวกรรมศาสตรดุษฎีบัณฑิต
สาขาวิชาวิศวกรรมไฟฟ้า ภาควิชาวิศวกรรมไฟฟ้า
คณะวิศวกรรมศาสตร์ จุฬาลงกรณ์มหาวิทยาลัย
ปีการศึกษา 2547
ISBN 974-17-6561-4

Thesis Title	RECEIVER AND PARAMETER ESTIMATION TECHNIQUES FOR QUASI-SYNCHRONOUS REVERSE LINK MULTICARRIER CDMA SYSTEM
By	Mr.Suwich Kunaruttanapruk
Field of Study	Electrical Engineering
Thesis Advisor	Associate Professor Somchai Jitapunkul, Dr.Ing.

Accepted by the Faculty of Engineering, Chulalongkorn University in Partial Fulfillment of the Requirements for the Doctor's Degree

. . . . . Dean of the Faculty of Engineering
(Professor Direk Lavansiri, Ph.D.)

THESIS COMMITTEE

. . . . . Chairman
(Professor Prasit Prapinmongkolkarn, D.Eng.)

. . . . . Thesis Advisor
(Associate Professor Somchai Jitapunkul, Dr.Ing.)

. . . . . Member
(Associate Professor Watit Benjapolakul, D.Eng.)

. . . . . Member
(Associate Professor Lunchakorn Wuttisittikulkij, Ph.D.)

. . . . . Member
(Assistant Professor Phaophak Sirisuk, Ph.D.)

. . . . . Member
(Nisachon Tangsangiumvisai, Ph.D.)

สุวิชช์ คุณารัตนพฤกษ์: เครื่องรับและเทคนิคการประมาณพารามิเตอร์สำหรับการเชื่อมโยงขากลับแบบควอไซชิงโครนัสของระบบมัลติแคเรียร์ซีดีเอ็มเอ (RECEIVER AND PARAMETER ESTIMATION TECHNIQUES FOR QUASI-SYNCHRONOUS REVERSE LINK MULTICARRIER CDMA SYSTEM), อ. ที่ปรึกษา: รองศาสตราจารย์ ดร.สมชาย จิตะพันธ์กุล, 99 หน้า, ISBN 974-17-6561-4

สมรรถนะของระบบมัลติแคเรียร์ซีดีเอ็มเอถูกจำกัดโดย ความเฉทางความถี่ การเติมหน้าแบบวนกลับที่ไม่เพียงพอ และการแทรกสอดจากการเข้าถึงหลายทาง ในข่ายเชื่อมโยงขากลับแบบควอไซชิงโครนัส เครื่องรับไม่สามารถปรับเท่าความเฉทางความถี่และการเติมหน้าแบบวนกลับที่ไม่เพียงพอ เนื่องจากความเป็นอิสระต่อกันของช่องสัญญาณและค่าความเฉทางความถี่ของผู้ใช้แต่ละคน เป็นผลให้เครื่องรับทั่วไปไม่สามารถตัดสินสัญลักษณ์ได้ถูกต้องแม้แต่ในระบบผู้ใช้เดียวซึ่งไม่มีการแทรกสอดจากการเข้าถึงหลายทาง วิธีการที่สามารถจัดการกับสถานะการณ์ที่ยุ่งยากเช่นนี้ได้คือ การรวมการขจัดการแทรกสอดจากการเข้าถึงหลายทางเข้ากับการชดเชยความเฉทางความถี่และการชดเชยการเติมหน้าแบบวนกลับที่ไม่เพียงพอ อย่างไรก็ตาม วิธีการที่มีอยู่ในปัจจุบันไม่ได้พิจาณาครอบคลุมปัญหาทั้งหมดนี้ แต่มุ่งเน้นเพียงระบบที่พิจารณาการแทรกสอดจากการเข้าถึงหลายทางและความเฉทางความถี่ หรือระบบที่พิจารณาการแทรกสอดจากการเข้าถึงหลายทางและการเติมหน้าแบบวนกลับที่ไม่เพียงพอเท่านั้น

วิทยานิพนธ์ฉบับนี้เสนอการตรวจวัดหลายผู้ใช้ที่มีการขจัดการแทรกสอดข้ามสัญลักษณ์ซึ่งก้าวล้ำกว่าวิธีการที่มีอยู่เดิมด้วยความสามารถที่จะเอาชนะปัญหาที่พิจารณาทั้งหมด นอกจากคุณลักษณะนี้แล้ว เครื่องรับที่นำเสนอยังสามารถนำวิธีการตรวจวัดแบบไม่เป็นเชิงเส้นมาใช้ได้ จึงมีความยืดหยุ่นมากกว่าเครื่องรับที่มีอยู่เดิมซึ่งมีการใช้เพียงการตรวจวัดแบบเชิงเส้นชนิดค่าเฉลี่ยกำลังสองของค่าผิดพลาดน้อยที่สุดเท่านั้น วิทยานิพนธ์ฉบับนี้ไม่เพียงแต่นำเสนอเครื่องรับใหม่ แต่ยังได้นำเสนอวิธีการประมาณค่าพารามิเตอร์ที่สามารถใช้งานในทางปฏิบัติได้ด้วย ตัวประมาณที่เสนอได้แก่ ตัวประมาณลำดับลายมือชื่อที่ถูกแปลง (transformed signature sequences) ตัวประมาณลำดับกำเนิดการแทรกสอดข้ามสัญลักษณ์ และตัวประมาณความแปรปรวนของสัญญาณรบกวน เนื่องจากการประมาณผลตอบสนองอิมพัลส์ของช่องสัญญาณและค่าความเฉทางความถี่มีความซับซ้อนสูงมาก จนเป็นที่เชื่อได้ว่าจะไม่สามารถนำมาปฏิบัติได้จริง ค่าพารามิเตอร์ที่ต้องการจึงถูกประมาณโดยตรง จากการวิเคราะห์ค่าเฉลี่ยกำลังสองของค่าผิดพลาด วิทยานิพนธ์ฉบับนี้ได้นำเสนอลำดับฝึกที่ทำให้ได้ค่าดังกล่าวน้อยที่สุด วิธีการประมาณค่าพารามิเตอร์ที่นำเสนอทำให้งานในวิทยานิพนธ์มีความน่าสนใจมากขึ้นกว่างานที่มีอยู่เดิม ซึ่งสนใจเพียงการออกแบบเครื่องรับโดยไม่ได้พิจารณาความเป็นไปได้ในทางปฏิบัติ

ผลการจำลองระบบสาธิตให้เห็นถึงคุณประโยชน์หลายประการของวิธีการที่นำเสนอที่เหนือกว่าเครื่องรับอื่น ๆ ผลยังได้ยืนยันข้อดีของลำดับฝึกที่ดีที่สุด จากผลการจำลองระบบค่าผิดพลาดบิตน้อยที่สุดได้รับจากระบบที่มีการเติมหน้าแบบวนกลับที่ไม่เพียงพอ ซึ่งแตกต่างจากการออกแบบระบบทั่วไปที่ต้องการเงื่อนไขการเติมหน้าแบบวนกลับที่เพียงพอ วิธีการที่นำเสนอไม่เพียงแต่มีค่าผิดพลาดบิตที่น้อยลงกว่าเดิม แต่ยังมีศักยภาพที่จะให้อัตราสัญลักษณ์ที่สูงขึ้นด้วย

ภาควิชา	วิศวกรรมไฟฟ้า	**ลายมือชื่อนิสิต**	. . . . .
สาขาวิชา	วิศวกรรมไฟฟ้า	**ลายมือชื่ออาจารย์ที่ปรึกษา**	. . . . .
ปีการศึกษา	2547		

##4471829121: MAJOR ELECTRICAL ENGINEERING
KEY WORD: REVERSE LINK / MULTICARRIER / CDMA / QUASI-SYNCHRONOUS / PARAMETER ESTIMATION / MULTIUSER DETECTION

SUWICH KUNARUTTANAPRUK: RECEIVER AND PARAMETER ESTIMATION TECHNIQUES FOR QUASI-SYNCHRONOUS REVERSE LINK MULTICARRIER CDMA SYSTEM, THESIS ADVISOR: SOMCHAI JITAPUNKUL, Dr.Ing., 99 pp., ISBN 974-17-6561-4

The performance of a multicarrier code division multiple access (MC-CDMA) system is limited by frequency offsets, insufficient cyclic prefix condition, and multiple access interference (MAI). In a quasi-synchronous reverse link, a receiver is unable to equalize the frequency offsets and the insufficient cyclic prefix due to the independence of each user's channel and frequency offset. As a consequence, conventional detectors cannot give accurate symbol decision even in a single user system, which is free from MAI. The viable approach to deal with such complicated situation is to integrate the MAI suppression with the compensation of frequency offsets and insufficient cyclic prefix. Unfortunately, the existing techniques do not consider all of these problems. They only focus on the system with MAI and frequency offsets or the system with MAI and insufficient cyclic prefix.

This dissertation proposes a multiuser detection with intersymbol interference cancellation (MUD-ISIC), which surpasses the existing techniques by the capability to jointly overcome all the concerned problems. Apart from this feature, the MUD-ISIC, which is able to adopt non-linear detection techniques, is more flexible than the existing techniques, which only accept a linear minimum mean square error detector. This dissertation does not only introduce the new receiver but it also proposes practical parameter estimation techniques, including the estimators for transformed signature sequences, ISI generation sequences, and noise variance, to realize the MUD-ISIC. Since the estimation of channel impulse response and frequency offsets has extremely high complexity and is unlikely to be able to implement, the required parameters are directly estimated. From the mean square error analyses, the training sequences, which achieve the minimum mean square error, are proposed. The proposed parameter estimation techniques enhance the attractiveness of this dissertation over other existing works, which only concentrate on the receiver design without clarifying its feasibility.

The simulation results demonstrate several relevant merits of the proposed techniques over the other known techniques. The results also confirm the benefits of the optimum training sequences. According to the simulation results, the lowest bit error rate (BER) is achieved in the system with insufficient cyclic prefix, which contrasts to the conventional system design where the sufficient cyclic prefix condition is normally imposed. The MUD-ISIC does not only gain better BER but it also has a potential to offer the higher symbol rate.

Department	Electrical Engineering	Student's signature	
Field of study	Electrical Engineering	Advisor's signature	
Academic year	2004		

Acknowledgements

I would like to express my sincere gratitude to my advisor, Dr.Somchai Jitapunkul. His encouragement, support, and expert guidance have been invaluable during my time at the Digital Signal Processing Research Laboratory. He has contributed both on a professional and on a personal level to my life as a graduate student.

My gratitude is extended to Dr.Prasit Prapinmongkolkarn, Dr.Watit Benjapolakul, Dr.Lunchakorn Wuttisittikulkij, Dr.Nisachon Tangsangiumvisai, and Dr.Phaophak Sirisuk for serving as members on the dissertation committee. Their valuable discussion and insightful comments have improved the quality of this dissertation.

I would also like to acknowledge the Chulalongkorn University's "Sit Kon Ku Ti" scholarship and the financial support from the Cooperation Project between Department of Electrical Engineering and Private Sector for Research and Development, Chulalongkorn University, Thailand.

I would also like to thank the laboratory and staffs of communication division for providing good facilities. Many thanks go to my colleagues for their help, suggestion, and enjoyment during my time at the laboratory.

Finally, I sincere thank my parents for their support, encouragement, and love. This work could not have been possible if it were not for them.

Table of Contents

Page

Abstract in Thai . . . . . **iv**

Abstract in English . . . . . **v**

Acknowledgements . . . . . **vi**

Table of Contents . . . . . **vii**

List of Tables . . . . . **x**

List of Figures . . . . . **xi**

Chapter

1 Introduction **1**
- 1.1 Multicarrier Modulation 1
- 1.2 Multicarrier Code Division Multiple Access 2
- 1.3 Guard Interval 3
- 1.4 Frequency Offset 5
- 1.5 Multiple Access Interference and Multiuser Detection 6
- 1.6 Scope of This Dissertation 7
- 1.7 Outline 8
- 1.8 Basic Notation 9

2 Basic Background and Related Topics **10**
- 2.1 System Models 10
  - 2.1.1 MC-CDMA Transmission Model 10
  - 2.1.2 Channel Model 12
  - 2.1.3 Received Signal Model 13
- 2.2 Receivers for the Forward Link MC-CDMA system 16
  - 2.2.1 Combining Techniques 16
    - 2.2.1.1 Equal Gain Combining 17
    - 2.2.1.2 Maximum Ratio Combining 18
    - 2.2.1.3 Orthogonal Restore Combining 18
    - 2.2.1.4 Controlled Equalization 18
    - 2.2.1.5 Minimum Mean Square Error Combining 18
    - 2.2.1.6 Other Receivers 19
  - 2.2.2 Frequency Offset Correction 19
  - 2.2.3 Frequency Offset Estimation 19
    - 2.2.3.1 Cyclic Prefix Based Frequency Offset Estimator 19

Table of Contents (Cont.)

Chapter Page

2.2.3.2 Virtual Carrier Based Frequency Offset Estimator 20
2.2.4 Channel Estimation 20
2.3 Receivers for the OFDM System with Insufficient Cyclic Prefix 21
2.3.1 Impulse Response Shortening Technique 21
2.3.2 Decision Feedback Equalization Technique 21
2.3.2.1 Minimum Mean Square Error ICI Compensation 22
2.3.2.2 Cyclic Reconstruction ICI Compensation 22
2.3.2.3 Windowed Maximum Likelihood Sequence Estimator ICI Compensation 23
2.4 Receivers for the Reverse Link MC-CDMA System 23
2.4.1 Conventional Channel Estimation Technique for Reverse Link 23
2.4.2 Recursive Estimation of Channels and Frequency Offsets Based on the Extended Kalman Filter 24
2.4.3 Frequency Offset Compensated Minimum Mean Square Error Detector . . 24
2.4.4 Truncated Time-Domain Minimum Mean Square Error Multiuser Detector 25
2.4.5 Minimum Mean Square Error Decision Feedback Equalizer 26

3 Multiuser Detection with Intersymbol Interference Cancellation 27
3.1 Motivation 27
3.2 Receiver Design 30
3.2.1 Matched Filter 31
3.2.2 Decorrelating Detector 31
3.2.3 Minimum Mean Square Error Detector 32
3.2.4 Weighted Multistage Interference Cancellation Detector 32
3.3 Simulation Results and Discussion 33
3.3.1 Simulation Configuration 33
3.3.2 Effect of Cyclic Prefix Insertion and Serial to Parallel Conversion 35
3.3.3 Effect of Frequency Offset 39
3.3.4 MUD-ISIC Employing Various Multiuser Detection Techniques 40
3.3.5 Performance Comparison With Other Receivers 43
3.3.5.1 The Receivers for the MC-CDMA System with Insufficient Cyclic Prefix 43
3.3.5.2 The Receivers for the MC-CDMA System with Frequency Offset 49
3.3.5.3 Sensitivity of Each Receiving Technique to the Frequency Offset 49
3.4 Summary 52

4 Parameter Estimation Techniques 54
4.1 Basic Concepts 54
4.2 ISI Generation Sequences and Transformed Signature Sequences Estimation . . . 55
4.2.1 Least Squares Estimator 55
4.2.2 Mean Square Error of the Least Squares Estimator 56
4.2.3 Criterion for the Optimum Training Sequences 57

Table of Contents (Cont.)

Chapter Page

4.2.4 Optimum Training Sequence Generation 58
4.2.4.1 Time Division Training Sequences 58
4.2.4.2 Odd-Even Training Sequences 59
4.2.4.3 Cyclically Orthogonal Training Sequences 59
4.2.4.4 Optimum Training Sequence Comparison 62
4.2.5 Adaptive Estimator 63
4.3 Noise Variance Estimation 64
4.4 Simulation Results and Discussion 64
4.4.1 Performance of the Transformed Signature Sequence and ISI Generation Sequence Estimator 65
4.4.2 Performance Over the Serial to Parallel Conversion Size - Cyclic Prefix Length Grid 66
4.4.3 Multiuser Detection Techniques Comparison 66
4.4.4 Performance Comparison with the Other Receivers 70
4.5 Sequences Estimation During a Data Period 78
4.6 Summary 80

5 Conclusions 84
5.1 Future Works 87

References 88

Appendices 95
Appendix A 96
Appendix B 98

Vitae 99

List of Tables

Table		Page
2.1	Interference for various system conditions	16
3.1	Simulation parameters	34
3.2	Weight factors of WMIC used in the simulations	42
3.3	WMIC configuration	42
4.1	Optimum training sequence comparison	63

List of Figures

Figure		Page
1.1	Spectrum of single carrier signal and multicarrier signal	2
1.2	Cyclic Prefix Insertion	5
1.3	Multiuser Detection Tree Diagram	7
2.1	Quasi-synchronous reverse link MC-CDMA system block diagram	11
2.2	Continuous subcarrier assignment and interleaved subcarrier assignment	12
2.3	Multipath channel	12
2.4	Cyclic prefix insersion and multipath signals	13
2.5	Block diagram of combining technique	17
2.6	Block diagram of impulse response shortening technique	22
2.7	Block diagram of decision feedback equalization technique	22
2.8	Block diagram of the truncated time-domain MMSE multiuser detector	26
3.1	BER versus CP duration	28
3.2	Average power spreading due to frequency offsets and insufficient cyclic prefix for the CSA scheme	29
3.3	Block diagram of the MUD-ISIC	30
3.4	Linear detector	31
3.5	WMIC detector	33
3.6	BER of the MUD-ISIC (perfect timing synchronization)	37
3.7	BER of the MUD-ISIC versus cyclic prefix length (perfect timing synchronization)	37
3.8	BER of the MUD-ISIC (imperfect timing synchronization)	37
3.9	BER of the MUD-ISIC versus cyclic prefix length (imperfect timing synchronization)	38
3.10	BER of the MUD-ISIC (perfect frequency synchronization)	38
3.11	BER of the MUD-ISIC (16 users)	38
3.12	BER of the MUD-ISIC (using MF, MF-WMIC, and MMSE-WMIC in the multiuser detection part)	39
3.13	BER versus serial to parallel conversion size for various frequency offset variances	40
3.14	BER versus cyclic prefix length for various frequency offset variances	40
3.15	BER versus frequency offset variance	41
3.16	Performance of various multiuser detection techniques, applied to the MUD-ISIC, for the system with 8 users under the uniform MIP channel	44
3.17	Performance of various multiuser detection techniques, applied to the MUD-ISIC, for the system with 16 users under the uniform MIP channel	44
3.18	Performance of various multiuser detection techniques, applied to the MUD-ISIC, for the system with 24 users under the uniform MIP channel	45
3.19	Performance of various multiuser detection techniques, applied to the MUD-ISIC, for the system with 32 users under the uniform MIP channel	45
3.20	Performance of various multiuser detection techniques, applied to the MUD-ISIC, for the system with 8 users under the exponentially decaying MIP channel	46
3.21	Performance of various multiuser detection techniques, applied to the MUD-ISIC, for the system with 16 users under the exponentially decaying MIP channel	46

List of Figures (Cont.)

Figure		Page
3.22	Performance of various multiuser detection techniques, applied to the MUD-ISIC, for the system with 24 users under the exponentially decaying MIP channel	47
3.23	Performance of various multiuser detection techniques, applied to the MUD-ISIC, for the system with 32 users under the exponentially decaying MIP channel	47
3.24	Performance of various multiuser detection techniques, applied to the MUD-ISIC, versus the number of users (uniform MIP channel)	48
3.25	Performance of various multiuser detection techniques, applied to the MUD-ISIC, versus the number of users (exponentially decaying MIP channel)	48
3.26	Performance of the modified truncated time-domain MMSE multiuser detector and the MUD-ISIC (linear MMSE detector) under the perfect frequency synchronization situation	50
3.27	Performance of the modified truncated time-domain MMSE multiuser detector, MMSE-DFE, and the MUD-ISIC (linear MMSE detector) under the imperfect frequency synchronization situation	50
3.28	Performance of the frequency offset compensated MMSE detector and the MUD-ISIC (linear MMSE detector) under the perfect frequency synchronization situation	51
3.29	Performance of the frequency offset compensated MMSE detector and the MUD-ISIC (linear MMSE detector) under the imperfect frequency synchronization situation	51
3.30	Performance of the modified truncated time-domain MMSE multiuser detector, MMSE-DFE, the frequency offset compensated MMSE detector, and the MUD-ISIC (linear MMSE detector) versus frequency offset variance	52
4.1	Time division training sequence diagram	60
4.2	Odd-even training sequence diagram	60
4.3	MSE of the transformed signature sequences and ISI generation sequence estimator for the system having only one active subcarrier group	67
4.4	MSE of the transformed signature sequences and ISI generation sequence estimator for the system with 8 fully active subcarrier groups	68
4.5	BER of MUD-ISIC (linear MMSE detector) employed various parameter estimation techniques	69
4.6	BER of MUD-ISIC (linear MMSE detector) using LS estimator	70
4.7	BER of the MUD-ISIC, employed various multiuser detection techniques, for 8 users system with LS estimator (cyclically orthogonal training sequences) under the uniform MIP channel	71
4.8	BER of the MUD-ISIC, employed various multiuser detection techniques, for 16 users system with LS estimator (cyclically orthogonal training sequences) under the uniform MIP channel	71
4.9	BER of the MUD-ISIC, employed various multiuser detection techniques, for 24 users system with LS estimator (cyclically orthogonal training sequences) under the uniform MIP channel	72

List of Figures (Cont.)

Figure		Page
4.10	BER of the MUD-ISIC, employed various multiuser detection techniques, for 32 users system with LS estimator (cyclically orthogonal training sequences) under the uniform MIP channel	72
4.11	BER of the MUD-ISIC, employed various multiuser detection techniques, for 8 users system with LS estimator (cyclically orthogonal training sequences) under the exponentially decaying MIP channel	73
4.12	BER of the MUD-ISIC, employed various multiuser detection techniques, for 16 users system with LS estimator (cyclically orthogonal training sequences) under the exponentially decaying MIP channel	73
4.13	BER of the MUD-ISIC, employed various multiuser detection techniques, for 24 users system with LS estimator (cyclically orthogonal training sequences) under the exponentially decaying MIP channel	74
4.14	BER of the MUD-ISIC, employed various multiuser detection techniques, for 32 users system with LS estimator (cyclically orthogonal training sequences) under the exponentially decaying MIP channel	74
4.15	BER of the MUD-ISIC, employed various multiuser detection techniques, versus the number of users in the system with LS estimator (cyclically orthogonal training sequences) under the uniform MIP channel	75
4.16	BER of the MUD-ISIC, employed various multiuser detection techniques, versus the number of users in the system with LS estimator (cyclically orthogonal training sequences) under the exponentially decaying MIP channel	75
4.17	BER of the MUD-ISIC (linear MMSE detector) versus the training symbol power in the system with LS estimator using cyclically orthogonal training sequences	76
4.18	Achievable symbol rate as a function of number of data symbol in a packet frame	77
4.19	Performance of the frequency offset compensated MMSE detector using conventional reverse link subcarrier coefficient estimator and the MUD-ISIC (linear MMSE detector) using the LS estimator with cyclically orthogonal training sequences under the perfect frequency synchronization situation	79
4.20	Performance of the frequency offset compensated MMSE detector using EKF estimator and the MUD-ISIC (linear MMSE detector) using the LS estimator with cyclically orthogonal training sequences under the imperfect frequency synchronization situation	79
4.21	Performance of the MUD-ISIC (linear MMSE detector) using various parameter estimation techniques during a data period for the system having 512 data symbols in each packet frame	81
4.22	Performance of the MUD-ISIC (linear MMSE detector) using various parameter estimation techniques during a data period for the system having 260 data symbols in each packet frame	82

CHAPTER I

INTRODUCTION

Since the launch of commercial mobile phone service in the late 1970s and early 1980s, the demand for new services with higher quality has rapidly increased [1]. The current third-generation systems offer the variety of services with transmission rate up to 2 Mbps over 5 MHz bandwidth [2–4]. However, the maximum transmission rate may require the whole capacity of a cell to run [5]. For the next generation systems, which will be in operation around the year 2010, there is an expectation of peak data rate at 10-20 Mbps [6, 7] to 100 Mbps [8]. The existing air interface techniques, such as frequency division multiple access (FDMA), time division multiple access (TDMA), and direct sequence code division multiple access (DS-CDMA), are not able to achieve this emerging requirement. Therefore, the new wireless access scheme, using an approximate 20-100 MHz bandwidth, is needed. The most promising techniques to enabling the fourth-generation systems are based on the multicarrier modulation technology. The multicarrier modulation is not a new technology. It was first implemented with analog oscillators in the 1960s [9]. At that time, the implementation encountered difficulty due to hardware limitation such as oscillator stability etc. The multicarrier modulation becomes more attractive after its digital implementation using the discrete Fourier transform (DFT) was successfully executed in the 1980s via its fast algorithm called the fast Fourier transform (FFT). The multicarrier modulation was earlier adopted for a digital audio broadcasting (DAB) and a digital terrestrial television broadcasting (dTTb) in Europe [10, 11]. Several wireless local area network (WLAN) standards such as IEEE802.11 and HIPERLAN have also selected multicarrier modulation as their physical layer standard [10]. For terrestrial mobile communication systems, the multicarrier modulation is also under the promising exploration [12]. The laboratory simulations of the multicarrier code division multiple access (MC-CDMA) system demonstrated the attractiveness of the MC-CDMA in the cellular systems.

1.1 Multicarrier Modulation

The basic principle of multicarrier modulation is to convert a high-rate serial data stream into low-rate parallel data streams. The parallel data streams are modulated on different frequencies, usually called subcarriers, which at baseband are multiples of a harmonic frequency. An orthogonal frequency division multiplexing (OFDM) is a special case of the multicarrier modulation where frequency spacing between subcarriers is set at the closest possible value. Because the symbol duration is prolonged by a serial to parallel conversion process, the OFDM system is less sensitive to the dispersion in time caused by physical channel delay spread. Moreover, the OFDM achieve higher bandwidth efficiency than a single carrier system due to the overlapping spectra of the

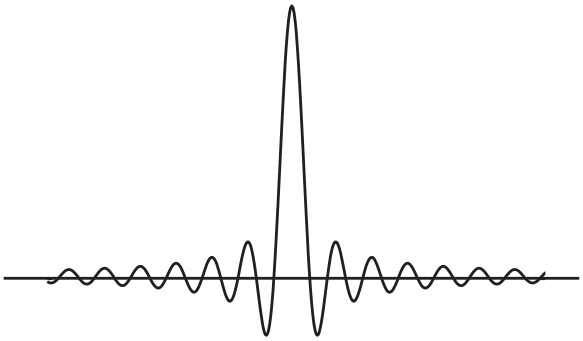

Spectrum of single carrier signal

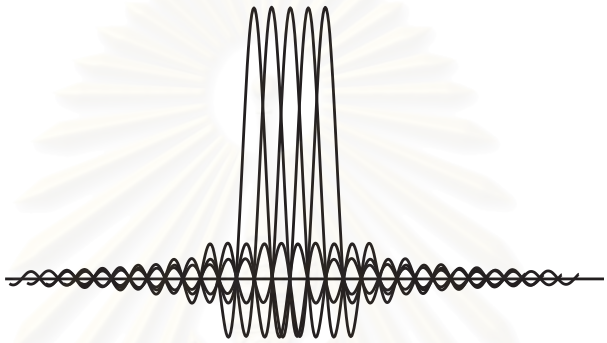

Spectrum of multicarrier signal

Figure 1.1 Spectrum of single carrier signal and multicarrier signal

subcarriers. The modulation of parallel data streams onto subcarriers can be realized by using the inverse discrete Fourier transform (IDFT). In practice, this transform can be efficiently implemented via the inverse fast Fourier transform (IFFT).

The OFDM has been employed to the applications in wireline as well as wireless environment. Many wireless OFDM based systems have been developed for both broadcasting and multiuser applications. For multiuser OFDM systems, termed as orthogonal frequency division multiple access (OFDMA), each user is assigned a disjoint set of subcarriers so that the multiple access is accomplished by means of frequency division. A data symbol can be encoded with error correcting codes and transmitted over several subcarriers to compensate for the loss of individual subcarriers due to frequency selective fading.

1.2 Multicarrier Code Division Multiple Access

In the very high-rate transmission, DS-CDMA system experiences severe inter-chip interference and difficulty in synchronizing the fast spreading code [13]. To overcome these limitations, a new system, which is a combination between DS-CDMA and OFDM signaling, has been proposed by various authors [14–16]. The advantages of the new hybrid system over the conventional

DS-CDMA systems have been reported [12]. This dissertation focuses on the MC-CDMA scheme, described by N.Yee [14]. In [15] and [16], the authors proposed the systems where each subcarrier is designated for an individual DS-CDMA system. These systems are refered as a multicarrier direct sequence code division multiple access (MC-DS-CDMA) system [15] and a multitone code division multiple access (MT-CDMA) system [16]. The considered MC-CDMA scheme provides higher spectral utilization efficiency and better resistance to frequency selective fading than the MC-DS-CDMA and MT-CDMA scheme [17]. In this scheme, the original data symbols are multiplied in parallel by the chips of spreading codes preassigned to the corresponding users. All the resultant chips are modulated onto different subcarriers, as in OFDM, and transmitted. This process can be viewed as direct-sequence spreading in the frequency domain.

The MC-CDMA system is different from the OFDMA system that one MC-CDMA data symbol occupies the whole subcarriers or a large number of subcarriers. The symbol detection in the MC-CDMA system exploits spreading code correlation properties rather than frequency seperation. In term of frequency diversity, the MC-CDMA system achieves much higher order of diversity than the OFDMA system. The MC-CDMA system succeeds many inherent advantages from the DS-CDMA system such as soft capacity, possible performance improvement by using multiuser detection techniques, and the utilization of soft handoff technique. Though the MC-CDMA system is different from the OFDMA system, both systems share many common features. Therefore, several techniques, initially proposed for the OFDMA system, can also be applied to the MC-CDMA system with slight modification.

1.3 Guard Interval

Guard interval in the form of cyclic prefix is normally introduced for each multicarrier symbol to avoid the intersymbol interference (ISI). In order to attain the ISI free communication, the duration of the cyclic prefix must be at least as long as the maximum channel delay. The graphical explanation of a guard interval insertion process is shown in figure 1.2. By using the cyclic prefix, the demodulation window can be selected from anywhere over the length of the symbol. This property provides symbol time synchronization tolerance as well as multipath immunity. If the cyclic prefix insertion is sufficient (communication is free from ISI), each subcarrier experiences flat fading where the channel is characterized by a multiplicative complex valued coefficient. This property offers more simplicity by converting the requirement of a complicated time-domain equalizer to a simple single-tap frequency domain combiner. Thus, the sufficient cyclic prefix condition is desirable for a forward link where the receivers are the complexity limited mobile stations.

In a reverse link, the delay of each user's signal to the basestation can be regarded as part of the effective channel impulse response. The sufficient cyclic prefix condition is possible for the reverse link, if the delay time of all the user signals can be maintained within a small synchronization window through the aid of a quasi-synchronous mechanism [18–21]. However,

since each user's signal experiences different channel fading in the reverse link, the simple frequency domain combiner cannot mitigate the effect from the multiple access interference (MAI) even with the sufficient cyclic prefix condition. Therefore, the complicated receiving techniques, such as the multiuser detectors, are required [13, 20–25]. Fortunately, a receiver in the reverse link is at a base station where the complexity constraint is not a crucial restriction. At the receiver, cyclic prefix is normally discarded to avoid the ISI. Thus, a symbol decision is made by considering only part of the entire MC-CDMA signal. This discarding leads to an inefficient use of the transmitted signal energy. Additionally, the introduction of cyclic prefix also decreases bandwidth utilization efficiency. To preserve these valuable resources, cyclic prefix should be used as less as possible. Due to a constraint on cyclic utilization, the maximum delay of channel may exceed the cyclic length in some cases. In the quasi-synchronous reverse link environment, time delay of each user signal relative to the beginning of the synchronization window lengthens the effective channel impulse response. This situation increases a possibility that the effective CIR duration exceeds the cyclic prefix duration.

The insufficient cyclic prefix situation does not only incur the ISI but also a crosstalk between each pair of subcarriers, which is generally referred as the intercarrier interference (ICI) [10, 26–35]. In this case, the single-tap frequency domain combiner and the conventional multiuser detection techniques are not sufficient to guarantee good quality of symbol detection. Many authors have proposed techniques for improving the symbol detection in the insufficient cyclic prefix situation [26–35]. The development of detectors for the insufficient cyclic prefix case introduces a new vision to the multicarrier system design where the cyclic prefix may be intentionally neglected [27, 28, 33–35]. It should be emphasized that the multicarrier systems without cyclic prefix provide better power and bandwidth utilization efficiency than the conventional cyclic prefix requisite system.

The works in [26–32] target the insufficient cyclic problem in the OFDM system. Unfortunately, the OFDM system is different from the MC-CDMA system. More specifically, the OFDM system does not consider the existence of the MAI, which is particular for the DS-CDMA related systems. Therefore, those OFDM based techniques are not directly applicable to the MC-CDMA system. To jointly cope with the MAI and the insufficient cyclic prefix problem in the MC-CDMA system, a multiuser detection with ISI cancellation (MUD-ISIC) [33] is a potential solution. The alternate solution, a truncated time-domain multiuser detection [34], suffers from the energy loss due to the discarding of the useful signal part. In [35], a receiver was derived from a well-known minimum mean square error (MMSE) decision feedback equalization (DFE) approach. The resultant receiver becomes a special case of the MUD-ISIC where a multiuser part is a MMSE detector.

In the previous works except the partial works of this dissertation in [32, 33], the receivers acquire the necessary parameters by calculating from the estimated channel impulse response. Many works concentrated on the receiver design and assume the perfect knowledge about the channel impulse response at the receiver without clarifying its feasibility. Some works in both the OFDM context and the MC-CDMA context misleadingly suggested the channel impulse response

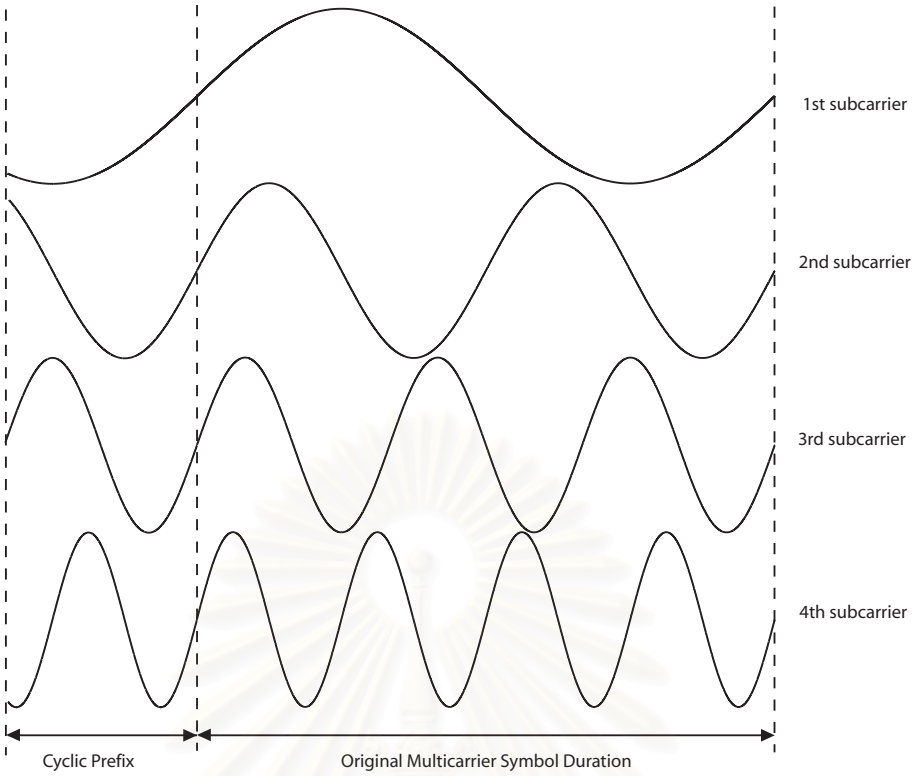

Figure 1.2 Cyclic Prefix Insertion

estimation based on the assumption of equally spaced finite impulse response (FIR) channel. In fact, this assumption is only ensured in the sufficient cyclic prefix case [36].

1.4 Frequency Offset

The MC-CDMA system inherits from OFDM the vulnerability to a frequency offset, which mainly results from a mismatch between the carrier frequencies at the transmitter and the receiver [10]. Even small amount of frequency offset can cause severe degradation of the desired signal power and cross talk among subcarriers.

For the forward link, if the frequency offset can be accurately estimated, the carrier synchronization error can be easily compensated. The frequency offset estimation can be accomplished by employing periodic pilots [37, 38], which cost bandwidth and power expense. In [39], the authors proposed the semi-blind frequency offset estimation technique by exploiting the redundancy (cyclic prefix) structure of a multicarrier symbol. In [40, 41], the authors further improved the accuracy of the technique in [39] by discarding part of the cyclic prefix, affected by ISI. The non-data aided or blind approaches for frequency offset estimation are also reported in the literatures. These methods exploit the known subspace structure due to the placement of unmodulated (virtual) subcarriers employed in the practical multicarrier modulation systems [42–44].

For the reverse link OFDMA system, each user is assigned a disjoint sub-band. Signal

for each user can be separated by using a bandpass filter. Therefore, it is possible to apply techniques initially proposed for a forward link to the reverse link OFDMA system [45, 46]. For the reverse link MC-CDMA system, each mobile station shares the same frequency band and incurs different frequency offset values. The correction of one user's frequency offset would mis-align the others. In [47, 48], the authors proposed the signal separation strategy for the reverse link MC-CDMA system. For this technique, each single user signal is extracted from a multi-dimensional composite signal by using an interference cancellation strategy. This separation technique enables the use of the existing frequency offset estimation and correction algorithms. However, the residual interference (from imperfect interference cancellation) severely degrades the performance of the signal separation based technique especially in a low signal to interference plus noise ratio (SINR) scenario. Moreover, signal separation requires the initial channel estimation. This requirement implies the necessity of performing channel estimation on the ICI disturbed signal. Such channel estimation technique is currently not available. In [47, 48], the receiver was optimistically assumed to have the perfect knowledge about channel. In [49, 50], the authors integrated signal detection and frequency offset compensation for the MC-CDMA system into a unified procedure. This technique eludes the need for individual frequency offset correction, hence; it is practically interesting. There was a report on a blind frequency offset estimation technique for the reverse link in [51]. However, since the frequency offsets still cannot be corrected, the channel estimation process is still in doubt. The more practical work was presented in [52] where the joint channel and frequency offset estimation technique based on the extended Kalman filtering method is proposed. However, this technique has slow convergence rate especially in the case of large number of users.

It is worth to note that all the mentioned techniques regarding the frequency offset problem for both the forward link and reverse link channel require the sufficient cyclic prefix condition.

1.5 Multiple Access Interference and Multiuser Detection

The performance of DS-CDMA based systems, including the MC-CDMA systems, is limited by the presence of MAI. Even if the systems employ orthogonal code such as Hadamard-Walsh sequence, channel fading can easily destroy such orthogonality. Additionally, different multipath attenuation causes a so-called near-far problem, which would intensify the adverse effect of MAI. The conventional matched filter (MF) detector, which is optimum in a single user system, is severely susceptible to MAI. The sensitivity of the MF to MAI has encouraged researchs on multiuser detections, which exploit the structure of the MAI in order to suppress it.

Since the main objective of this dissertation is not on the development of the multiuser detection techniques, only the multiuser detectors without channel decoding are considered for simplicity. These detectors have low complexity and promising potential for implementation. The multiuser detection stage of the proposed receiver does not limit to any particular multiuser detection techniques. In general, the channel decoding aided multiuser detectors (Turbo multiuser detectors)

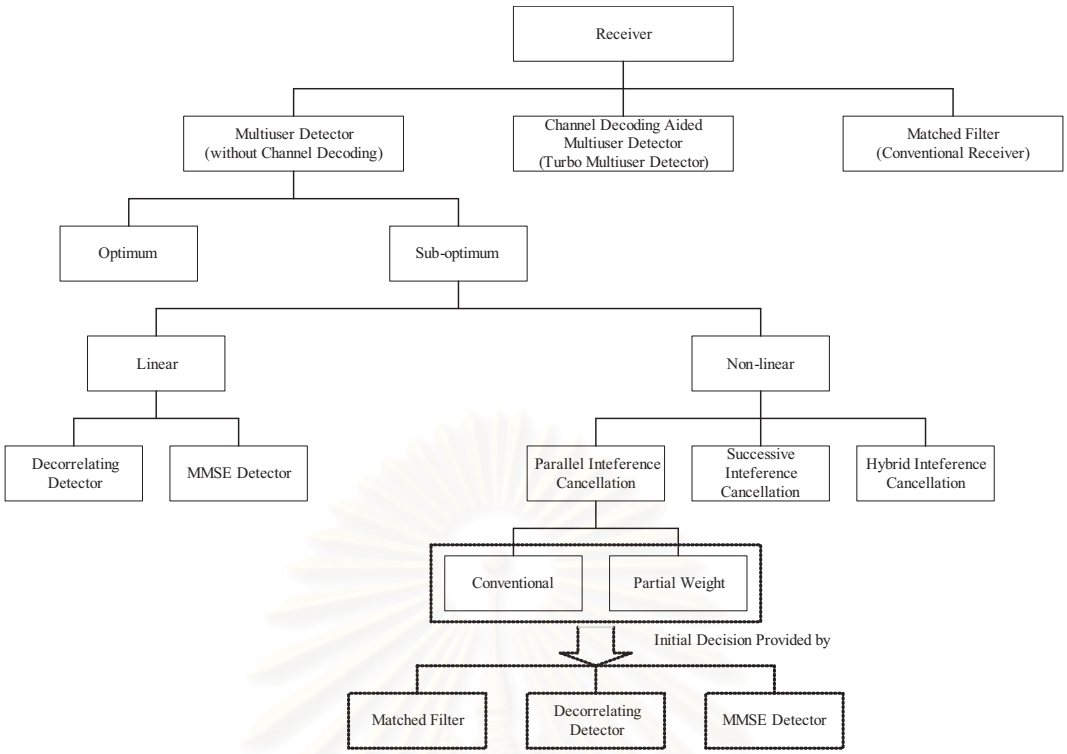

Figure 1.3 Multiuser Detection Tree Diagram

as well as the conventional matched filter can be applied in place of the multiuser detectors without channel decoding. Figure 1.3 illustrates a hierarchy diagram of multiuser detection classes.

An optimal multiuser detector based on an exhaustive search was proposed in [53] and it was applied to the MC-CDMA systems in [54]. Due to its high complexity which exponentially increases in the number of users, several sub-optimum linear and non-linear multiuser detectors have been studied such as in [55–62] for the DS-CDMA system and in [13, 17, 20–25, 63] for the MC-CDMA system. In this dissertation, both linear and non-linear sub-optimum multiuser detectors will be studied. For linear multiuser detectors, this dissertation will consider the decorrelating detector (DD) and the MMSE detector. For non-linear multiuser detectors, this dissertation will consider the weighted multistage interference cancellation (WMIC) detector [22, 61, 62]. In addition to the conventional WMIC with MF first stage, the WMIC with linear multiuser detection first stage will also be studied.

1.6 Scope of This Dissertation

A MC-CDMA system will be considered in this dissertation, due to its potential to support high-rate transmission, which will be necessary in several different aspects for the future wireless applications. In the past, a forward link has usually been targeted because most of the high-rate traffic is in the forward link. However, due to the increasing demand for some high rate applications in a reverse link such as real time interactive applications, the researches in various aspects for

the reverse link inevitably become more important. The difference of channel fading, delay time, and frequency offset, experienced by each user's signal, introduces considerable complication to the implementation of the reverse link with high quality of services. Fortunately, the limitation on hardware complexity in the reverse link is much more relaxed than that in the forward link. These significant issues will be addressed in this dissertation.

As earlier mentioned, the MC-CDMA system is susceptible to the MAI, ISI, and ICI. The main causes of the later two interference types are the insufficient cyclic prefix condition and the presence of the frequency offset. This dissertation will start by exploring the mathematical models of the MC-CDMA system under the presence of all the concerned interference. From the obtained models, a MUD-ISIC will be proposed to improve the overall performance by mitigating the effect from all the interference. The proposed MUD-ISIC will be able to employ many existing multiuser detection techniques, both linear and non-linear detectors. Performance of the proposed receiver will be evaluated and compared with other known receiving techniques by using the computer simulations under the assumption of perfect knowledge of all the necessary parameters. This dissertation will also study the influence of the cyclic prefix insertion and the data serial to parallel conversion process to the bit error rate.

In order to implement the proposed MUD-ISIC, this dissertation will also study the parameter acquisition techniques. The concerned parameters are the ISI generation sequences, the transformed signature sequences, and the noise variance. The estimation techniques for the ISI generation sequences and the transformed signature sequences will be proposed in 2 different approaches, least squares (LS) estimator and adaptive estimator. The asymtotic mean square error (MSE) analyses of the estimator and the criteria for the training sequences to achieve minimum MSE will be presented. Several systematic generation schemes of the optimum training sequences will be proposed and discussed. Comparative studies of several estimators will be presented in this dissertation. Performance of the proposed MUD-ISIC with the proposed parameter estimation techniques will also be studied and compared with the other receivers with the existing estimation techniques.

In this dissertation, the communication will be carried out using bursts (packets) mode. The parameter estimation is only performed in the training period. The techniques for interpolation or tracking (decision direct computation) of the estimated parameters during the data transmission period will also be proposed and evaluated.

1.7 Outline

In chapter 2, the quasi-synchronous reverse link MC-CDMA system model, frequency offset model, multipath fading channel model, and background noise model will be described. Many existing receiving and parameter estimation techniques will be reviewed.

In chapter 3, the MUD-ISIC will be developed and the adoption of several classes of multiuser detection will be discussed. Key simulation parameters, such as the multipath intensity

profile, frequency offset variance, cell size, etc., will be presented. The simulation results by assuming perfect information of all the necessary parameters will be presented.

In chapter 4, the transformed signature sequences and ISI generation sequences estimation techniques will be proposed. The MSE of the estimator will be analyzed and the criteria for the training sequence to achieve the minimum MSE will also be presented. The systematic generation of the optimum training sequence will be developed. The techniques for acquiring the sequence estimates during the data period will also be demonstrated. In order to implement some classes of multiuser detection, the noise variance estimation technique will also be proposed. The performance of the estimator and the optimum training sequences is evaluated and the results will be given in chapter 4. The results on the MUD-ISIC using the proposed estimator will also be presented and discussed.

Finally, Chapter 5 will conclude this dissertation. The results and contributions will be summarized.

1.8 Basic Notation

In this dissertation, bold character denotes a column vector and bold capital character denotes a matrix as it will be clear from the context. $(.)^T$ denotes transposition, $(.)^H$ denotes hermitian transposition, $(.)^*$ denotes complex conjugate, $(.)^{-1}$ denotes square matrix inversion, and $(.)^\dagger$ denotes Moore-Penrose generalized inversion. If $\mathbf{X}$ is a given $M \times M$ square matrix, $diag(\mathbf{X})$ is the $M \times 1$ vector of the diagonal entries of $\mathbf{X}$.

CHAPTER II

BASIC BACKGROUND AND RELATED TOPICS

This chapter reviews a basic background and the related topics of a quasi-synchronous reverse link MC-CDMA system. A mathematical model of the quasi-synchronous reverse link MC-CDMA system under the presence of frequency offset and intersymbol interference is investigated. This model is analyzed under various special cases in order to understand the characteristic of the system and the influence of each factor. The receiving techniques for a conventional MC-CDMA system as well as the more advanced techniques for an error-prone situation are presented and the existing parameter estimation techniques are reviewed.

2.1 System Models

2.1.1 MC-CDMA Transmission Model

A block diagram of the quasi-synchronous reverse link MC-CDMA system is shown in figure 2.1. The entire bandwidth is divided into N_C equally spaced subcarriers. The system is supposed to service N_U active users, being assigned a unique signature sequence of length N_S,

$$\mathbf{c}_k = \begin{bmatrix} c_k^0 & c_k^1 & \cdots & c_k^{N_S-1} \end{bmatrix}^T \tag{2.1}$$

where $c_k^n \in \{1, -1\}$. At a transmitter, each user generates input symbols, which are independent and identically distributed (i.i.d.) with zero mean. A block of successive symbols is serial-to-parallel converted and each parallel symbol is multiplied by a corresponding signature sequence.

Each chip of the resultant sequence is mapped onto different subcarrier according to a continuous subcarrier assignment (CSA) scheme. In general, an interleaved subcarrier assignment (ISA) scheme, which offers higher level of frequency diversity than the CSA scheme, can also be employed. However in the presence of ICI, the CSA scheme, which maximizes the frequency separation among subcarriers assigned to different parallel symbols, simplifies a detector by neglecting cross parallel symbol interference [50]. This simplification also helps reducing a number of parameters to be estimated, thus; a number of pilot symbols can be greatly lessened. Since the ICI is commonly occurred in the real applications, the CSA scheme is considered in this dissertation. For the CSA scheme, a group of adjacent subcarriers is assigned to each parallel symbol so that the m^{th} chip of the p^{th} parallel symbol is mapped onto the $(m + pN_S)^{th}$ subcarrier (see also figure 2.2). After subcarrier mapping, the data are modulated in baseband by the IDFT and converted into serial data. The cyclic prefix is inserted between the successive MC-CDMA symbols. The signal is RF up-converted and then transmitted. The complex equivalent lowpass transmitted signal can be described as

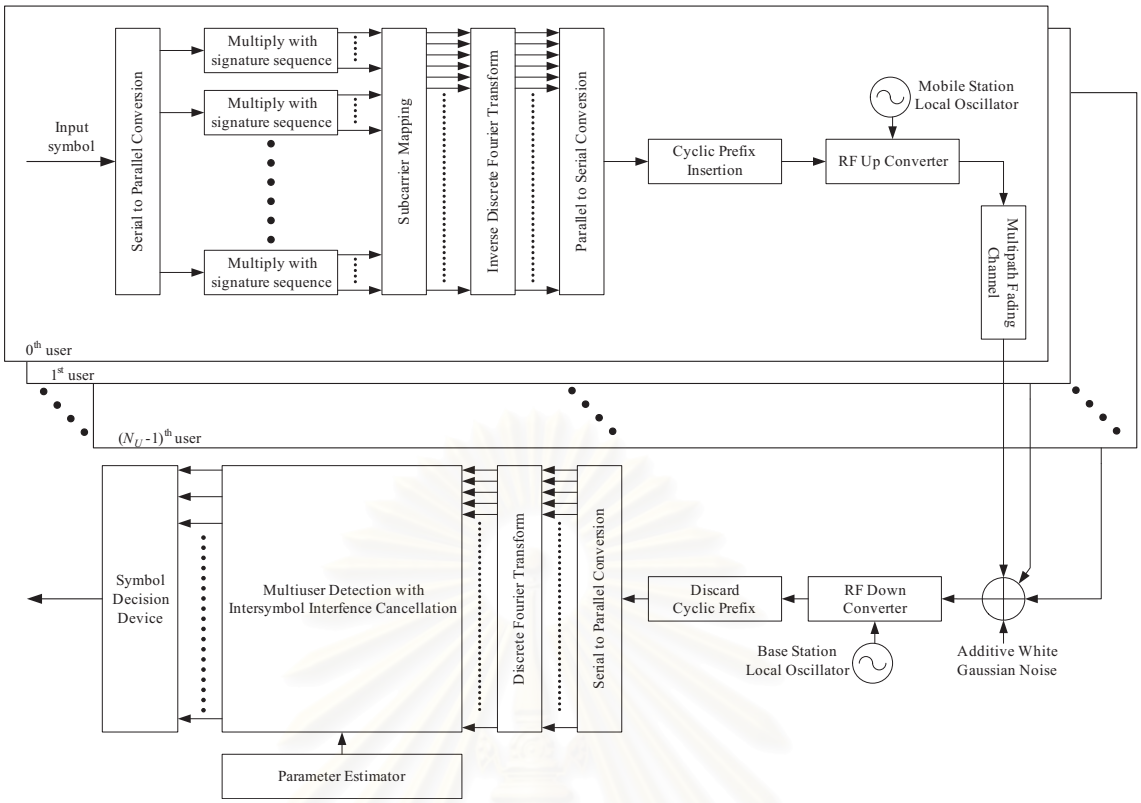

Figure 2.1 Quasi-synchronous reverse link MC-CDMA system block diagram

$$s_k(t) = \sum_{i=-\infty}^{\infty} s_k^i(t - iT_S) \tag{2.2}$$

where

$$s_k(t) = s_k^i(t) = \frac{\sigma_k}{N_C} \sum_{p=0}^{N_P-1} \sum_{m=0}^{N_S-1} c_k^m b_{k,p}^i e^{j2\pi f_{map}(m,p)\frac{(t-T_{CP})}{T_B}} p_T\left(\frac{t}{T_S}\right), \tag{2.3}$$

T_S is the MC-CDMA symbol duration, T_{CP} is the cyclic prefix duration, $T_B = T_S - T_{CP}$ is the duration of a MC-CDMA symbol without cyclic prefix, $(\sigma_k)^2$ is the transmit power of the k^{th} user's signal, $p_T(t)$ is a rectangular waveform defined as

$$p_T(t) = \begin{cases} 1 & (0 \le t < 1) \\ 0 & (otherwise) \end{cases}, \tag{2.4}$$

and

$$f_{map}(m,p) = m + pN_S \tag{2.5}$$

is a subcarrier mapping function.

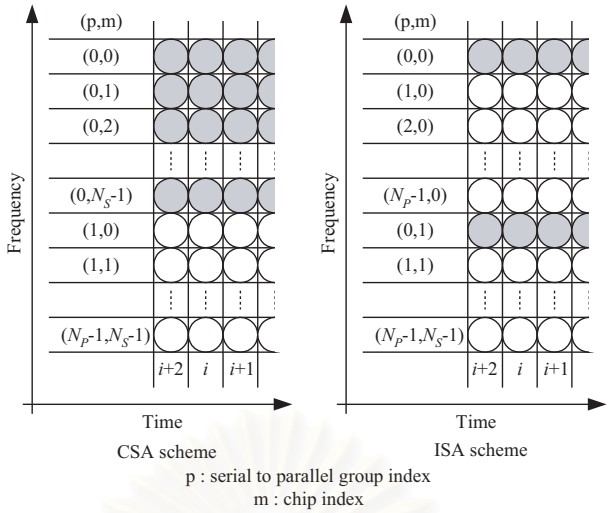

Figure 2.2 Continuous subcarrier assignment and interleaved subcarrier assignment

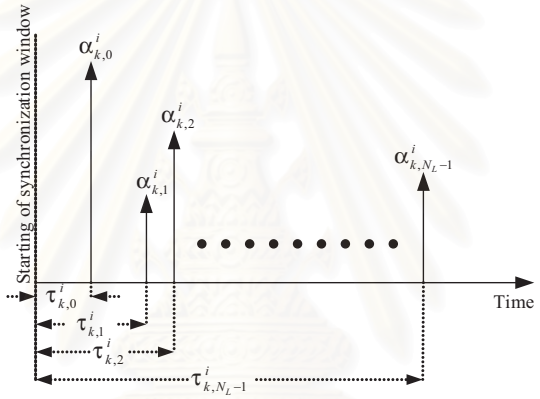

Figure 2.3 Multipath channel

2.1.2 Channel Model

In quasi-synchronous systems, mobile units attempt to synchronize with a synchronization window, specified by the base station, before initiating the communication link. As a consequence, the relative time-offsets among users are limited to a fraction of a symbol, and can, thus, be incorporated as part of the unknown channel impulse response. In such cases, the time offset is compensated as part of the equalization performed at the receiver. In this dissertation, the channel will be assumed to be quasi-static so that it will be constant over a MC-CDMA block and it will vary from block to block. Since this dissertation considers a reverse link where each transmitted signal is emitted from a different location, the channel of each user is assumed to be independent. Moreover, each transmitter introduces different frequency offset relative to the frequency of the base station's local oscillator. The channel is modeled as a wide sense stationary uncorrelated scattering (WSSUS) multipath channel as shown in figure 2.3 [64, 65]. The channel consists of

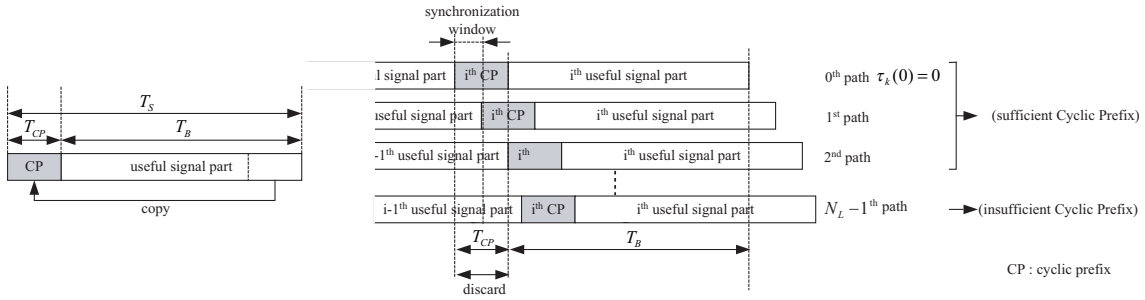

Figure 2.4 Cyclic prefix insersion and multipath signals

N_L paths, each of which has its particular delay $\tau_{k,l}^i$ and complex value coefficient $\alpha_{k,l}^i$. The channel of the k^{th} user is described by

$$h_k^i(\tau) = \sum_{l=0}^{N_L-1} \alpha_{k,l}^i \delta\left(\tau - \tau_{k,l}^i\right) \tag{2.6}$$

where $\delta(\tau)$ is a Dirac function defined as

$$\delta(\tau) = \begin{cases} 1 & (\tau = 0) \\ 0 & (otherwise) \end{cases} . \tag{2.7}$$

The path delay value is relative to the beginning of the synchronization window. For example, $\tau_{k,l}^i = 0$ implies that the l^{th} delay version of the k^{th} user's signal synchronizes with the beginning of the synchronization window (see also figure 2.3 and 2.4).

2.1.3 Received Signal Model

In practical systems, A MC-CDMA symbol period is usually designed to be much larger than the maximum delay of channel [10]. As a consequence, only signal from the i^{th} symbol interval and signal from the $(i-1)^{th}$ symbol interval are involved in the receiving process during the i^{th} symbol interval.

The received signal is an aggregate of the linear convolution of each transmitted signal with the corresponding channel impulse response. The received signal in the complex baseband representation can be expressed as

$$r(t) = \sum_{k=0}^{N_U-1} r_k(t) + \eta(t) \tag{2.8}$$

where

$$r_k(t) = \left[\sum_{l=0}^{N_L-1} \alpha_{k,l}^i \sum_{i=-\infty}^{\infty} s_k^i\left(t - \tau_{k,l}^i - iT_S\right)\right] e^{j2\pi\Delta_{f,k}(t-iT_S-T_{CP})}, \tag{2.9}$$

$\Delta_{f,k}$ is a frequency offset value of the k^{th} user signal, and $\eta(t)$ denotes an additive complex Gaussian noise term, modeled as a normal distributed random variable with zero mean and variance

$(\sigma_\eta)^2$. The received data after the cyclic prefix removal is sampled at $t = iT_S + T_{CP} + nT_C$ over the i^{th} symbol interval, where $T_C = T_B/N_C$ is a sampling interval. A discrete-time data sample during the i^{th} symbol interval is expressed as

$$r^i[n] = \sum_{k=0}^{N_U-1} \left(r^i_{k,D}[n] + r^i_{k,I}[n]\right) + \eta^i[n] \tag{2.10}$$

where $\eta^i[n]$ is a noise sample, $r^i_{k,D}[n]$ is the contribution from the transmitted signal in the i^{th} symbol interval, and $r^i_{k,D}[n]$ is the contribution from the transmitted signal in the $(i-1)^{th}$ symbol interval. The terms $r^i_{k,D}[n]$ and $r^i_{k,D}[n]$ are given, respectively, by

$$r^i_{k,D}[n] = \left[\sum_{l=0}^{N_L-1} u\left(nT_C + T_{CP} - \tau^i_{k,l}\right)\alpha^i_{k,l} \sum_{p=0}^{N_P-1}\sum_{m=0}^{N_S-1} c^m_k b^i_{k,p} e^{j\frac{2\pi f_{map(m,p)}\left(nT_C-\tau^i_{k,l}\right)}{T_B}}\right] e^{j2\pi\frac{n\varepsilon_k}{N_C}} \tag{2.11}$$

and

$$r^i_{k,I}[n] = \left[\sum_{l=0}^{N_L-1} \bar{u}\left(\tau^i_{k,l} - T_{CP} - nT_C\right)\alpha^i_{k,l} \sum_{p=0}^{N_P-1}\sum_{m=0}^{N_S-1} c^m_k b^{i-1}_{k,p} e^{j\frac{2\pi f_{map(m,p)}\left(nT_C-\tau^i_{k,l}+T_S\right)}{T_B}}\right] e^{j2\pi\frac{n\varepsilon_k}{M}} \tag{2.12}$$

where $\varepsilon_k = \frac{\Delta_{f,k}}{1/T_B}$ is a frequency offset value normalized by a carrier spacing, $u(n)$ is an unit step function defined as

$$u(n) = \begin{cases} 1 & (n \geq 0) \\ 0 & (\text{otherwise}) \end{cases} \tag{2.13}$$

and $\bar{u}(n)$ is a function defined as

$$\bar{u}(n) = u(n) - \delta(n). \tag{2.14}$$

A sequence of the received samples $\{r^i[n]\}_{n=0}^{N_C-1}$ is demodulated by taking the N_C-point DFT. An element of the DFT output sequence $\{x^i[n']\}_{n'=0}^{N_C-1}$ is given by

$$x^i[n'] = \sum_{k=0}^{N_U-1}\sum_{p=0}^{N_P-1} x^i_{k,p}[n'] + \bar{\eta}^i[n'] \tag{2.15}$$

where $\bar{\eta}^i[n']$ is the DFT of $\eta^i[n]$. The term $x^i_{k,p}[n']$ can be expressed as

$$x^i_{k,p}[n'] = \bar{c}^{i,n'}_{k,p,D} b^i_{k,p} + \bar{c}^{i,n'}_{k,p,I} b^{i-1}_{k,p} \tag{2.16}$$

where

$$\bar{c}^{i,n'}_{k,p,D} = \sum_{m=0}^{N_S-1} \beta^{i,n',m}_{k,p,D} c^m_k, \tag{2.17}$$

$$\bar{c}^{i,n'}_{k,p,I} = \sum_{m=0}^{N_S-1} \beta^{i,n',m}_{k,p,I} c^m_k, \tag{2.18}$$

$$\beta^{i,n',m}_{k,p,D} = \sum_{l=0}^{N_L-1}\sum_{n=0}^{N_C-1} \alpha^i_{k,l} u\left(nT_C + T_{CP} - \tau^i_{k,l}\right) e^{j\frac{-2\pi f_{map(m,p)}\tau^i_{k,l}}{T_B}} e^{j2\pi\frac{\left(f_{map(m,p)}-n'+\varepsilon_k\right)n}{N_C}} \tag{2.19}$$

and

$$\beta_{k,p,I}^{i,n',m} = \sum_{l=0}^{N_L-1} \sum_{n=0}^{N_C-1} \alpha_{k,l}^{i} \bar{u}\left(\tau_{k,l}^{i} - T_{CP} - nT_C\right) e^{j\frac{2\pi f_{map(m,p)}\left(-\tau_{k,l}^{i}+T_S\right)}{T_B}} e^{j2\pi\frac{\left(f_{map(m,p)}-n'+\varepsilon_k\right)n}{N_C}}. \tag{2.20}$$

From (2.17) and (2.18), Each element of the sequence $\bar{\mathbf{c}}_{k,D}^{i} = \left\{\bar{c}_{k,p,D}^{i,n'}\right\}_{n'=0}^{N_C-1}$ and $\bar{\mathbf{c}}_{k,I}^{i} = \left\{\bar{c}_{k,p,I}^{i,n'}\right\}_{n'=0}^{N_C-1}$ is a linear combination of the original signature sequences $\mathbf{c}_k$ with the coefficients $\beta_{k,p,D}^{i,n',m}$ and $\beta_{k,p,I}^{i,n',m}$, respectively. From the expressions of DFT output sequence in (2.15)-(2.20), we can view the receiving part of the MC-CDMA system with insufficient cyclic prefix and frequency offset as the receiving part of the ISI corrupted MC-CDMA system, provided signature sequences $\bar{\mathbf{c}}_{k,D}^{i}$ and $\bar{\mathbf{c}}_{k,I}^{i}$ for the i^{th} symbols and the $(i-1)^{th}$ symbols, respectively. To reflect their physical meanings, the sequence $\bar{\mathbf{c}}_{k,D}^{i}$ will be referred as the transformed signature sequence and the sequence $\bar{\mathbf{c}}_{k,I}^{i}$ will be referred as the ISI generation sequence.

At the transmitting end, the $(n')^{th}$ subcarrier, which lies within the p^{th} subcarrier group ($pN_S \leq n' < (p+1)N_S$), is the p^{th} parallel symbols multiplied by the corresponding chips of the signature sequences. However, the $(n')^{th}$ DFT output entry at the receiver does not only capture the contribution from the p^{th} parallel symbols but also the other $N_P - 1$ parallel symbol. The interference from the other $N_P - 1$ parallel symbols will be referred as the cross parallel symbol interference. Unlike the signal at the transmitter that only the corresponding chip of the signature sequences characterizes the signal at the particular subcarrier, all the N_S chips of the signature sequences factor the contribution from the p^{th} parallel symbol to each DFT output entry at the receiver. Apart from the cross parallel symbol interference, the $(n')^{th}$ DFT output entry is also affected by the ISI from all the N_P parallel symbols of the previous symbol interval.

For a sufficient cyclic prefix environment, i.e. $\tau_k[i,n,l] \leq T_{CP}$, the coefficient $\beta_{k,p,I}^{i,n',m}$ becomes zero. As a consequence, the second term on the right hand side of equation (2.16), which denotes the ISI, vanishes. The sufficient cyclic prefix condition also simplifies the expression of $\beta_{k,p,D}^{i,n',m}$ in (2.19) as

$$\begin{aligned}\beta_{k,p,D}^{i,n',m} &= \sum_{l=0}^{N_L-1} \sum_{n=0}^{N_C-1} \alpha_{k,l}^{i} e^{j\frac{-2\pi f_{map(m,p)}\tau_{k,l}^{i}}{T_B}} e^{j2\pi\frac{\left(f_{map(m,p)}-n'+\varepsilon_k\right)n}{N_C}} \\ &= \sum_{l=0}^{N_L-1} \alpha_{k,l}^{i} e^{j\frac{-2\pi f_{map(m,p)}\tau_{k,l}^{i}}{T_B}} \sum_{n=0}^{N_C-1} e^{j2\pi\frac{\left(f_{map(m,p)}-n'+\varepsilon_k\right)n}{N_C}}\end{aligned}. \tag{2.21}$$

In case of perfect frequency synchronization, i.e. $\varepsilon_k = 0$, the above equation can be further simplified as

$$\beta_{k,p,D}^{i,n',m} = \begin{cases} \sum_{l=0}^{N_L-1} \alpha_{k,l}^{i} e^{j\frac{-2\pi n'\tau_{k,l}^{i}}{T_B}} & \text{for } f_{map}(m,p) = n' \\ 0 & (\text{otherwise}) \end{cases}. \tag{2.22}$$

Then,

$$x^i[n'] = \sum_{k=0}^{N_U-1} \beta_{k,p,D}^{i,n',m} c_k^m b_{k,p}^i + \bar{\eta}^i[n'] \tag{2.23}$$

for $f_{map}(m,p) = n'$.

The above equation indicates that, for the systems with perfect frequency synchronization and sufficient cyclic prefix, each DFT output entry is basically the transmitted signal ($c_k^m b_{k,p}^i$), multiplied by the channel coefficient ($\beta_{k,p,D}^{i,n',m}$). In this case, there is neither ISI nor cross parallel symbol interference.

For the case of non-zero frequency offset, i.e. $\varepsilon_k \neq 0$, the term $\beta_{k,p,D}^{i,n',m}$ cannot be simplified as in (2.22). Hence, the cross parallel symbol interference still exists. For the insufficient cyclic prefix case, the cross parallel symbol interference occurs even in the system with perfect frequency synchronization. Before continuing to the next topic, it is worth to note that the OFDM system can be regarded as a special case of the MC-CDMA system that has processing gain of one. Under the presence of frequency offset and ISI, subcarriers of the OFDM system, which carry different data symbols, are mutually interfered. Therefore, the cross parallel symbol interference in the OFDM system is usually referred as the intercarrier interference (ICI).

Table 2.1 Interference for various system conditions

		MAI	CPSI	ISI
Sufficient cyclic prefix	without frequency offset	Yes	No	No
	with frequency offset	Yes	Yes	No
Insufficient cyclic prefix	without frequency offset	Yes	Yes	Yes
	with frequency offset	Yes	Yes	Yes

*CPSI : cross parallel symbol interference

2.2 Receivers for the Forward Link MC-CDMA system

In the forward link, all the users' signals share the same communication channel. With perfect frequency synchronization and sufficient cyclic prefix insertion, the DFT output element is given by

$$x^i[n'] = \beta_{p,D}^{i,n',m} \sum_{k=0}^{N_U-1} c_k^m b_{k,p}^i + \bar{\eta}^i[n'] \tag{2.24}$$

for m and p satisfying $f_{map}(m,p) = n'$, where channel coefficient $\beta_{p,D}^{i,n',m}$ is defined similar to (2.22) by taking off the subscript indicating the user index k.

2.2.1 Combining Techniques

From (2.24), transmitted power of each parallel symbol is spread across the N_S DFT output entries. The decision variable for each data symbol is conventionally obtained by coherently

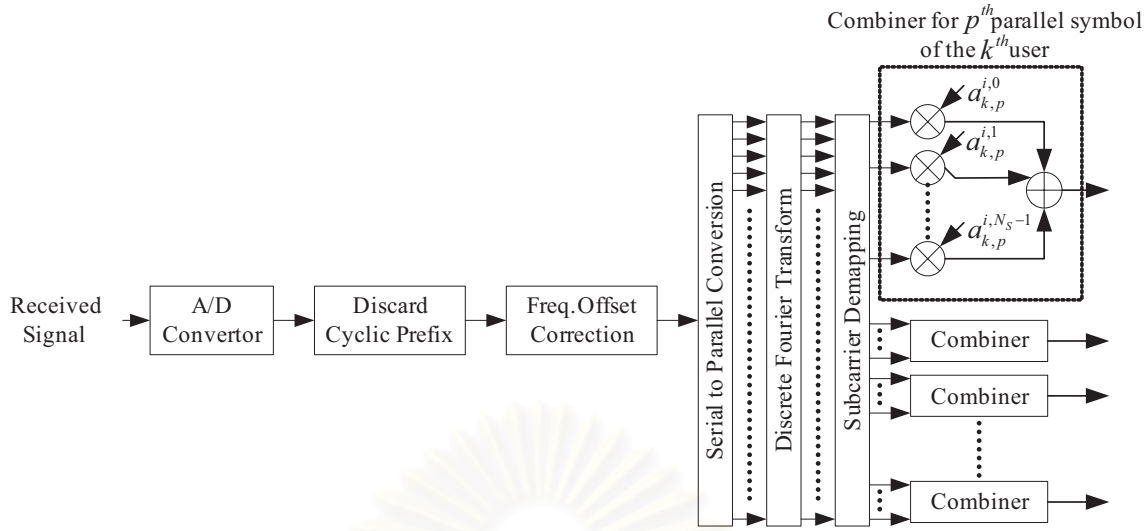

Figure 2.5 Block diagram of combining technique

combining all the scattered power as

$$z_{k,p}^{i} = \sum_{m=0}^{N_S-1} \left(a_{k,p}^{i,m}\right)^{*} x^{i}\left[f_{map}\left(m,p\right)\right] \tag{2.25}$$

where $a_{k,p}^{i,m}$ is a combining coefficient.

Several authors have proposed many criteria in designing the combining coefficients. Some techniques only consider the background noise or only consider the MAI, whereas some techniques try to compromise the effect from these 2 factors. In the following, the five most famous combining techniques, namely equal gain combining (EGC), maximum ratio combining (MRC), orthogonal restore combining (ORC), controlled equalization (CE), and minimum mean square error combining (MMSEC), will be reviewed. The MRC maximizes the signal to noise ratio (SNR) but it tends to increase the MAI. On the other hand, the ORC perfectly recovers the orthogonality but it is susceptible to the noise amplification. The EGC only compensates the phase shift. As a consequence, it does not effect the level of MAI and SNR. The CE and MMSEC compromise the MAI suppression with the noise enhancement.

2.2.1.1 Equal Gain Combining

The EGC only coherently combines the signal power at each subcarrier. It does not equalize the effect of the channel. The EGC coefficient is given by

$$a_{k,p}^{i,m} = \frac{\beta_{p,D}^{i,f_{map}(m,p),m}}{\left|\beta_{p,D}^{i,f_{map}(m,p),m}\right|} c_k^m . \tag{2.26}$$

2.2.1.2 Maximum Ratio Combining

The MRC maximizes the SNR of the decision statistics. In the case of one user, the MRC method can minimize the bit error rate (BER). The motivation behind MRC is that the components of the received signal with large amplitudes are likely to contain relatively less noise. Thus, their effect on the decision process is increased by squaring their amplitudes. The MRC coefficient is given by

$$a_{k,p}^{i,m} = \beta_{p,D}^{i,f_{map}(m,p),m} c_k^m. \tag{2.27}$$

2.2.1.3 Orthogonal Restore Combining

In the forward link, the orthogonal codes are normally employed as signature sequence. Unfortunately, the channel fading coefficients destroy such orthogonality. The ORC attempts to restore the orthogonality among user's signature sequences by normalizing the amplitudes of the subcarriers. The ORC coefficient is given by

$$a_{k,p}^{i,m} = \frac{\beta_{p,D}^{i,f_{map}(m,p),m}}{\left|\beta_{p,D}^{i,f_{map}(m,p),m}\right|^2} c_k^m. \tag{2.28}$$

With ORC, the decision statistics are free from MAI. However, weak-amplitude subcarriers tend to be multiplied by strong gains. As a consequence, noise components are amplified at weaker subcarriers. This noise amplification effect degrades the BER performance.

2.2.1.4 Controlled Equalization

This method suppresses the excessive noise amplification in the ORC by only combining the subcarriers with substantially high amplitude (amplitude exceed the certain threshold level). The CE coefficient is given by

$$a_{k,p}^{i,m} = \frac{\beta_{p,D}^{i,f_{map}(m,p),m}}{\left|\beta_{p,D}^{i,f_{map}(m,p),m}\right|^2} u\left(\left|\beta_{p,D}^{i,f_{map}(m,p),m}\right| - \gamma\right) c_k^m \tag{2.29}$$

where γ is a detection threshold and $u(n)$ is the unit step function as defined in (2.13).

2.2.1.5 Minimum Mean Square Error Combining

The MMSEC compromises the orthogonality restoration with the noise amplification. Based on the minimum mean square error (MMSE) criterion, the MMSEC coefficient is given by

$$a_{k,p}^{i,m} = \frac{\beta_{p,D}^{i,f_{map}(m,p),m}}{N_U \left|\beta_{p,D}^{i,f_{map}(m,p),m}\right|^2 + \mathrm{var}\left(\bar{\eta}^i\left[n'\right]\right)} c_k^m \tag{2.30}$$

where $\mathrm{var}\left(\bar{\eta}^{i}\left[n'\right]\right)$ is the noise power. For large $\left|\beta_{p,D}^{i,f_{map}(m,p),m}\right|$, the MMSEC coefficients become in proportion to the inverse of the subcarrier envelop, whereas the gains are small for the small $\left|\beta_{p,D}^{i,f_{map}(m,p),m}\right|$.

2.2.1.6 Other Receivers

Apart from the aforementioned combining techniques, many other advanced receivers have also been proposed for the detection of forward link MC-CDMA systems. These receiving techniques include the maximum likelihood multiuser detection, interference cancellation, etc. The details on these detectors are summarized in [17]. Even though the performance of these detectors is relatively good, their implementation is limited by the fact that they perform simultaneous detection of all the active users, which is not suitable for the forward link where the receiving process is at the mobile stations. In addition, the complexity of these advanced receivers is much higher than that of the combining techniques.

2.2.2 Frequency Offset Correction

The receivers for the forward link require the frequency offset correction prior to the symbol detection. Since all the user's signals are modulated by the common local oscillator at the base station, the frequency offsets of all the users as seen from a mobile terminal are the same. The compensation of frequency offset can be achieved by either using the voltage control oscillator to adjust the mobile station's local oscillator or pre-multiplying the compensation factors to the received signal samples. As shown in (2.11) and (2.12), the compensation factor for the n^{th} sample is $e^{-j2\pi\frac{n\varepsilon}{N_C}}$.

2.2.3 Frequency Offset Estimation

The two most renowned frequency offset estimation techniques for the forward link do not require any pilot symbol transmission. The first technique exploits the duplicate structure of the cyclic prefix, whereas the other technique makes use of the unmodulated subcarriers, being use in the practical systems.

2.2.3.1 Cyclic Prefix Based Frequency Offset Estimator

Because of the cyclic prefix, the first part with duration T_{CP} seconds of each multicarrier symbol is identical to the last part. This property can be exploited for frequency offset estimation. The estimator correlates a T_{CP} long part of the signal with a part that is T_B seconds delayed. The phrase of the correlation output is equal to the phase drift between samples that are T_B seconds apart. Hence, the estimate of frequency offset can simply be obtained as the correlation phrase

divided by $2\pi T_B$:

$$\frac{1}{2\pi T_B}\tan^{-1}\left(\int_0^{T_{CP}} r\left(t-\tau\right) r\left(t-T_B-\tau\right)^* d\tau\right). \tag{2.31}$$

The accuracy of the cyclic prefix based method could not be guaranteed for multipath fading channels as the ISI disrupts parts of the cyclic prefix. The cyclic prefix based estimator can be improved by considering the channel impulse response length [40, 41]. This improved scheme requires that the cyclic prefix is strictly longer than the channel delay spread and, that the exact channel order is known.

2.2.3.2 Virtual Carrier Based Frequency Offset Estimator

This method takes advantage of the inherent null, or virtual, subcarriers to enforce frequency synchronization. Even though the presence of virtual subcarriers can be seen as the transmission of known (null) symbols, there is a practical difference because the transmission of null symbols does not imply any lost of power. Furthermore, null subcarriers are intrinsically present in any nonfully loaded multicarrier systems. The basic idea for the virtual carrier based approach is simple. The algorithm measures the average power in the virtual subcarriers and updates the oscillator frequency (or equivalently update the frequency offset compensation factors) until the algorithm reaches the minimum measured energy. Ideally, in the system with perfect frequency synchronization and without noise, a null energy should be observed from the virtual subcarriers. If some power is detected, the algorithm will adjust the oscillator frequency in order to minimize such energy. Following the average power cost function, the conventional steepest gradient descent algorithm is applied.

2.2.4 Channel Estimation

For packet transmission as in a wireless LAN, each packet starts with special pilot multicarrier symbols for which all data values are known. These pilot multicarrier symbols are used to obtain channel estimates. There is no spreading process for pilot symbols at each subcarrier and the pilot symbols are common for all the users. In order to perform channel estimation, frequency offset has to be compensated. Then, by assuming that the frequency offset correction is perfect, the $\left(n'\right)^{th}$ DFT output entry during the pilot period is given in the same way as in (2.24) as following

$$x^i\left[n'\right] = \beta_{k,p,D}^{i,n',m}\bar{b}_p^i\left[n'\right] + \bar{\eta}^i\left[n'\right] \tag{2.32}$$

where $\bar{b}_p^i\left[n'\right]$ is a pilot symbol at the $\left(n'\right)^{th}$ subcarrier. The subcarrier coefficient estimate, $\hat{\beta}_{k,p,D}^{i,n',m}$, can basically be obtained by

$$\hat{\beta}_{k,p,D}^{i,n',m} = x^i\left[n'\right]/\bar{b}_p^i\left[n'\right]. \tag{2.33}$$

The subcarrier coefficient estimates can be further refined by using the Wiener filtering which exploits time-frequency correlation statistics [66]. Unfortunately, the information of channel

correlation statistics is usually unknown. In [67], the robust technique, which is independent of channel statistics, was proposed. The robust technique uses 2-D DFT and IDFT with diamond shape filter.

2.3 Receivers for the OFDM System with Insufficient Cyclic Prefix

The insufficient cyclic prefix problem has been addressed in the OFDM context by many authors. A number of approaches have been proposed to alleviate such problem. These approaches can be divided into 2 main categories, an impulse response shortening approach and a decision feedback equalization (DFE) approach.

2.3.1 Impulse Response Shortening Technique

For the impulse response shortening technique, a shortened impulse response filter (SIRF) is placed following the analog-to-digital (A/D) converter as shown in figure 2.6. The purpose of this filter is to shorten the impulse response of the effective channel, which is the convolution of physical channel and SIRF, to be shorter than the length of the cyclic prefix. In [26], a traditional least squares algorithm was proposed to fit a pole-zero model to the channel impulse response. The channel impulse response is assumed to be represented as a transfer function

$$h\left(z^{-1}\right) = \frac{a\left(z^{-1}\right)}{1 + b\left(z^{-1}\right)}. \tag{2.34}$$

If the poles of the model, $1 + b\left(z^{-1}\right)$, are used as the SIRF coefficients, the SIRF cancels the poles of the physical channel, leaving the zeros of the model. If the number of zeros are chosen to be less than the cyclic prefix duration, the effective impulse response will be shorter than the length of cyclic prefix. Reference [29] reviewed other criteria for designing the filter. The impulse response shortening approach sometimes suffers from slow convergence and noise amplification. Therefore, this technique has not received much interest.

2.3.2 Decision Feedback Equalization Technique

The alternate DFE approach allows the ISI and ICI due to the insufficient cyclic prefix to occur. Then, the receiver later eliminates the ISI and ICI before the symbol detection. Several DFE based techniques have been proposed in the past literatures. These techniques share the common ISI cancellation structure in the feedback part but they differ in the ICI compensation strategy which is governed by the feed-forwarded part. In the ISI cancellation part, the ISI replica is constructed from the previously detected symbols and the channel impulse response. Then the ISI replica is subtracted from the received signal.

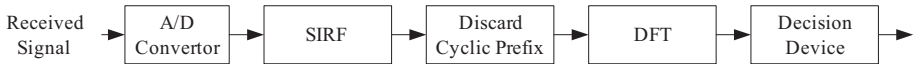

Figure 2.6 Block diagram of impulse response shortening technique

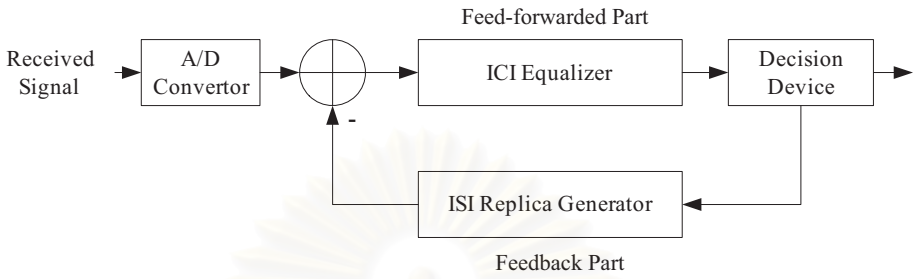

Figure 2.7 Block diagram of decision feedback equalization technique

2.3.2.1 Minimum Mean Square Error ICI Compensation

In [27,28], The ICI is equalized by using the MMSE criteria. The DFE in [27,28] is directly applied to the A/D output samples. The entire process does not involve the DFT for multicarrier demodulation. The work in [29] also optimizes the feed-forward filter by using the MMSE criteria but the DFE is operated in the frequency domain (after the DFT). In fact, the DFE in [27, 28] is an equivalent form of the DFE in [29] by incorporating the DFT matrix into the feed-forwarded matrix and the feedback matrix.

2.3.2.2 Cyclic Reconstruction ICI Compensation

In [31], the ICI is mitigated by using the non-linear approach. After the ISI cancellation process, the resulting sequence is converted into frequency domain by using the DFT and symbol decisions are made. Afterwards, the detected symbols are used in the cyclic reconstruction process. The cyclic reconstruction process simulates the cyclic prefix, manipulated by the channel impulse response. The part of the missing cyclic prefix is then reconstructed and added back to the ISI cancelled sequence. If the reconstruction is perfect, the sequence is virtually of sufficient cyclic prefix. In practical, the accuracy of the reconstruction in the first iteration is not good due to the ICI. After the reconstruction, the ICI power is partially suppressed, hence; the decision based on the DFT of the reconstructed sequence is more reliable. The improved decisions are then used in the cyclic reconstruction process for the next iteration.

2.3.2.3 Windowed Maximum Likelihood Sequence Estimator ICI Compensation

The optimal maximum likelihood sequence estimator (MLSE) was explored in [30] for the symbol detection under the presence of ICI. It is well recognized that the complexity of the MLSE is very large and exponentially increases with a number of subcarriers. This complexity burden issue has been cited in [27, 28] and motivated the authors of [27, 28] to the MMSE approach. In [30], this complexity is substantially reduced by using the windowing technique. The windowing technique can suppress the sidelobe spectrum which results in a reduced number of subcarriers affecting the desired subcarrier. Also, [30] claimed that only two adjacent subcarriers of the desired subcarrier have substantial influence and require consideration.

2.4 Receivers for the Reverse Link MC-CDMA System

2.4.1 Conventional Channel Estimation Technique for Reverse Link

Similar to the forward link, the channel impulse response has to be estimated for enabling the coherent reception in the reverse link. The sufficient cyclic prefix condition and the perfect frequency synchronization simplify the requirement of channel impulse response information to only the subcarrier coefficient estimates. The major difference between the forward link and the reverse link is that signals of each user in the forward link share the same physical channel, but, for the reverse link, they experience different channel fading. The pilot symbols for the reverse link need some degree of orthogonality to decoupling each user's signal. The conventional channel estimation technique for the reverse link [68] uses the pilot OFDM modulated symbols, inserted in a preamble of a packet frame. A set of orthogonal sequences, such as Walsh-Hadamard sequences having length of at least N_U, is served as pilot sequences in order for the estimator to separate N_U dimensional signal simultaneously arriving at the receiver. A unique sequence from the set of orthogonal sequences is assigned to each user. During a pilot period, each pilot OFDM modulated symbol contains the same chip of the given sequence in all subcarriers. The estimation process is carried out after a DFT block. For estimation of a desired subcarrier coefficient of a desired user, DFT outputs corresponding to the desired subcarrier during a pilot period are multiplied by respective chips of the user's pilot sequence. Then the resulting sequence is integrated and normalized. This estimation process is repeated for all subcarriers and all users.

In [69], a sampled spaced channel impulse response estimator was proposed. This estimator considers the time-domain equivalent samples, which is the IDFT of the subcarrier coefficients. Only some of the time-domain samples, which have relatively high amplitudes, are estimated. These desired samples are usually some of the first samples and some of the last samples. The estimated time-domain samples are converted to the subcarrier coefficients by taking DFT. This channel estimation technique can reduce a number of parameters to be estimated but its accuracy is substantially degraded due to the negligent of some time-domain samples. Moreover, it can

support only few concurrent users.

2.4.2 Recursive Estimation of Channels and Frequency Offsets Based on the Extended Kalman Filter

In the reverse link, the problem of frequency offsets is much more complicated than the forward link because each user has different frequency offset value. A simple channel estimator, as described in the previous subsection, suffers from the ICI and cannot estimate the frequency offsets. Even in a case that perfect knowledge of frequency offsets is available, the frequency synchronization is impossible because the correction of one user frequency offset would misalign the others.

In [52], a technique for jointly estimating channels and frequency offsets under the sufficient cyclic prefix condition was proposed. The work in [70], which considers the estimation of the frequency offset in a single user system by using an extended Kalman filter, was extended to a multiuser system in [52]. The extended Kalman filter is used because the observation is a non-linear function with respect to the frequency offsets. A state-space equation is assumed to be a simple first order equation and an observation equation is formulated similar to (2.15)-(2.21).

The disadvantages of the EKF based estimator are that it has slow convergence rate in the system with large number of users and it can easily be trapped in the saddle points.

2.4.3 Frequency Offset Compensated Minimum Mean Square Error Detector

In [49, 50], the authors proposed a receiver based on the MMSE criterion for the reverse link MC-CDMA system with frequency offsets. The cyclic prefix is assumed to be longer than the maximum channel delay. The receiver capitalizes on the sub-band structure of the CSA scheme to reduce the complexity. Only the subcarriers, being used for transmitting the considered parallel symbol, are involved in the detection of the considered parallel symbol. Block diagram of the frequency offset compensated MMSE detector is similar to a combining technique (figure 2.5) with only difference in the derivation of the combining weights. Since the cyclic prefix is longer than the maximum channel delay, equation (2.15) is simplified as

$$x^i\left[n'\right] = \sum_{k=0}^{N_U-1}\sum_{p=0}^{N_P-1} \bar{c}^{i,n'}_{k,p,D} b^i_{k,p} + \bar{\eta}^i\left[n'\right]. \tag{2.35}$$

From the above equation, the DFT outputs associated with the p^{th} parallel symbol, $pN_S \leq n' < (p+1)N_S$, can be written in the matrix notation as

$$\mathbf{x}^i_p = \sum_{p'=0}^{N_P-1} \bar{\mathbf{C}}^i_{p',p,D}\mathbf{b}^i_{p',D} + \bar{\eta}^i_p \tag{2.36}$$

where

$$\mathbf{x}^i_p = \left[\begin{array}{cccc} x^i\left[pN_S\right] & x^i\left[(pN_S)+1\right] & \cdots & x^i\left[(p+1)N_S-1\right] \end{array}\right]^T, \tag{2.37}$$

$$\bar{\eta}_p^i = \left[\begin{array}{cccc} \bar{\eta}^i\left[pN_S\right] & \bar{\eta}^i\left[(pN_S)+1\right] & \cdots & \bar{\eta}^i\left[(p+1)N_S-1\right] \end{array} \right]^T, \tag{2.38}$$

$$\mathbf{b}_{p',D}^i = \left[\begin{array}{cccc} b_{0,p'}^i & b_{1,p'}^i & \cdots & b_{N_U-1,p'}^i \end{array} \right]^T, \tag{2.39}$$

and

$$\bar{\mathbf{C}}_{p',p,D}^i = \left[\begin{array}{cccc} \bar{c}_{0,p',D}^{i,pN_S} & \bar{c}_{1,p',D}^{i,pN_S} & \cdots & \bar{c}_{N_U-1,p',D}^{i,pN_S} \\ \bar{c}_{0,p',D}^{i,pN_S+1} & \bar{c}_{1,p',D}^{i,pN_S+1} & \cdots & \bar{c}_{N_U-1,p',D}^{i,pN_S+1} \\ \vdots & \vdots & \ddots & \vdots \\ \bar{c}_{0,p',D}^{i,(p+1)N_S-1} & \bar{c}_{1,p',D}^{i,(p+1)N_S-1} & \cdots & \bar{c}_{N_U-1,p',D}^{i,(p+1)N_S-1} \end{array} \right]. \tag{2.40}$$

The frequency offset compensated minimum mean square error detector has the form

$$\hat{\mathbf{b}}_{p,D}^i = D\left(\left(\mathbf{W}_{p,FO-MMSE}^i\right)^H \mathbf{x}_p^i\right) \tag{2.41}$$

where $\mathbf{W}_{p,FO-MMSE}^i$ is the weight matrix of the frequency offset compensated MMSE detector. The weight matrix is designed to minimize the following error function:

$$E\left\{\left|\left(\mathbf{W}_{p,FO-MMSE}^i\right)^H \mathbf{x}_p^i - \mathbf{b}_{p,D}^i\right|^2\right\}. \tag{2.42}$$

By applying the orthogonal principle, the weight matrix is derived as

$$\mathbf{W}_{p,FO-MMSE}^i = \left(\mathbf{R}_{p,D}^i\right)^{-1} \bar{\mathbf{C}}_{p,D}^i \tag{2.43}$$

where

$$\begin{aligned} \mathbf{R}_{p,D}^i &= E\left\{\mathbf{x}_p^i \left(\mathbf{x}_p^i\right)^H\right\} \\ &= \sum_{p'=0}^{N_P-1} \bar{\mathbf{C}}_{p',p,D}^i \left(\bar{\mathbf{C}}_{p',p,D}^i\right)^H + N_C\left(\sigma_\eta\right)^2 \mathbf{I} \end{aligned}. \tag{2.44}$$

2.4.4 Truncated Time-Domain Minimum Mean Square Error Multiuser Detector

This receiving technique was proposed in [34] for the reverse link MC-CDMA system without cyclic prefix. The frequency synchronization is assumed to be perfect. The MC-CDMA system without cyclic prefix is interpreted as an equivalent time-domain ISI-corrupted DS-CDMA system. The considered MC-CDMA system does not have serial to parallel conversion process ($N_P = 1$). In the equivalent time-domain model (see also figure 2.8), the IDFT of a signature sequence can be regarded as a time-domain signature sequence similar to the DS-CDMA system. The time-domain signature sequence propagates through a physical channel, which distorts and prolongs the original signal. The extended signal duration will overlap with the following symbol interval resulting in ISI. With aid of the cyclic prefix, the ISI is discarded along with the part of useful signal during the cyclic prefix interval.

The truncated time-domain MMSE multiuser detector discards part of the signal affected by the ISI. This part can be either the cyclic prefix or the normal signal. For the system without cyclic prefix, the discarded part is purely the normal signal. The remaining time-domain signature sequence is used in the MMSE multiuser detector [55].

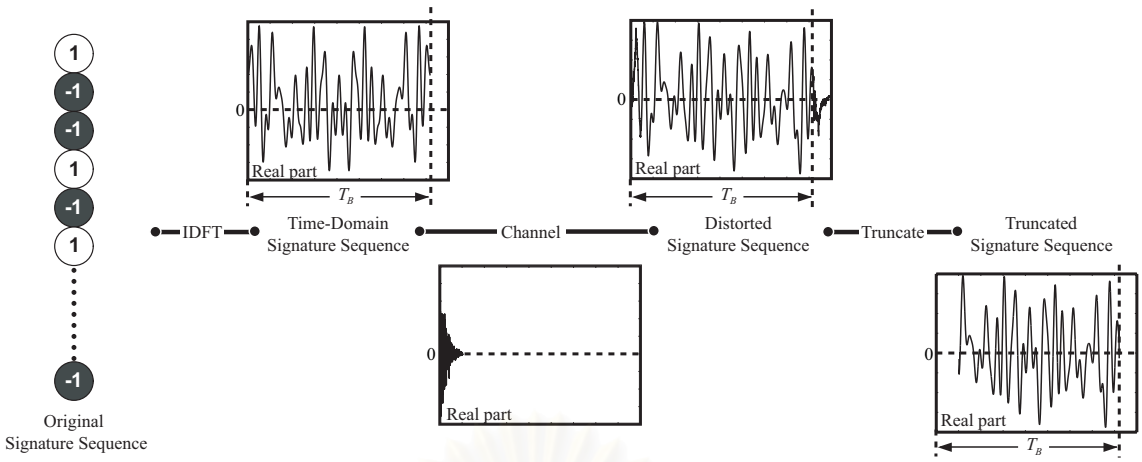

Figure 2.8 Block diagram of the truncated time-domain MMSE multiuser detector

The major disadvantage of this technique is the requirement of channel impulse response information. Since the system does not have cyclic prefix, the conventional channel estimation technique, which targets the subcarrier coefficients, cannot be applied. The other drawback of this technique is due to the discarding of the part of the useful signal resulting in lower signal to noise ratio. The derivation of this technique is on the time-domain. The time-domain processing cannot distinguish multiple frequency-domain parallel symbols, transmitted at the same time. In order to apply this technique to a system with serial to parallel conversion process, a truncated time-domain signature sequence has to be transformed into frequency-domain by taking the DFT. Similar MMSE multiuser detection technique can directly be applied to the frequency-domain versions of the signature sequences. The frequency-domain implementation will be referred as the modified truncated time-domain MMSE multiuser detector.

2.4.5 Minimum Mean Square Error Decision Feedback Equalizer

Similar to the truncated time-domain MMSE multiuser detector, the MMSE-DFE [35] was originally proposed for the system with no serial to parallel conversion and perfect frequency synchronization. The MMSE-DFE uses the feedback ISI cancellation process to remove the ISI instead of discarding the ISI affected part. Even though the MMSE-DFE does not explicitly use the MMSE multiuser detector, the derivation based on the MMSE criterion leads the feed-forwarded part to be the MMSE multiuser detector. Therefore, the MMSE-DFE and the truncated time-domain MMSE multiuser detector are only different in the ISI removal strategies.

The implementation of the MMSE-DFE is also obstructed by the requirement of channel impulse response estimation. However, the MMSE-DFE does not require knowledge about maximum channel delay and has more efficient power utilization than the truncated time-domain MMSE multiuser detector.

CHAPTER III

MULTIUSER DETECTION WITH INTERSYMBOL INTERFERENCE CANCELLATION

From the models described in the previous chapter, a key idea and the foundation of the MUD-ISIC will be presented in this chapter. Having difference from other known techniques, the MUD-ISIC provides a unified approach in suppressing the MAI, cancelling the ISI, and compensating the frequency offsets. At the end of this chapter, the simulation results, demonstrating the merits of the MUD-ISIC over the other existing techniques under the same assumption of perfect parameter information, will be presented.

3.1 Motivation

From (2.16), the estimate of ISI, generated by using the previously detected symbols, may be subtracted from the DFT output to yield the ISI free sequence. The detector is then applied to the ISI cancelled sequence to detect all the $N_U N_P$ transmitted symbols. The detector may be performed in a full band manner so that all the $N_U N_P$ transmitted symbols are simultaneously detected. In such approach, all the $N_U N_P$ transmitted symbols are regarded as virtual $N_U N_P$ distinct users and each virtual user occupies the entire N_S subcarriers. For the full band scheme, $2N_U N_P N_C$ parameters, which are $\bar{c}_{k,p,D}^{i,n'}$ and $\bar{c}_{k,p,I}^{i,n'}$ for $0 \leq n' \leq N_C - 1$, $0 \leq k \leq N_U - 1$, and $0 \leq p \leq N_P - 1$, have to be estimated. This requirement implies the demand for large number of pilot symbols, which would incur several disadvantages such as loss of bandwidth efficiency, loss of power, etc. The work in this dissertation will adopt the alternative sub-band approach, which exploits a sub-band structure of the CSA scheme. In the sub-band technique, the cross parallel symbol interference is neglected so that the detection of the desired parallel symbol is independent of the detection of other parallel symbols. The N_C entries of the ISI removed sequence are grouped into N_P groups, each of which is processed by a dedicated detector. Each detector is designated for the detection of N_U transmitted symbols. For the sub-band technique, all the N_P detectors requires estimation of only $2N_U N_P N_S$ parameters, which are $\bar{c}_{k,p,D}^{n'}$ and $\bar{c}_{k,p,I}^{n'}$ for $0 \leq n' \leq N_S - 1$, $0 \leq k \leq N_U - 1$, and $0 \leq p \leq N_P - 1$. The number of required parameter for the sub-band scheme is less than that required for the full band detector by a ratio of N_P. It should be noted that guard subcarriers may be inserted between the group of subcarriers assigned to each parallel symbol to maintain the power of cross parallel symbol interference at the negligible level. The graphical diagrams of the full band detector and the sub-band detector are shown in figure 3.1. Figure 3.2 shows the average leakage power from the 3^{th} parallel symbols to all the subcarriers due to the frequency offsets and the insufficient cyclic prefix for the CSA

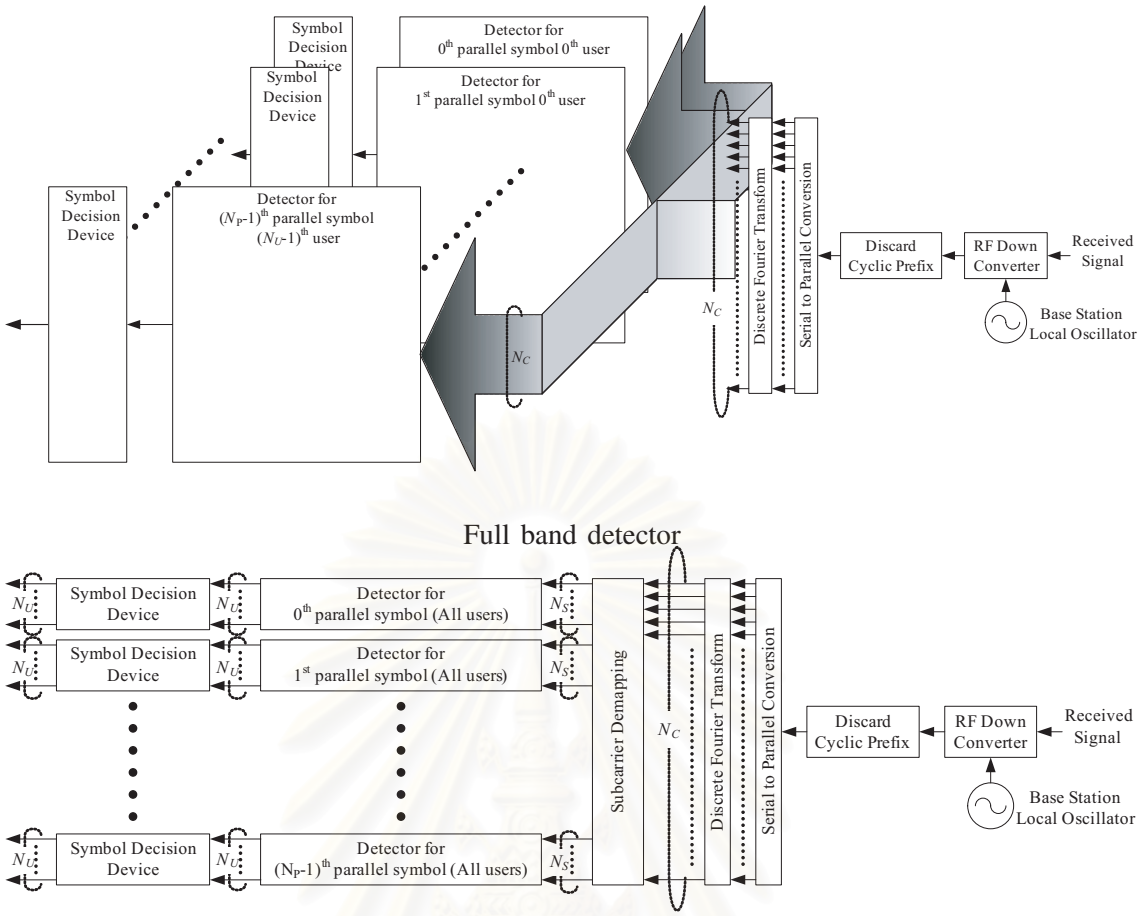

Figure 3.1 BER versus CP duration

scheme. For the plot of figure 3.2, the frequency offset normalized by carrier spacing is assumed to be the normal distributed random variable with variance 0.5, the channel is 12 paths with equal mean power, and the multicarrier signal is transmitted without cyclic prefix.

For a quantitative example, a reverse link MC-CDMA system in [49, 50] is considered. The key parameters for this system are $N_S = N_U = N_P = 16$ and $N_C = N_S N_P = 256$. Therefore, $2N_U N_P N_C = 131072$ parameters are needed for the full band detector and $2N_U N_P N_P = 8192$ parameters are needed for the sub-band detector. For the least squares estimator, which will be presented in the next chapter, the full band scheme requires 257 pilot MC-CDMA symbols whereas the sub-band scheme only requires 33 pilot MC-CDMA symbols. This difference emphasizes the necessity of the sub-band approach.

Considering the sub-band detection of the p^{th} parallel symbols, the N_S DFT output entries, $x^i[n']$ for $pN_S \leq n' < (p+1)N_S$, are fed into the detector. Next, the vector representation of the input of the detector is introduced to facilitate a receiver design.

Let

$$\mathbf{x}_p^i = \left[\begin{array}{cccc} x^i[pN_S] & x^i[(pN_S)+1] & \cdots & x^i[(p+1)N_S - 1] \end{array} \right]^T, \tag{3.1}$$

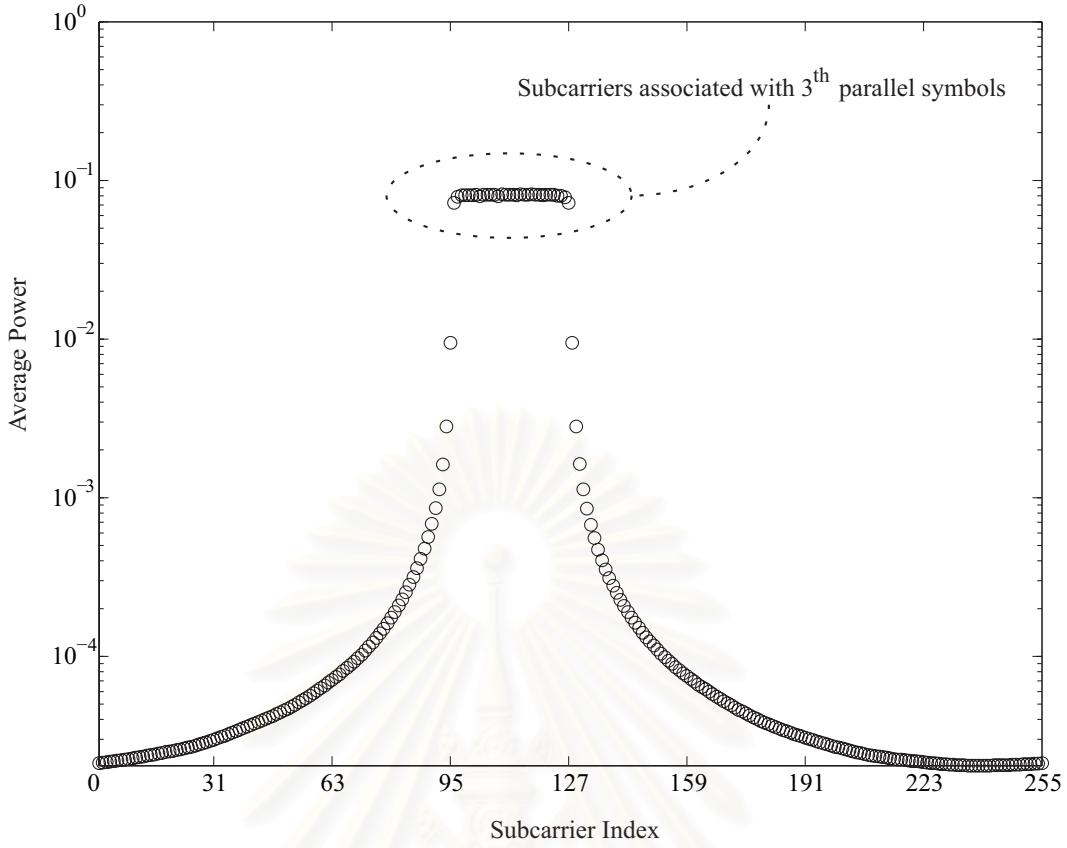

Figure 3.2: Average power spreading due to frequency offsets and insufficient cyclic prefix for the CSA scheme

$$\bar{\eta}_p^i = \left[\begin{array}{cccc} \bar{\eta}^i\left[pN_S\right] & \bar{\eta}^i\left[(pN_S)+1\right] & \cdots & \bar{\eta}^i\left[(p+1)N_S-1\right] \end{array} \right]^T, \tag{3.2}$$

$$\mathbf{b}_{p,D}^i = \left[\begin{array}{cccc} b_{0,p}^i & b_{1,p}^i & \cdots & b_{N_U-1,p}^i \end{array} \right]^T, \tag{3.3}$$

$$\mathbf{b}_{p,I}^i = \left[\begin{array}{cccc} b_{0,p}^{i-1} & b_{1,p}^{i-1} & \cdots & b_{N_U-1,p}^{i-1} \end{array} \right]^T, \tag{3.4}$$

$$\bar{\mathbf{c}}_{k,p,D}^i = \left[\begin{array}{ccc} \bar{c}_{k,p,D}^{i,pN_S} & \bar{c}_{k,p,D}^{i,(pN_S)+1} & \cdots \quad \bar{c}_{k,p,D}^{i,(p+1)N_S-1} \end{array} \right]^T, \tag{3.5}$$

$$\bar{\mathbf{c}}_{k,p,I}^i = \left[\begin{array}{ccc} \bar{c}_{k,p,I}^{i,pN_S} & \bar{c}_{k,p,I}^{i,(pN_S)+1} & \cdots \quad \bar{c}_{k,p,I}^{i,(p+1)N_S-1} \end{array} \right]^T, \tag{3.6}$$

$$\bar{\mathbf{C}}_{p,D}^i = \left[\begin{array}{cccc} \bar{\mathbf{c}}_{0,p,D}^i & \bar{\mathbf{c}}_{1,p,D}^i & \cdots & \bar{\mathbf{c}}_{N_U-1,p,D}^i \end{array} \right], \tag{3.7}$$

and

$$\bar{\mathbf{C}}_{p,I}^i = \left[\begin{array}{cccc} \bar{\mathbf{c}}_{0,p,I}^i & \bar{\mathbf{c}}_{1,p,I}^i & \cdots & \bar{\mathbf{c}}_{N_U-1,p,I}^i \end{array} \right] \tag{3.8}$$

denote, respectively, a corresponding DFT output vector, a corresponding noise sample vector, an i^{th} symbol interval-p^{th} parallel symbol data vector, an $(i-1)^{th}$ symbol interval-p^{th} parallel symbol data vector, a shortened transformed signature sequence vector, a shortened ISI generation sequence vector, a shortened transformed signature sequence matrix, and a shortened ISI generation

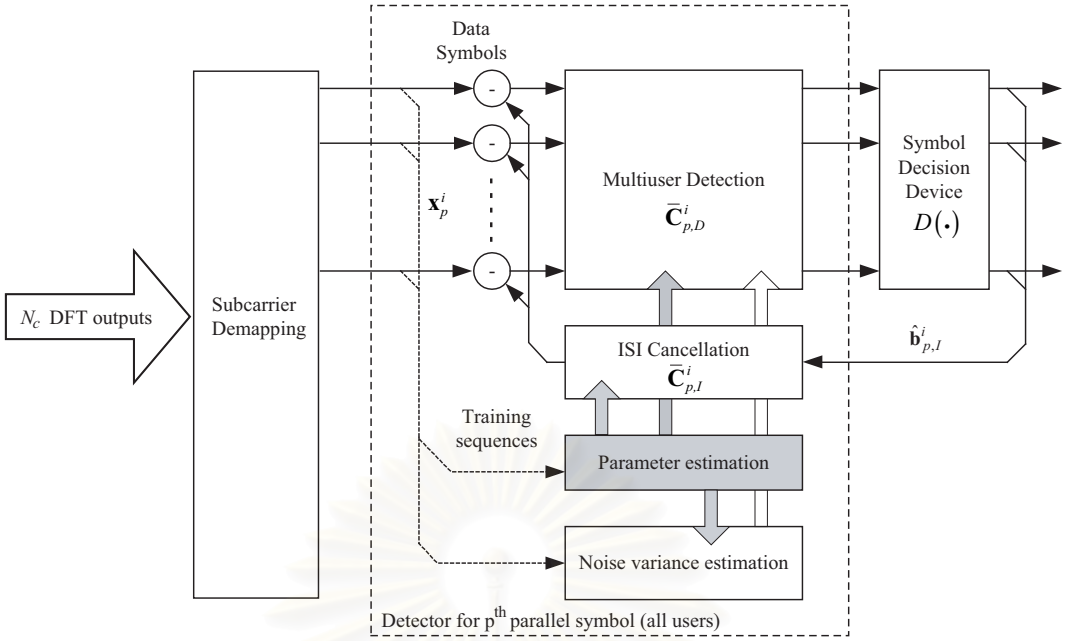

Figure 3.3 Block diagram of the MUD-ISIC

sequence matrix. By neglecting the cross parallel symbol interference terms, the corresponding DFT output vector is simplified as

$$\mathbf{x}_p^i = \bar{\mathbf{C}}_{p,D}^i \mathbf{b}_{p,D}^i + \bar{\mathbf{C}}_{p,I}^i \mathbf{b}_{p,I}^i + \bar{\eta}_p^i. \tag{3.9}$$

3.2 Receiver Design

A block diagram of the MUD-ISIC is depicted in figure 3.3. The MUD-ISIC is composed of an ISI cancellation part, a multiuser detection part, a parameter estimation part, and a noise variance estimation part. The ISI cancellation block is designed to remove the ISI introduced by the insufficient cyclic prefix condition. The multiuser detection block then gives the decision statistics from The ISI cancelled signal. The parameter estimator delivers the necessary parameters, which are the transformed signature sequences and the ISI generation sequence, to the others blocks whereas the noise variance estimator provides the statistical information of the background noise to the detector. The parameter estimation block and the noise variance estimation block will be presented in the next chapter.

From the previous section, an ISI term can be approximated by using the previously detected symbols as $\bar{\mathbf{C}}_{p,I}^i \hat{\mathbf{b}}_{p,I}^i$ where $\hat{\mathbf{b}}_{p,I}^i$ is a vector of these symbols. The approximated ISI term is then subtracted from the DFT output to yield the ISI free data as

$$\tilde{\mathbf{x}}_p^i = \mathbf{x}_p^i - \bar{\mathbf{C}}_{p,I}^i \hat{\mathbf{b}}_{p,I}^i. \tag{3.10}$$

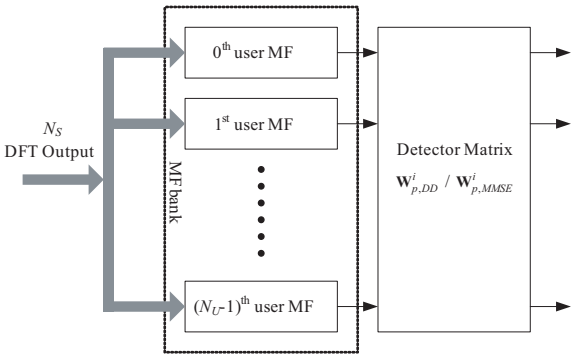

Figure 3.4 Linear detector

Assuming that the generation of the ISI replica is perfect, the resultant data can be expressed as

$$\tilde{\mathbf{x}}_p^i = \bar{\mathbf{C}}_{p,D}^i \mathbf{b}_{p,D}^i + \bar{\eta}_p^i. \tag{3.11}$$

3.2.1 Matched Filter

From (3.11), a vector of simple decision statistics is obtained by applying a matched filter (MF) bank to the ISI free vector:

$$\mathbf{y}_p^i = \left(\bar{\mathbf{C}}_{p,D}^i\right)^H \tilde{\mathbf{x}}_p^i. \tag{3.12}$$

Substituting (3.11) into (3.12) yields

$$\mathbf{y}_p^i = \mathbf{R}_{p,D}^i \mathbf{b}_{p,D}^i + \left(\bar{\mathbf{C}}_{p,D}^i\right)^H \bar{\eta}_p^i \tag{3.13}$$

where $\mathbf{R}_{p,D}^i = \left(\bar{\mathbf{C}}_{p,D}^i\right)^H \bar{\mathbf{C}}_{p,D}^i$ is a correlation matrix. The non-zero off-diagonal entries of the correlation matrix represent the MAI among all user signals [55]. This MAI raises the error probability of symbol decisions based on the MF outputs.

In order to improve the symbol detection accuracy, the MF outputs are further processed by the multiuser detectors, which suppress the MAI by exploiting the estimates of $\bar{\mathbf{C}}_{p,D}^i$. Various classes of multiuser detectors have been extensively explored in the past literatures. This dissertation will consider three well-known multiuser detectors, a linear decorrelating detector (DD), a linear minimum mean square error (MMSE) detector, and a weighted multistage interference cancellation (WMIC) detector. Figure 3.4 and figure 3.5 illustrate the block diagrams of linear multiuser detectors and WMIC detector, respectively.

3.2.2 Decorrelating Detector

For the DD, the improved decision statistics are obtained by multiplying a vector of MF bank outputs by a detector matrix $\mathbf{W}_{p,DD}^i$:

$$\begin{aligned} \mathbf{z}_p^i &= \mathbf{W}_{p,DD}^i \mathbf{y}_p^i \\ &= \mathbf{W}_{p,DD}^i \mathbf{R}_{p,D}^i \mathbf{b}_{p,D}^i + \mathbf{W}_{p,DD}^i \left(\bar{\mathbf{C}}_{p,D}^i\right)^H \bar{\eta}_p^i \end{aligned}. \tag{3.14}$$

The derivation of $\mathbf{W}^i_{p,DD}$ is based on the zero-forcing approach such that the product $\mathbf{W}^i_{p,DD}\mathbf{R}^i_{p,D}$ is forced to be an identity matrix. Thus, the detector matrix is given by

$$\mathbf{W}^i_{p,DD} = \left(\mathbf{R}^i_{p,D}\right)^{\dagger}. \tag{3.15}$$

As observed from (3.14), the drawback of the DD is the enlargement of noise variance by the detector matrix. The so-called noise enhancement effect degrades the performance of the DD.

3.2.3 Minimum Mean Square Error Detector

A structure of the linear MMSE detector is slightly different from the DD by only replacing matrix $\mathbf{W}^i_{p,DD}$ with matrix $\mathbf{W}^i_{p,MMSE}$. The linear MMSE detector matrix is designed to compromise the suppression of the MAI and the noise enhancement with the additional requirement of noise variance information. This requirement is a drawback when it is compared with the DD, which does not need any information about the noise variance. An error in the noise variance estimation may degrade the performance of the linear MMSE detector. The linear MMSE detector matrix is given by

$$\mathbf{W}^i_{p,MMSE} = \left(\mathbf{R}^i_{p,D} + N_C\left(\sigma_\eta\right)^2\mathbf{I}\right)^{-1}. \tag{3.16}$$

3.2.4 Weighted Multistage Interference Cancellation Detector

The WMIC is in a class of the non-linear MUD techniques. It has received considerable attention as an alternative to the linear approaches such as the DD and the linear MMSE detector. One of its major advantages is that it does not require a matrix inversion. Though the closed form analyses of the WMIC are intractable, the simulation results have supported its advantages over the linear counterparts [22, 33, 55]. A concept of one such stage of the WMIC is to generate the interfering signal replicas based on the estimated data from the previous stage and subtract them from the ISI free vector to obtain more reliable estimated data for the user of interest. The interfering signal replicas at each stage are multiplied by a weight factor before subtracting from the ISI free vector. This weight factor is used to alleviate the effect from incorrect interfering signal replicas, which are mainly caused from the wrong estimated data in the previous stage [71]. The weight factor reflects the confident level of the estimated data at each stage. In general, the reliability of the estimated data is improved at each stage. Therefore, the smaller weight factor values are usually used in the former stages [71]. The decision statistic of the k^{th} user symbol at the $\left(n_{IC}\right)^{th}$ stage is given by

$$z^i_{k,p,n_{IC}} = \left(\bar{\mathbf{c}}^i_{k,p,D}\right)^H\left\{\tilde{\mathbf{x}}^i_p - \sum_{\substack{\bar{k}=0\\ \bar{k}\neq k}}^{N_U-1}\bar{\mathbf{c}}^i_{\bar{k},p,D}\rho_{n_{IC}}D\left(z^i_{\bar{k},p,n_{IC}-1}\right)\right\} \tag{3.17}$$

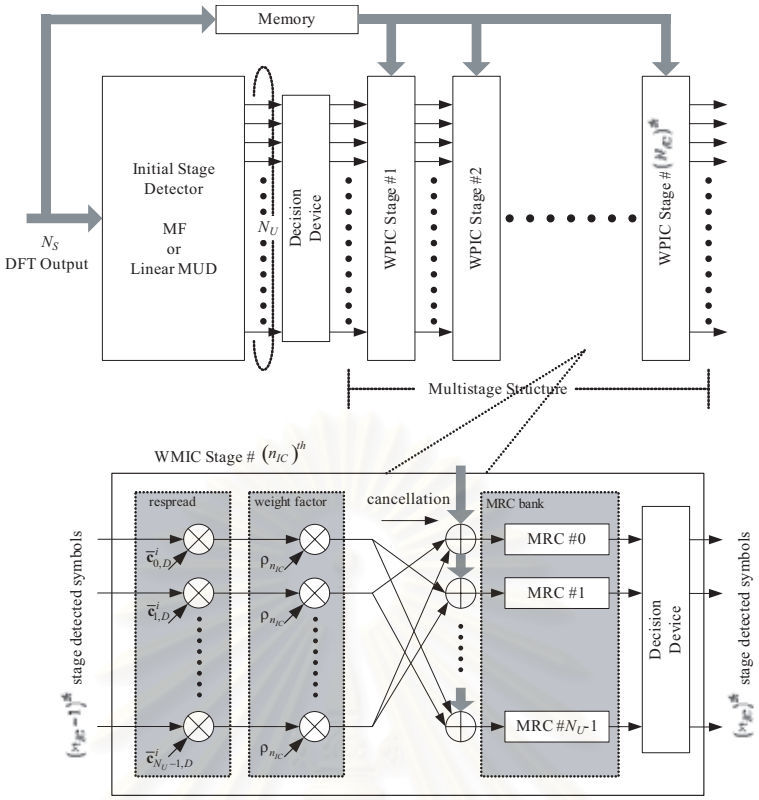

Figure 3.5 WMIC detector

where $\rho_{n_{IC}}$ is a weight factor of the $(n_{IC})^{th}$ stage and $D()$ is a quantizer used by a decision device. The estimated data at the initial stage are conventionally provided by the MF bank. The DD and the linear MMSE detector may also be employed following the MF bank to yield a more accurate symbol decision in the initial stage. However, it has to make a trade-off between the complexity burden and the performance improvement.

3.3 Simulation Results and Discussion

In this section, a bit error rate (BER) performance of the proposed receiver is evaluated and compared with other known techniques through the computer simulations. For all the simulations in this chapter, perfect knowledge of all the required parameters are provided to the receivers.

3.3.1 Simulation Configuration

The simulation parameters are summarized in Table 3.1. Many parameters, used in the simulations, are taken from [12, 72] where the practical MC-CDMA systems are considered. Each user is assigned a random binary signature sequence of length $N_S = 32$, which implies that each transmitted symbol occupies 32 subcarriers. The 40 MHz bandwidth is divided into N_C

Table 3.1 Simulation parameters

Bandwidth	40 MHz
Spreading factor (N_S)	32
Spreading sequence	Binary random sequence
Modulation	Quadrature phase shift keying (QPSK)
Cell	Macro cell (radius 1 km)
Maximum delay spread	1 μ sec
Maximum asynchronous delay	1 μ sec
Multipath intensity profile	Uniform, Exponentially decaying
Frequency offset variance	$\left(\sigma_{\Delta_f}\right)^2 = 62.5$ kHz

subcarriers, which is determined by a serial to parallel conversion size N_P and signature sequence length N_S as $N_C = N_P N_S$.

For the recent IEEE 802.11g standard, the specification for the oscillator stability is ± 25 ppm [73], which is equivalent to ± 62.5 kHz frequency offset for 2.5 GHz carrier frequency. In this dissertation, frequency offsets of each user are modeled as independent zero mean Gaussian random variables with variance $\left(\sigma_{\Delta_f}\right)^2 = 62.5$ kHz [49,50]. The acceptable level of the frequency offset for the conventional matched filter without frequency offset compensation is approximately 7 percent of the subcarrier spacing [63]. This requirement implies the frequency offset to be less than 10 kHz for the targeted system with subcarrier separation of 156.25 kHz. This consideration indicates that the experienced frequency offset of 62.5 kHz is far beyond the limitation and, thus, the special measures must be taken to handle the frequency offset.

In the future mobile communication systems, there will be strong potential for a microcell with a cell radius of less than 1 km in an urban area [12]. The microcell configuration allows the high data rate and high quality link with attainable transmission power. Therefore, the microcell model will be considered in the simulations. The maximum multipath delay for such model has been measured in Japan. From the field experiments, there was a report of an approximate 1 μ sec delay spread [12, 72]. Similar to [72], the simulated channel is modeled as 12 paths Rayleigh fading channel under the wide sense stationary uncorrelated scattering (WSSUS) assumption. Delay of the first path is fix at 0 μ sec and delays of the other paths are uniformly random in the 0 to 1 μ sec interval. Two different shapes of multipath intensity profile (MIP), i.e. exponentially decaying with 0.3 μ sec rms delay spread and uniform [12, 72], are assumed in the simulations.

A quasi-synchronous mechanism considered in this dissertation is realized by 2 techniques. For the first technique, every mobile user is provided a global positioning system (GPS) receiver, with the user bit epoch triggered by the GPS clock waveform [74]. If the distant to base station is unknown to the mobile station, the maximum time offset is determined by the cell size and the maximum GPS timing error. In this case, the maximum time offset is

$$\Delta_t = \pm \left(\frac{r}{2c} + 2T_{GPS} \right) \tag{3.18}$$

where r is a cell radius, c is the speed of light, and T_{GPS} is the maximum GPS timing error. If the distance to a base station is obtained by using the local GPS estimate of position and a database of base station coordinate, the maximum time offset is greatly reduced to

$$\Delta = \pm \left(\frac{P_{GPS}}{c} + 2T_{GPS} \right) \tag{3.19}$$

where P_{GPS} is a GPS position uncertainty. For the current GPS specifications [75, 76], the GPS timing error is approximately 0.1 μ sec and the GPS position error is approximately 20 m. As a consequence, the maximum time offset is approximately $\pm 1.86 \mu \sec$ and $\pm 0.26 \mu \sec$ for (3.18) and (3.19), respectively.

The other technique to attain the quasi-synchronous signaling is a closed loop timing synchronization technique [10]. For this technique, a mobile station monitors a special forward link channel. After the mobile station has detected the base station's timing, it immediately sends a packet to the base station through a special random access channel. The base station measures the time offset for the received packet and sends back the necessary timing advance to the mobile. There is currently no report on the achievable timing offset for this technique in the MC-CDMA system. However, it was reported the $\pm 0.40 \mu \sec$ timing offset in the DS-CDMA system using similar synchronization technique [77].

In this dissertation, the negative delay is pre-compensated. The additional pre-compensation for negative delay may slightly enlarge the timing offset. By considering the closed loop timing synchronization technique, the maximum $1.0 \mu \sec$ asynchronous delay is assumed in the simulations. The asynchronous delay for each user is independent and identically distributed between 0 and $1.0 \mu \sec$. By considering both the asynchronous delay and the channel delay spread, the maximum effective delay is $2.0 \mu \sec$.

3.3.2 Effect of Cyclic Prefix Insertion and Serial to Parallel Conversion

In the conventional sufficient cyclic prefix requisite systems, large amount of cyclic prefix must be added to compensate the channel delay spread and the asynchronous delay. To minimize the signal to noise ratio (SNR) loss caused by the introduction of cyclic prefix, it is desirable to have the symbol duration much larger than the cyclic prefix duration. In this sense, the large serial to parallel conversion size is needed to prolong the symbol duration. However, it cannot be arbitrarily large because the larger serial to parallel conversion size results in higher number of subcarriers, which means smaller subcarrier spacing, a larger implementation complexity, more sensitivity to frequency offset, as well as an increased peak-to-average power ratio (PAPR). This section presents the simulation results, showing an influence of cyclic prefix insertion and serial to parallel conversion. The ideal amplifier is assumed so that there is no effect from high peak-to-average power ratio.

Figure 3.6 shows BER of the MUD-ISIC as a joint function of cyclic prefix length (T_{CP}) and serial to parallel conversion size (N_P) in the system with perfect timing synchronization

(asynchronous delay = 0) for the uniform MIP and the exponentially decaying MIP. The linear MMSE detector is used in the multiuser detection part of the MUD-ISIC. It is seen from figure 3.6 that the lowest BER is achieved from $N_P = 6$ and $T_{CP} = 0\mu\,\mathrm{sec}$ for both the uniform MIP and the exponentially decaying MIP. Adding more cyclic prefix worsen the BER regardless of the serial to parallel conversion size. This result does not only demonstrate the robustness of the proposed detector against the insufficient cyclic prefix scenario but it also encourages a new system design where the insufficient cyclic prefix condition is intentionally enforced. For the system with small cyclic prefix length, increasing the serial to parallel conversion size degrades the BER. In contrast, the large serial to parallel conversion size is desirable in the system with large amount of cyclic prefix. Figure 3.7 compares the uniform MIP and the exponentially decaying MIP. As expected, the detector obviously gains from higher diversity of the uniform MIP. The BER is better for the uniform MIP than the exponentially decaying MIP.

Figure 3.8, where the system with imperfect timing synchronization (the maximum asynchronous delay is $1.0\mu\,\mathrm{sec}$) is considered, illustrates similar results as figure 3.6. The best BER is obtained from $N_P = 8$ and $T_{CP} = 0.5\mu\,\mathrm{sec}$ for the uniform MIP, whereas $N_P = 6$ and $T_{CP} = 0\mu\,\mathrm{sec}$ gives the lowest BER for the exponentially decaying MIP. The requirement of some cyclic prefix and moderate serial to parallel conversion size in the uniform MIP arises from the fact that asynchronous delay increases the level of useful power dissipating to the adjacent symbol. Small amount of cyclic prefix and moderate serial to parallel conversion size help storing useful power within the detection window. They also help reducing the ratio between the ISI power and the useful signal power. Note that with $T_{CP} = 0.5\mu\,\mathrm{sec}$, the considered system, having the maximum effective 2 $\mu\,\mathrm{sec}$ delay, still undergoes an insufficient cyclic prefix scenario. For the exponentially decaying MIP, the power of the high delay components is lower than that of the uniform MIP. Therefore, the power dissipation has less impact on the detector performance for the exponentially decaying MIP channel. As a result, the best BER is still achieved from the system without cyclic prefix.

The BER comparison between perfect and imperfect timing synchronization is shown in figure 3.9. As seen from the figure, a signal timing mismatch slightly increases BER of the system with small amount of cyclic prefix. It is worth to note that a research on timing synchronization is currently underway. In the future, as a cell size becomes smaller, a more accurate timing synchronization technique may be successfully developed. As a consequence, a small amount of cyclic prefix may not be required for a channel having relatively strong amplitude components at the high delay.

In figure 3.10, BER of the MUD-ISIC in the system with imperfect timing synchronization but perfect frequency synchronization ($\left(\sigma_{\Delta_f}\right)^2 = 0$) is presented. From the figure, similar results as in the case of imperfect frequency synchronization can be observed. The results in the optimistic perfect frequency synchronization case also favor the insufficient cyclic prefix scenario.

BER of the MUD-ISIC in the system with 16 concurrent users is presented in figure 3.11. The result is similar to that in figure 3.8 where the system with 8 active users is evaluated. The insufficient cyclic prefix condition is still needed for achieving the lowest BER. The effect from

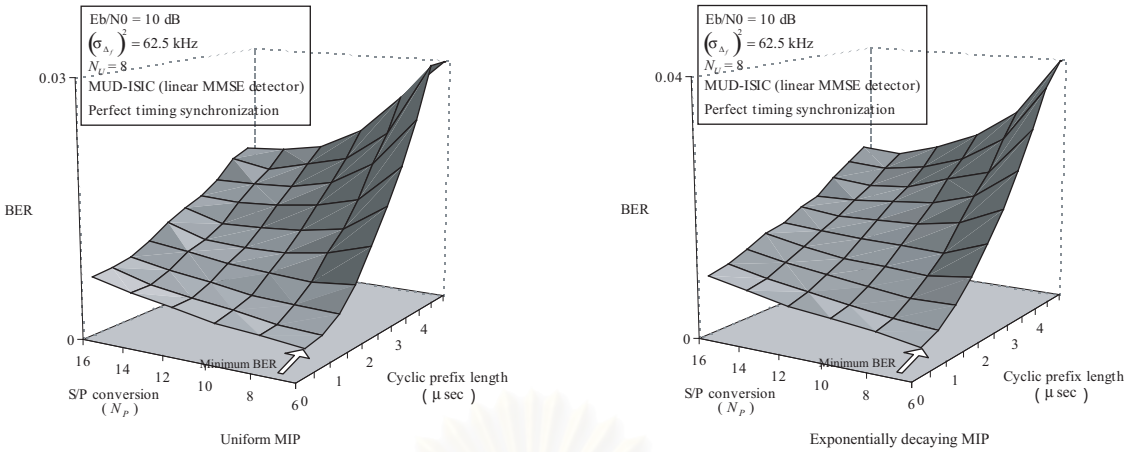

Figure 3.6 BER of the MUD-ISIC (perfect timing synchronization)

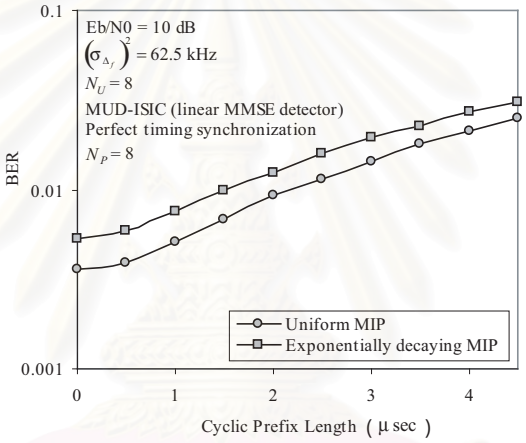

Figure 3.7 BER of the MUD-ISIC versus cyclic prefix length (perfect timing synchronization)

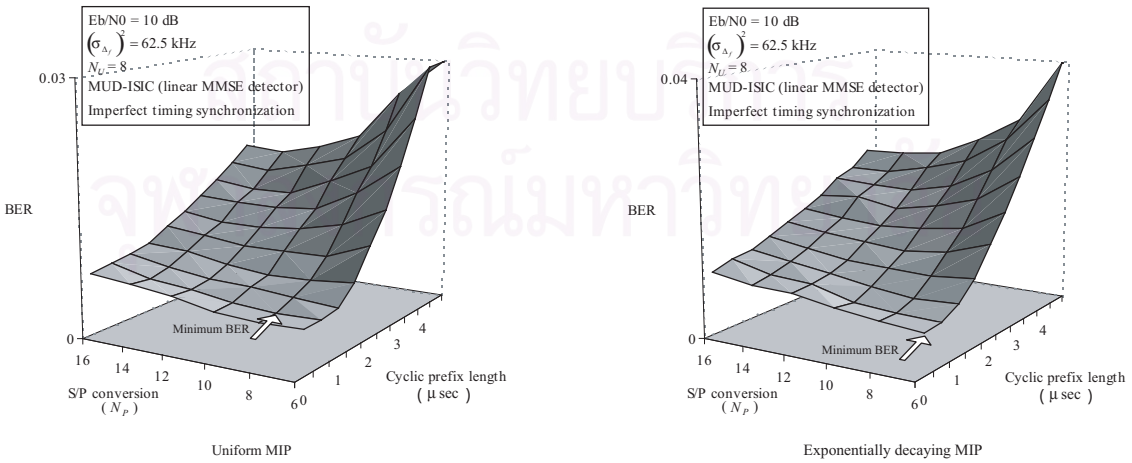

Figure 3.8 BER of the MUD-ISIC (imperfect timing synchronization)

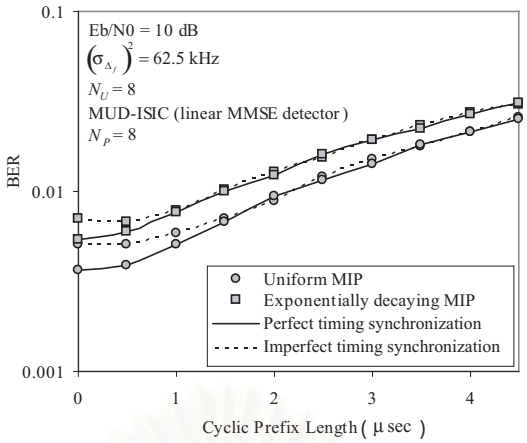

Figure 3.9 BER of the MUD-ISIC versus cyclic prefix length (imperfect timing synchronization)

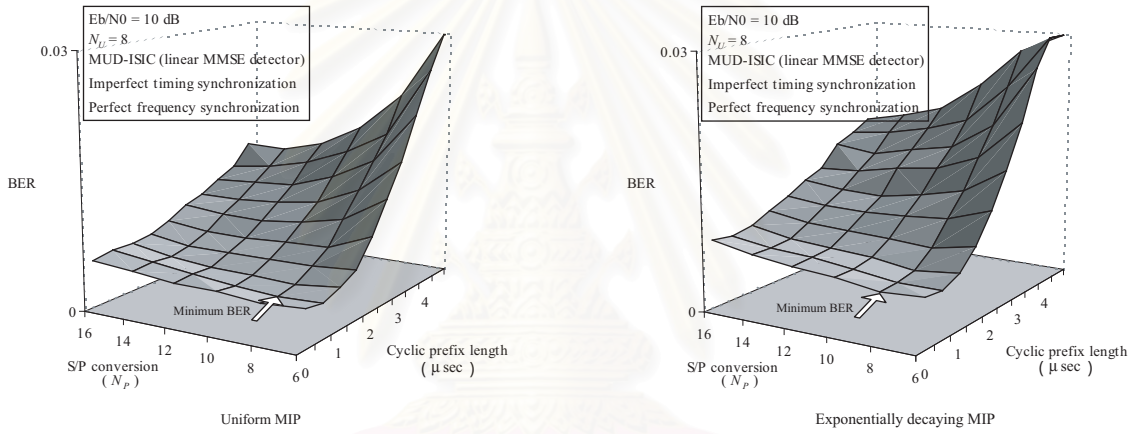

Figure 3.10 BER of the MUD-ISIC (perfect frequency synchronization)

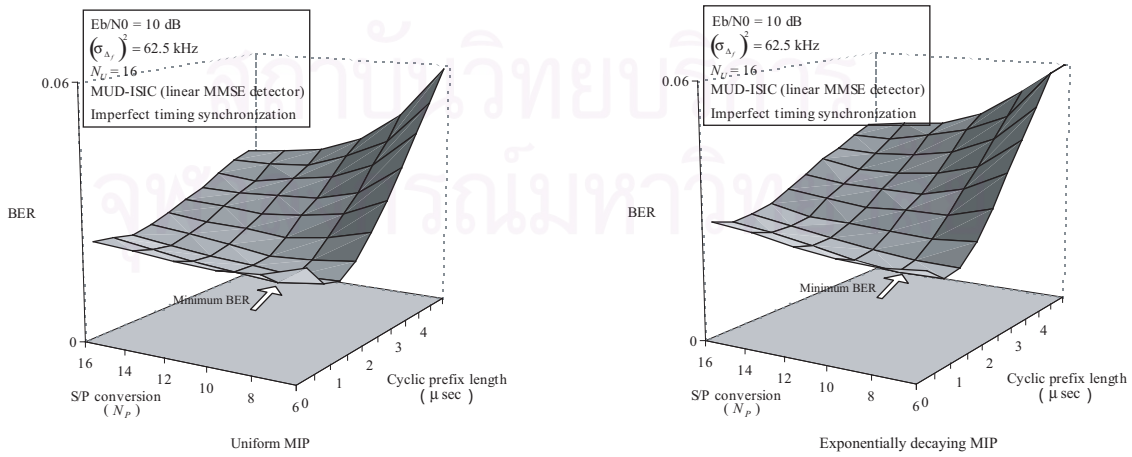

Figure 3.11 BER of the MUD-ISIC (16 users)

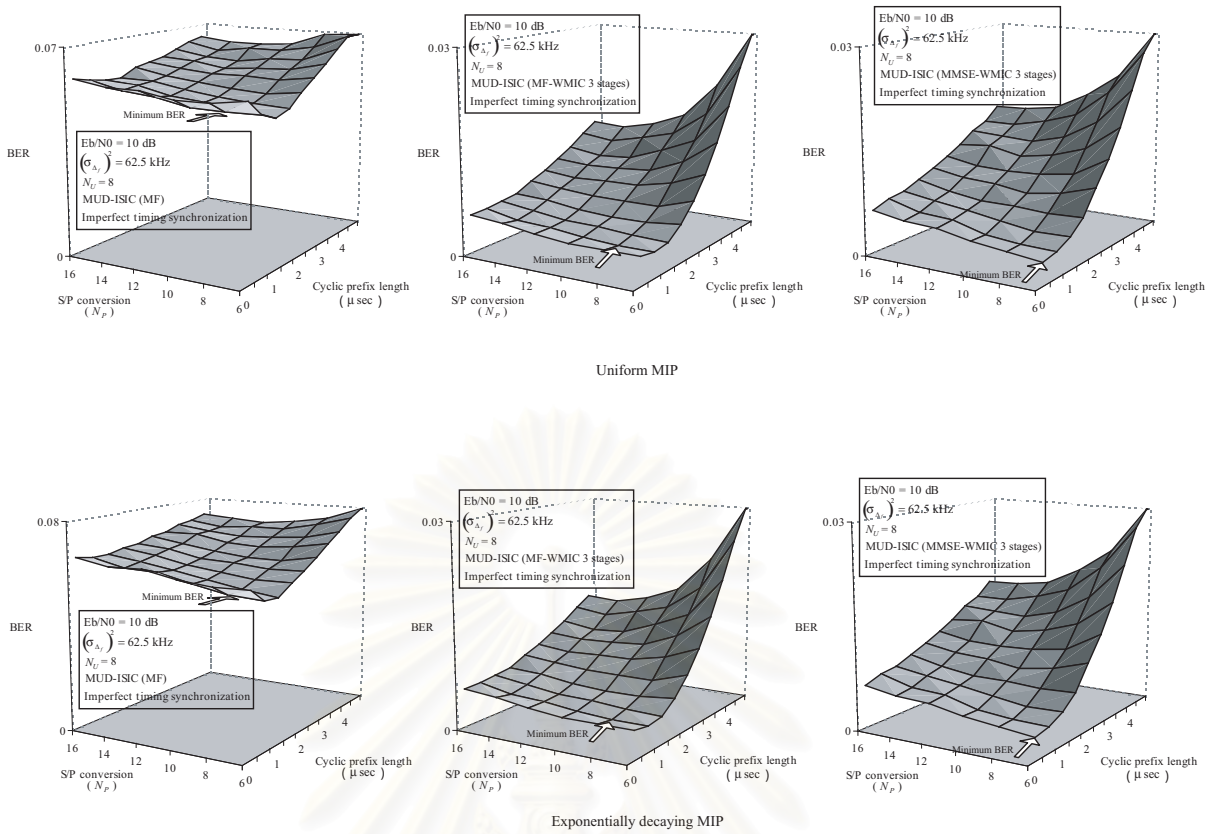

Figure 3.12: BER of the MUD-ISIC (using MF, MF-WMIC, and MMSE-WMIC in the multiuser detection part)

the useful power leakage is more obvious in the system with 16 users than the system with 8 users.

Figure 3.12 shows the BER of MUD-ISIC, using MF and WMIC in the multiuser detection part. Two different WMIC configurations are evaluated. For the first WMIC configuration, the MF is used for providing the initial decision data. The other WMIC configuration uses the linear MMSE detector to improve the accuracy of the initial data decision. Both WMIC detectors have 3 stages with unit cancellation weight for every stage. Comparing figure 3.12 with figure 3.8, both WMIC configurations as well as the MF concordantly favor the insufficient cyclic prefix condition. They are only different on the achievable BER.

3.3.3 Effect of Frequency Offset

An influence of the frequency offset to the system design and the performance of MUD-ISIC is presented in this section. The computer simulations were carried out by assuming imperfect timing synchronization. The considered MUD-ISIC employs the linear MMSE detector in its multiuser detection part. In figure 3.13, the BER is plotted as a function of the serial to parallel conversion size for $\left(\sigma_{\Delta_f}\right)^2 = 0$ kHz, $\left(\sigma_{\Delta_f}\right)^2 = 31.25$ kHz, and $\left(\sigma_{\Delta_f}\right)^2 = 62.5$ kHz. The figure shows that the BER is degraded by the increasing of the frequency offset variance. The

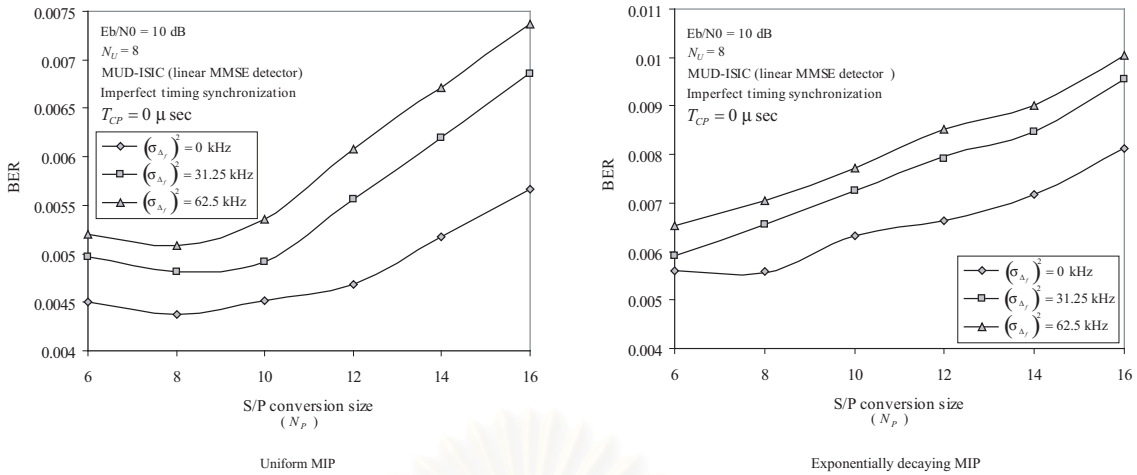

Figure 3.13 BER versus serial to parallel conversion size for various frequency offset variances

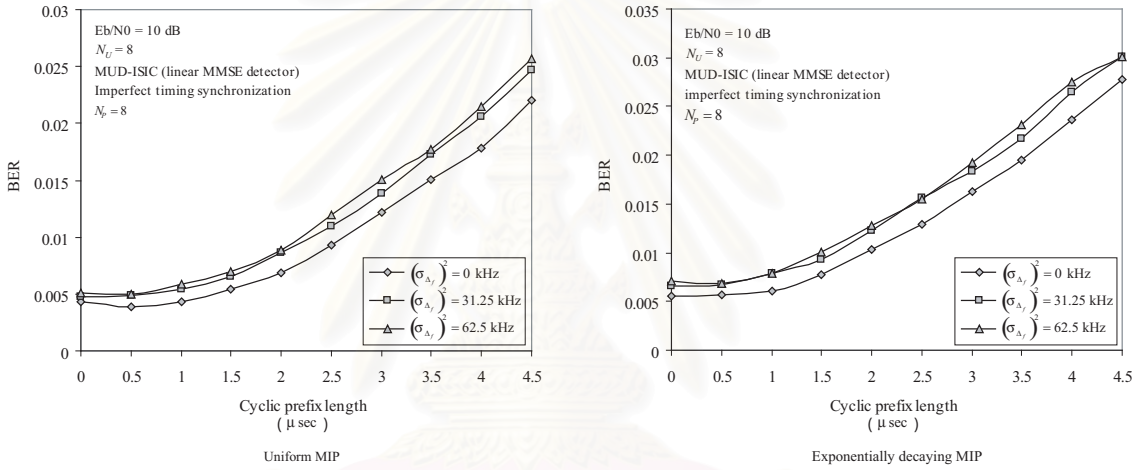

Figure 3.14 BER versus cyclic prefix length for various frequency offset variances

frequency offset has slightly more adverse impact on BER for the system with higher serial to parallel conversion size than the system with smaller serial to parallel conversion size. This is because the space between the subcarriers is closer for the system with larger serial to parallel conversion size. Figure 3.14 shows BER versus the cyclic prefix length for the system with 3 different frequency offset variances as in figure 3.13. As seen from the figure, introducing more cyclic prefix does not enhance the effect of the frequency offset to the achievable BER. Figure 3.15 plots BER as a function of frequency offset variance. The figure clearly shows the robustness of the proposed receiver to the frequency offset in the system with $N_P = 8$.

3.3.4 MUD-ISIC Employing Various Multiuser Detection Techniques

This section investigates the performance of various multiuser detection techniques, applied to the MUD-ISIC. The performance of MUD-ISIC, employing a simple MF, is also plotted as reference. The WMIC, having 3 stages, is considered. Two weight factor assignment schemes, all

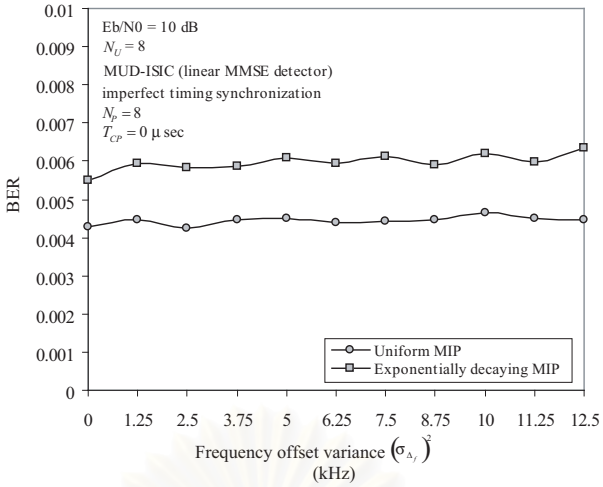

Figure 3.15 BER versus frequency offset variance

unit weight factor scheme and increasing weight factor scheme, are considered. Weight factors at each stage for both weight factor assignment schemes are given in table 3.2. The number of stages and weight factor assignment of the considered WMIC are based on the guideline in [71]. The work in [71] has shown that the WMIC is likely saturated after 3 stages. Adding more stage than 3 stages only incurs excessive complexity and delay with almost no improvement in BER. The work in [71] also demonstrated the advantages of the increasing weight factor scheme over the all unit weight factor scheme. Noted that the optimum weight factors in [71] and other reference works are obtained by trial and error experiments. The derivation of the optimum weight factor is very complicated because of the non-linear structure of the WMIC. Owing to this fact, the weight factors, used in this dissertation, are appropriated by following the recommendation in [71] but may not be the global optimum values. Several configurations of the WMIC are evaluated in the simulations. These configurations are summarized in table 3.3.

The MUD-ISIC receivers employing various multiuser detection techniques are compared in figure 3.16-3.19 for the uniform MIP channel and figure 3.20-3.23 for the exponentially decaying MIP channel. The MC-CDMA systems without cyclic prefix having 8, 16, 24, and 32 users are considered. The serial to parallel conversion size is set at 8.

From figure 3.16-3.23, the DD can perform well in a system with moderate number of users but it gives the worst result in a heavily loaded system (a number of users is comparable to a processing gain). In the system with 8 users (figure 3.16 and 3.20), the DD, which does not require an information about noise variance, can perform in the similar level as the linear MMSE detector. The susceptibility of the DD to the noise enhancement is more obvious in the system with higher number of users. The performance gap between the DD and the linear MMSE detector becomes significant in the low signal to noise ratio per bit (Eb/N0) region of the system with 16 users (figure 3.17 and 3.21). In the system with 24 users (figure 3.18 and 3.22), the DD requires Eb/N0 at least 10 dB and 8 dB to overcome the MF for the uniform MIP channel and exponentially decaying MIP channel, respectively. In addition, its performance is worse than that

of the linear MMSE detector for all the Eb/N0 range. The DD is totally inoperable in the system with 32 users (figure 3.19 and 3.23). The linear MMSE detector outperforms the MF regardless of the number of users and Eb/N0. It also performs better than the DD in almost cases. The performance of the DD is comparable to that of the MMSE detector in 8 and 16 users system at a high Eb/N0 region.

Table 3.2 Weight factors of WMIC used in the simulations

Weight factor assignment scheme	n_{IC}	$\rho_{n_{IC}}$
All unit weight factor scheme (1)	0	1.0
	1	1.0
	2	1.0
Increasing weight factor scheme (2)	0	0.6
	1	0.85
	2	1.0

Table 3.3 WMIC configuration

Name	N_{IC}	Initial stage	Weight factor
MF-WMIC.(1)	3	MF	All unit weight factor scheme
MF-WMIC.(2)	3	MF	Increasing weight factor scheme
DD-WMIC.(1)	3	DD	All unit weight factor scheme
DD-WMIC.(2)	3	DD	Increasing weight factor scheme
MMSE-WMIC.(1)	3	linear MMSE detector	All unit weight factor scheme
MMSE-WMIC.(2)	3	linear MMSE detector	Increasing weight factor scheme

The non-linear WMIC shows a very impressive performance. The MF-WMIC, which does not require a matrix inversion, can outperform the linear multiuser detectors (DD and linear MMSE detector) in many cases. The increasing weight factor scheme significantly improves the BER of the MF-WMIC over the all unit weight factor scheme. With the all unit weight factor scheme, the MF-WMIC can perform well only in the system with moderate number of users. In the system with large number of users, the MF provides erroneous initial symbol estimates. The cancellation based on the wrong initial symbol decisions injects additional interference to the received signal. A small weight factor in the early stage of the increasing weight factor scheme helps controlling the level of interference from the incorrect initial symbol decisions.

A use of the linear MMSE detector for providing initial stage decision in the WMIC (MMSE-WMIC) leads to significant performance improvement over the WMIC using MF (MF-WMIC) whereas a use of the DD for providing initial stage decision in the WMIC (DD-WMIC) can improve the performance over MF-WMIC only in the system with moderate number of users.

The limitation of the DD-WMIC to the system with large number of users is due to the inferior performance of the DD in such system.

For the DD-WMIC and the MMSE-WMIC operating in a system with moderate number of users, the BER improvement by introducing the increasing weight factor scheme is only marginal because the linear MMSE detector and the DD can deliver the initial symbol decisions with substantially low error rate. In this case, the weight factors, originally introduced for mitigating the effect from the incorrect estimated symbols in the early stage, have less impact on the performance. The performance gain, achievable by introducing the appropriate weight factors to the DD-WMIC and the MMSE-WMIC, becomes more remarkable in the heavily loaded systems.

Figure 3.24 and 3.25 illustrate the BER of the MUD-ISIC employing various multiuser detection techniques versus a number of users. From the figures, the robustness of the linear MMSE detector and the MMSE-WMIC to the system load is evident.

In conclusion, the best multiuser detection technique for applying to the MUD-ISIC is the MMSE-WMIC with increasing weight factor scheme. The benefits of the non-linear multiuser detection techniques in various aspects support the proposed MUD-ISIC, which does not limit to only the linear detector as other known receivers.

3.3.5 Performance Comparison With Other Receivers

Apart from the capability of the MUD-ISIC to employ various multiuser detection techniques as presented in the previous subsection, other merits of the MUD-ISIC are investigated in this section. For a fair comparison with other receivers, which are mainly relied on the MMSE approach, the MUD-ISIC employing the linear MMSE detector is considered.

3.3.5.1 The Receivers for the MC-CDMA System with Insufficient Cyclic Prefix

As reviewed in chapter 1 and chapter 2, two techniques [34, 35] have been independently proposed for the MD-CDMA systems without cyclic prefix. These techniques can also be adopted to the MC-CDMA system with insufficient cyclic prefix as well. Both techniques presume the perfect frequency synchronization condition which likely obstruct their application in the practical systems. The performance of the two previously proposed techniques is investigated under both perfect and imperfect frequency synchronization situation. As earlier discussed in the previous chapter, the original truncated time-domain MMSE multiuser detector, presented in [34], does not consider the serial to parallel conversion. For the system having serial to parallel conversion, the DFT is required for parallel symbols separation. As a consequence, the time-domain detector has to be converted to the frequency-domain.

Figure 3.26 shows the BER of the receivers as a function of the cyclic prefix length in the MC-CDMA system with perfect frequency synchronization for the uniform MIP channel and the exponentially decaying MIP channel. In this case, the MMSE decision feed back equalizer

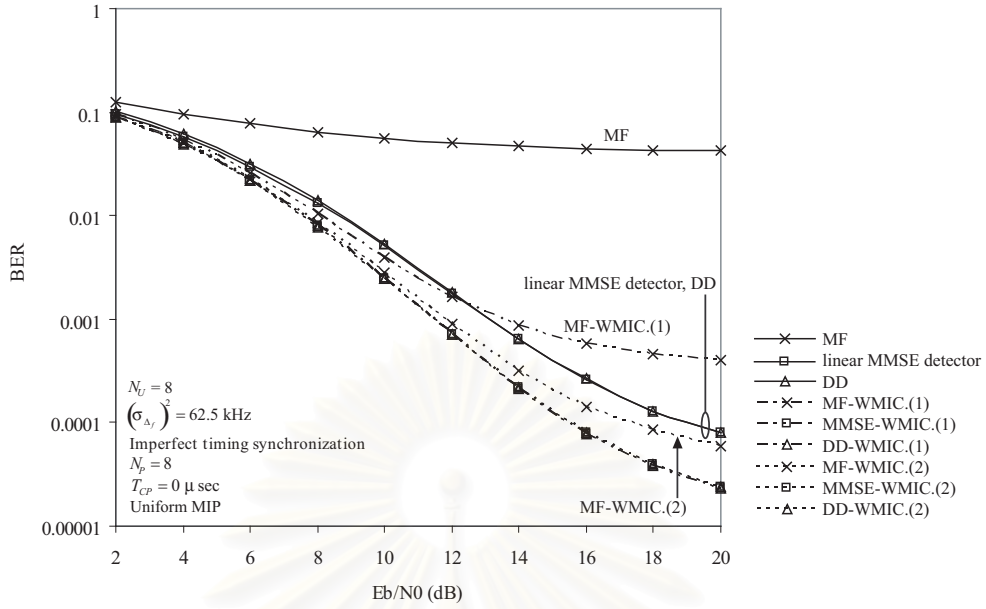

Figure 3.16: Performance of various multiuser detection techniques, applied to the MUD-ISIC, for the system with 8 users under the uniform MIP channel

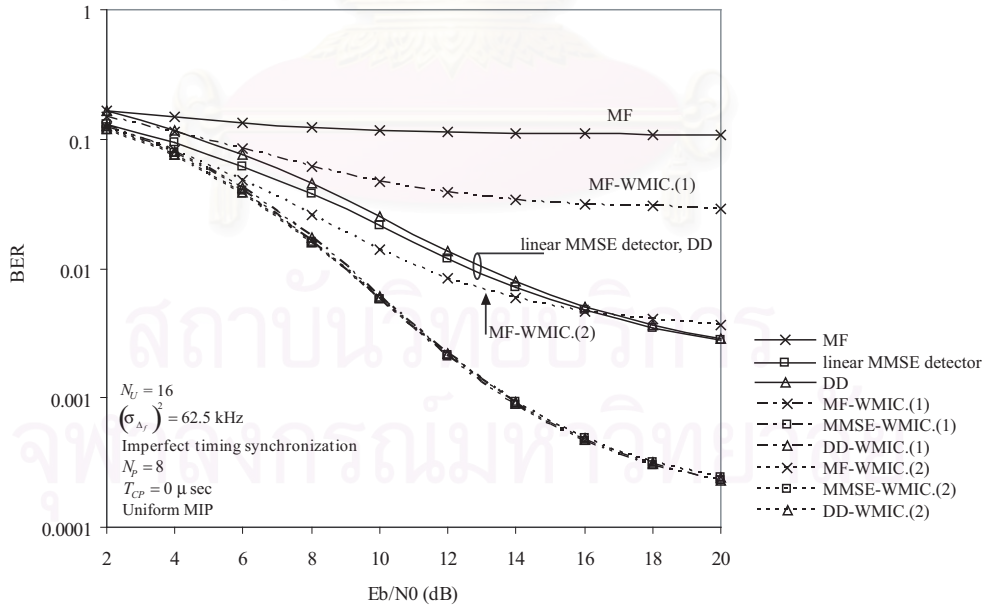

Figure 3.17: Performance of various multiuser detection techniques, applied to the MUD-ISIC, for the system with 16 users under the uniform MIP channel

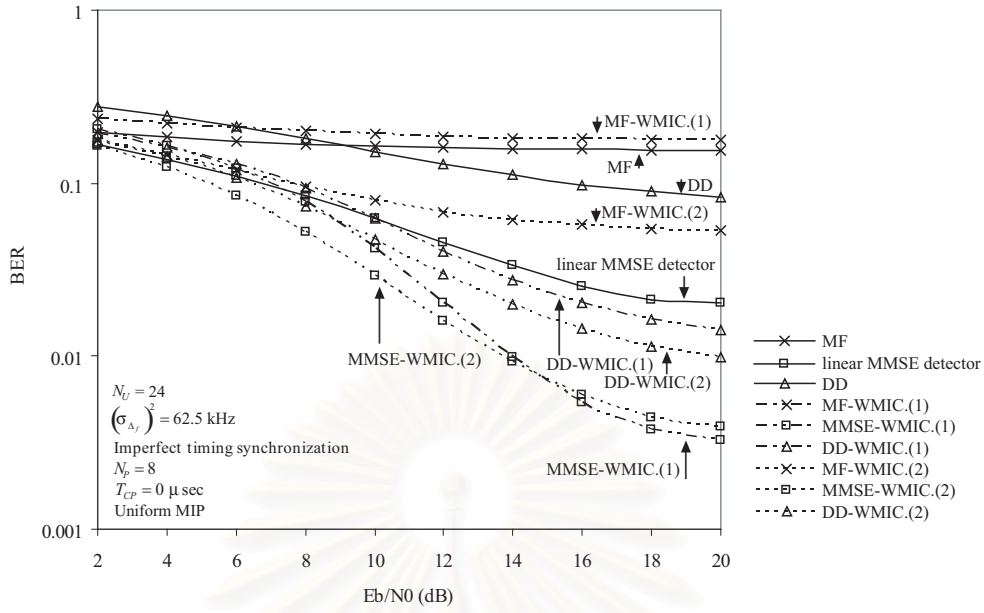

Figure 3.18: Performance of various multiuser detection techniques, applied to the MUD-ISIC, for the system with 24 users under the uniform MIP channel

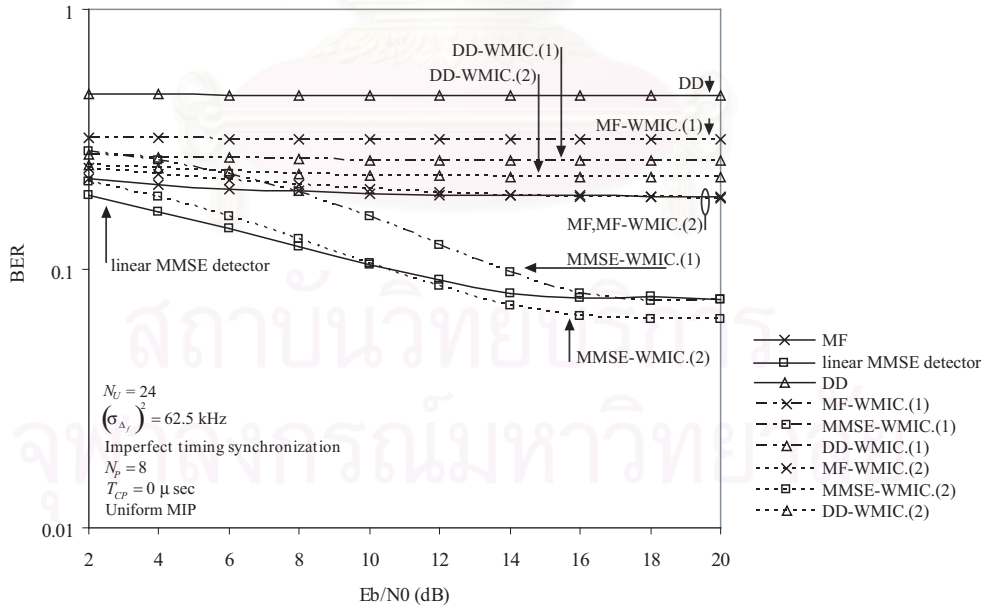

Figure 3.19: Performance of various multiuser detection techniques, applied to the MUD-ISIC, for the system with 32 users under the uniform MIP channel

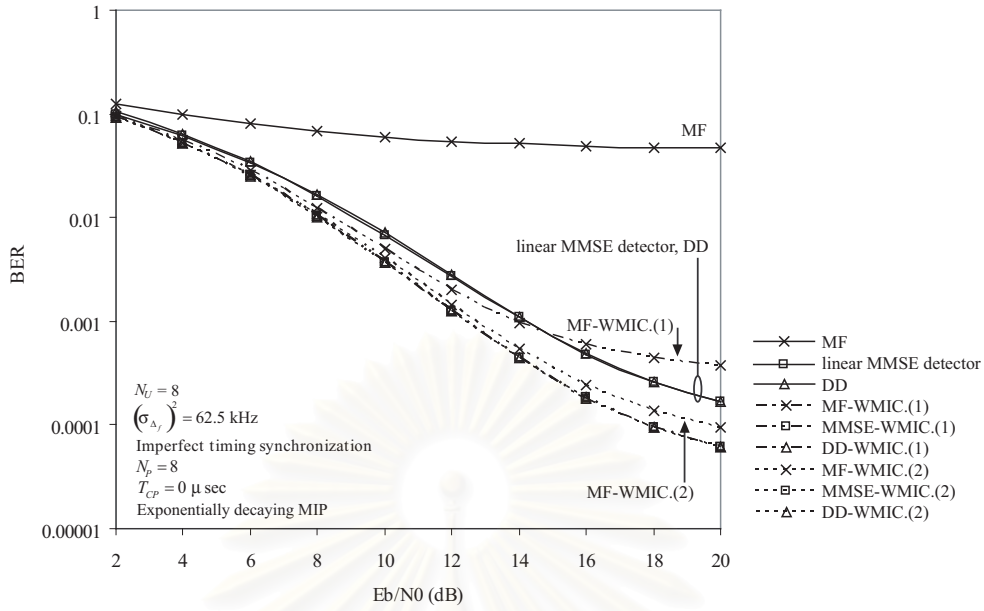

Figure 3.20: Performance of various multiuser detection techniques, applied to the MUD-ISIC, for the system with 8 users under the exponentially decaying MIP channel

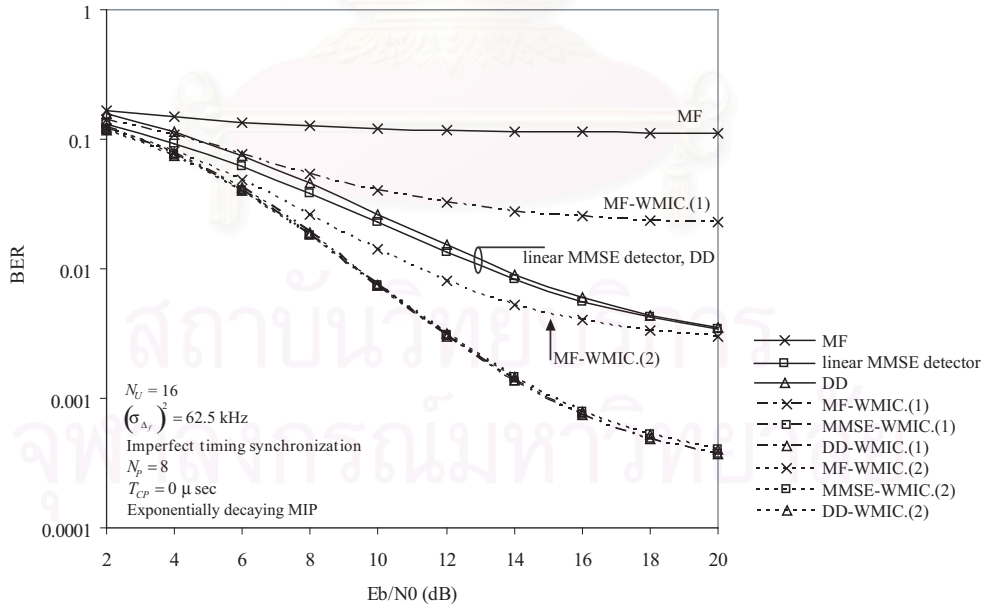

Figure 3.21: Performance of various multiuser detection techniques, applied to the MUD-ISIC, for the system with 16 users under the exponentially decaying MIP channel

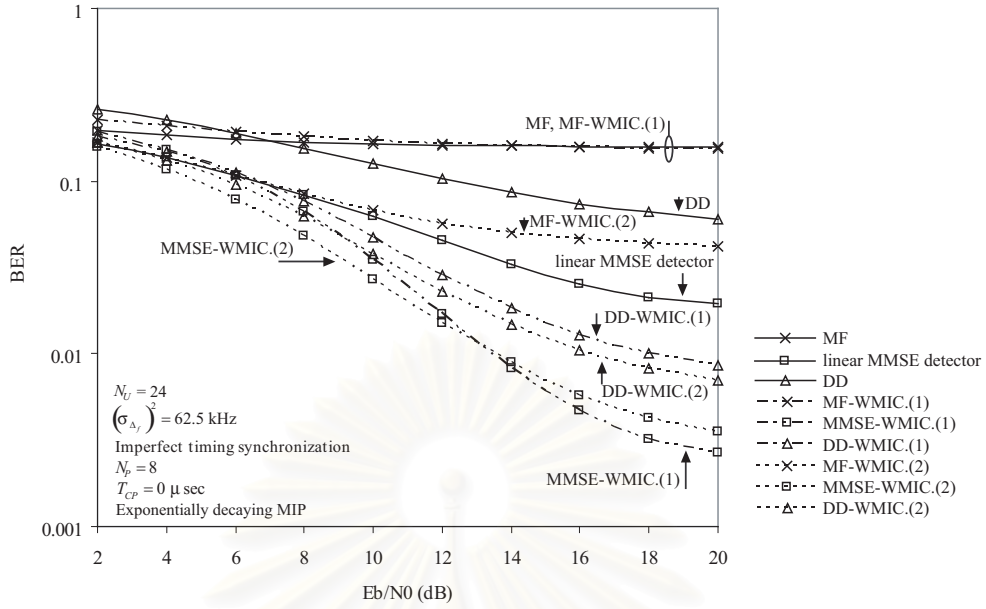

Figure 3.22: Performance of various multiuser detection techniques, applied to the MUD-ISIC, for the system with 24 users under the exponentially decaying MIP channel

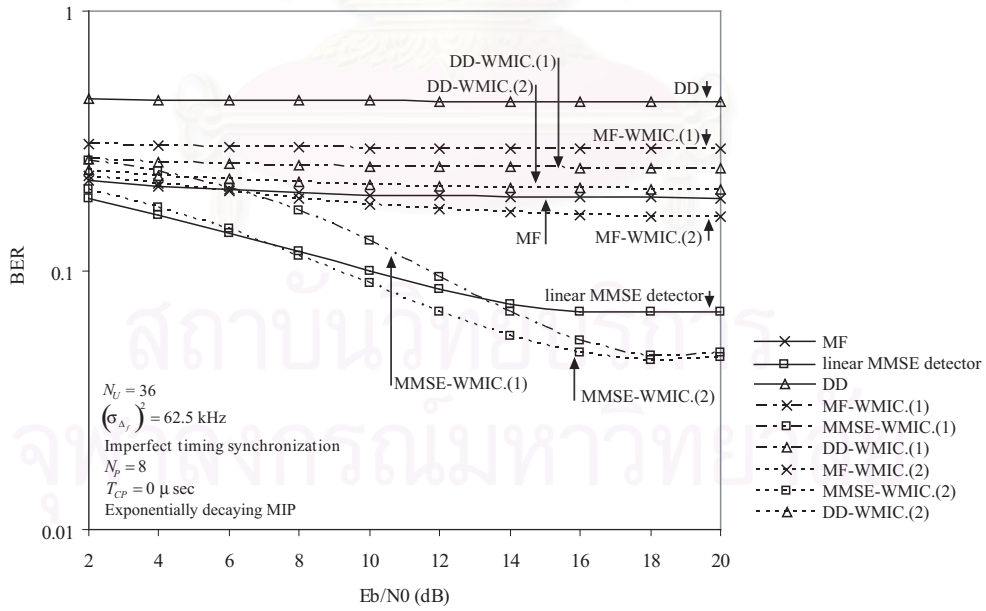

Figure 3.23: Performance of various multiuser detection techniques, applied to the MUD-ISIC, for the system with 32 users under the exponentially decaying MIP channel

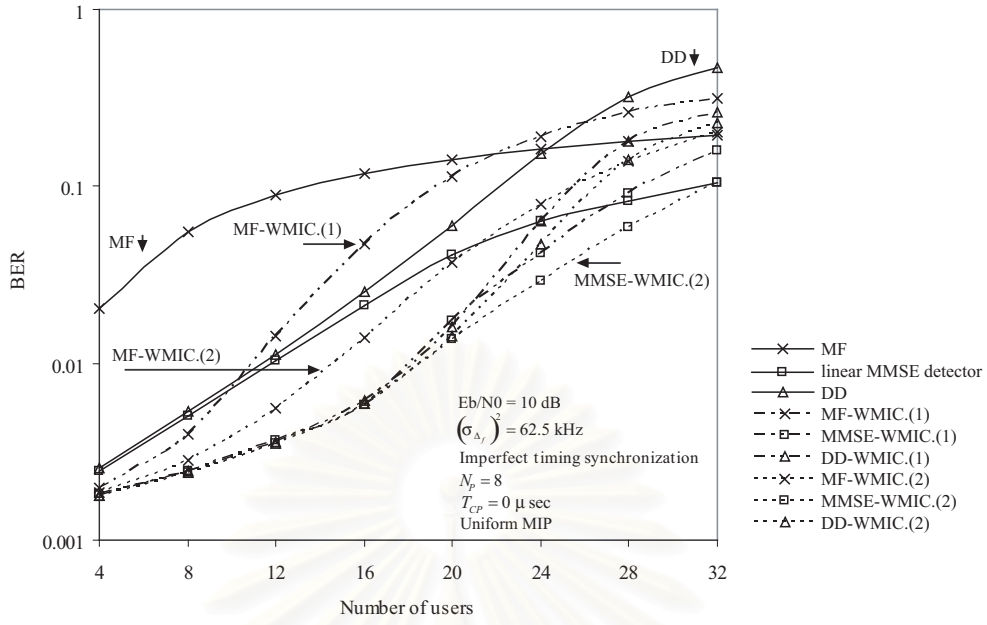

Figure 3.24: Performance of various multiuser detection techniques, applied to the MUD-ISIC, versus the number of users (uniform MIP channel)

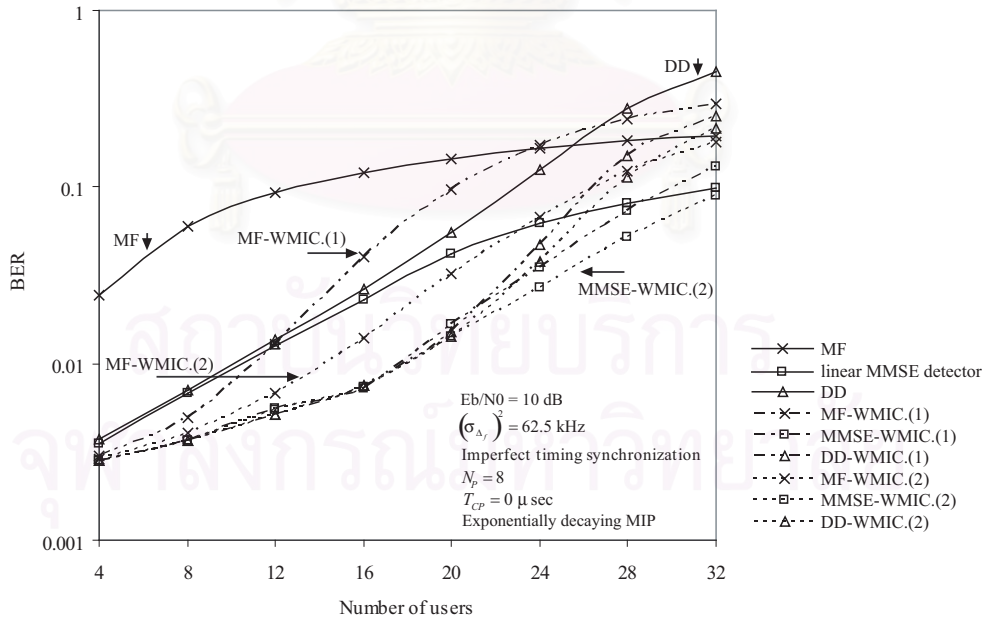

Figure 3.25: Performance of various multiuser detection techniques, applied to the MUD-ISIC, versus the number of users (exponentially decaying MIP channel)

(MMSE-DFE) [35] is equivalent to the MUD-ISIC employing the linear MMSE detector. For the simulation, a number of users is 8 and a serial to parallel conversion size is 8. From the figure, the modified truncated time-domain MMSE multiuser detector suffers from the useful power loss due to the discarding of an ISI disturbed part in the system with short cyclic prefix length. In the sufficient cyclic prefix case, the modified truncated time-domain MMSE multiuser detector and the MUD-ISIC employing the linear MMSE detector give the same BER.

Performance of the receivers in the MC-CDMA system with imperfect frequency synchronization is presented in figure 3.27 for the uniform MIP channel and the exponentially decaying MIP channel. Other simulation parameters are the same as those used in figure 3.26. As expected, the results show that both the modified truncated time-domain MMSE multiuser detector and the MMSE-DFE fail to work in the presence of frequency offset. In contrast, the MUD-ISIC can still perform well.

3.3.5.2 The Receivers for the MC-CDMA System with Frequency Offset

This section compares the MUD-ISIC employing the linear MMSE detector with the frequency offset compensated MMSE detector [49, 50]. Both receivers have a capability to work under the presence of frequency offset, but only the MUD-ISIC also considers the ISI. Figure 3.28 show the effect of the cyclic prefix length to the performance of both receivers in system with perfect frequency synchronization for the uniform MIP channel and the exponentially decaying MIP channel. The figure shows that the frequency offset compensated MMSE detector requires the cyclic prefix length at least as long as the effective delay in order to attain the same BER level as the MUD-ISIC. The similar observation is obtained from figure 3.29 where the system with imperfect frequency synchronization is considered. Compare the frequency offset compensated MMSE detector with the modified truncated time-domain MMSE multiuser detector in the perfect frequency synchronization case (figure 3.28 and figure 3.26), the superior performance of the modified truncated time-domain MMSE multiuser detector over the frequency offset compensated MMSE detector can be observed in the insufficient cyclic prefix environment. For the imperfect frequency synchronization case (figure 3.29 and figure 3.27), the frequency offset compensated MMSE detector performs much better than the modified truncated time-domain MMSE multiuser detector and the MMSE-DFE. Therefore, it may be able to conclude that the frequency offset poses more significant influence to the performance than the insufficient cyclic prefix.

3.3.5.3 Sensitivity of Each Receiving Technique to the Frequency Offset

Figure 3.30 depicts the BER as a function of frequency offset variance in the system without cyclic prefix. The BER of the modified truncated time-domain MMSE multiuser detector, the MMSE-DFE, the frequency offset compensated MMSE detector, and the MUD-ISIC employing the linear MMSE detector, are compared. Obviously, the MUD-ISIC and the frequency offset compensated MMSE detector show impressive robustness against the frequency offset whereas the

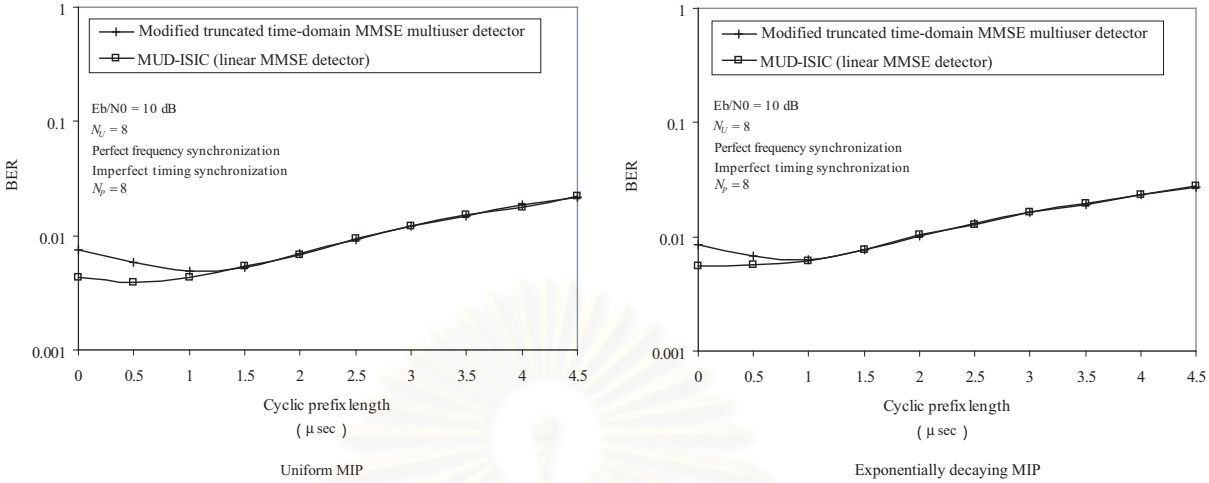

Figure 3.26: Performance of the modified truncated time-domain MMSE multiuser detector and the MUD-ISIC (linear MMSE detector) under the perfect frequency synchronization situation

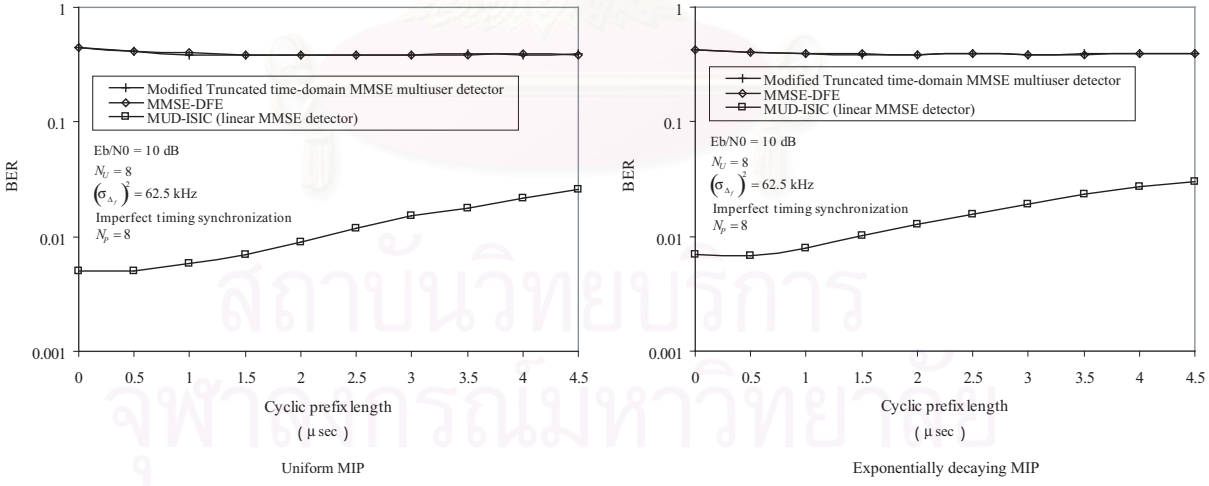

Figure 3.27: Performance of the modified truncated time-domain MMSE multiuser detector, MMSE-DFE, and the MUD-ISIC (linear MMSE detector) under the imperfect frequency synchronization situation

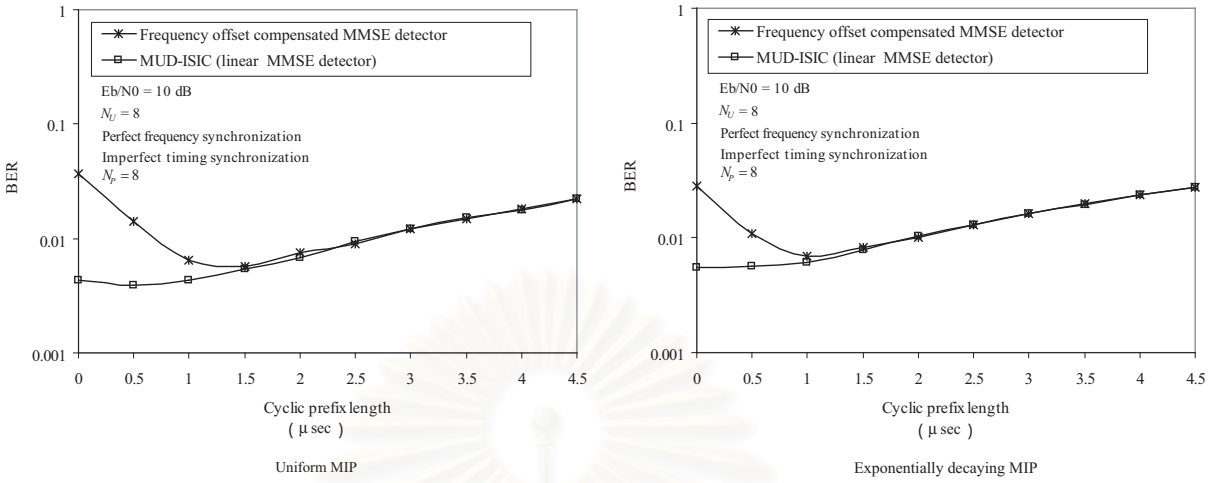

Figure 3.28: Performance of the frequency offset compensated MMSE detector and the MUD-ISIC (linear MMSE detector) under the perfect frequency synchronization situation

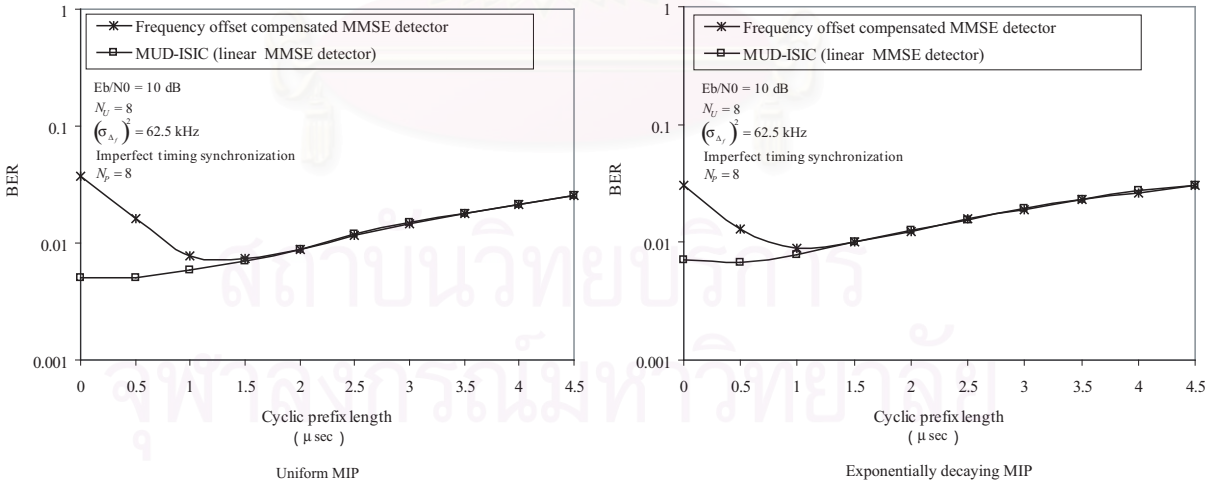

Figure 3.29: Performance of the frequency offset compensated MMSE detector and the MUD-ISIC (linear MMSE detector) under the imperfect frequency synchronization situation

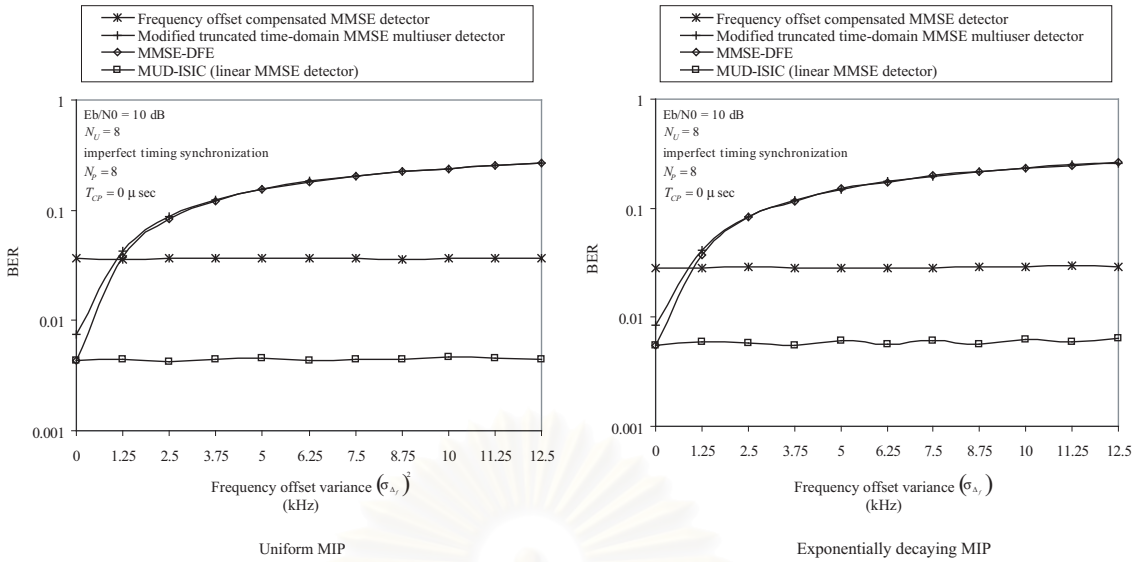

Figure 3.30: Performance of the modified truncated time-domain MMSE multiuser detector, MMSE-DFE, the frequency offset compensated MMSE detector, and the MUD-ISIC (linear MMSE detector) versus frequency offset variance

performance of the modified truncated time-domain MMSE multiuser detector and the MMSE-DFE rapidly drops as the frequency offset variance increases.

3.4 Summary

In this chapter, the motivation and the foundation of the MUD-ISIC have been presented. As seen from the previous chapter, the insufficient cyclic prefix, the frequency offset, and channel impulse response distort the original signature sequences. In addition, the insufficient cyclic prefix incurs the ISI. Instead of trying to separately compensate each factor, the integrated approach, which concentrated on the transformed signature sequences and the ISI generation sequences, is proposed. The proposed MUD-ISIC has two main functions, the ISI cancellation part and the multiuser detection part.

The merits of the proposed MUD-ISIC are twofold. Firstly, the MUD-ISIC is robust to both the insufficient cyclic prefix and the frequency offset. This robustness makes the proposed receiver more attractive than other receivers. Secondly, the structure of the MUD-ISIC does not limit to the particular classes of multiuser detectors, but it is flexible to adopt various multiuser detection techniques. This flexibility benefits system designer in compromising the complexity and performance. From the simulation results, the non-linear multiuser detection shows considerable potential over the linear counterparts. Since the WMIC employing the linear MMSE detector is the best multiuser detector (according to the simulation results), it is not wise to neglect the non-linear multiuser detection technique.

The simulation results also indicate that the best performance is achieved in the insufficient

cyclic prefix environment for both the uniform MIP channel and the exponentially decaying MIP channel. This result encourages a new system design where the cyclic prefix is intentionally inserted shorter than the effective channel delay or even neglected. The need for cyclic prefix has a trend to decrease as the advancement in timing synchronization can shorten the asynchronous delay.

CHAPTER IV

PARAMETER ESTIMATION TECHNIQUES

In order to implement the MUD-ISIC, presented in chapter 3, the ISI generation sequences and the transformed signature sequences have to be estimated. In addition, some multiuser detection techniques, such as the linear MMSE detector, further require an information about the noise variance. This chapter presents the techniques for acquiring these essential parameters. The proposed estimators will be evaluated at the end of this chapter.

4.1 Basic Concepts

Generally, the ISI generation sequences and the transformed signature sequences can be calculated from channel parameters, i.e. channel path coefficients ($\alpha_{k,l}^{i}$), channel path delay values ($\tau_{k,l}^{i}$), number of paths (N_L), and frequency offset values ($\Delta_{f,k}$), by using (2.17)-(2.20). Unfortunately, the existing channel estimation techniques are based on the sufficient cyclic prefix assumption where the fading of the subcarriers is described by multiplicative channel coefficients. The sufficient cyclic prefix presumed channel estimation techniques cannot be applied to the insufficient cyclic prefix case. Moreover, most of these techniques require the frequency offset compensation prior to the channel estimation.

Unlike the forward link, frequency offset of each user in the reverse link is not necessary the same. The frequency offset compensation for multiple frequency offset values is impossible because the frequency offset correction of one user would misalign the others. As a consequence, the conventional channel estimation techniques, which require frequency offset compensation, cannot be applied. In order to jointly estimate channel and frequency offset in the reverse link, the recursive estimation based on the extended Kalman filter (EKF) was proposed in [52]. This technique also requires the sufficient cyclic prefix condition.

Most of the channel estimation techniques focus on obtaining the multiplicative channel coefficients whereas very few techniques explicitly estimate multipath coefficients and delay by using ESPRIT algorithm [78]. The direct computation of the delays is a nonlinear estimation problem and, therefore, it suffers from threshold effects at low signal to noise ratio environment [79]. When a number of paths are large or the delay between each path is small, the estimator in [78] becomes ill-conditioned and, thus, the performance is degraded. Moreover, the complexity burden and the requirement of large number of training symbols even for the forward link case limit the application of this technique [80]. It should be noted that this technique was originally designed for only the forward link case. Hence, it cannot be applied to the concerned reverse link channels.

From the aforementioned reasons, this dissertation presents a novel estimation approach,

which directly estimates the ISI generation sequences and the transformed signature sequences in order to avoid several disadvantages in explicitly estimating the channel coefficients and delays. With the optimum training sequence, the proposed estimator has low computational load as will be discussed later in this chapter.

4.2 ISI Generation Sequences and Transformed Signature Sequences Estimation

By considering the detection of the p^{th} parallel symbols and neglecting the cross parallel symbol interference terms (according to the sub-band detection scheme), the m^{th} element of the corresponding DFT output vector (2.16) can be expressed as

$$\begin{aligned} x_p^i[m] &= x^i\left[pN_S+m\right] \\ &= \sum_{k=0}^{N_U-1} \bar{c}_{k,p,D}^{i,pN_S+m} b_{k,p}^i + \sum_{k=0}^{N_U-1} \bar{c}_{k,p,I}^{i,pN_S+m} b_{k,p}^{i-1} + \bar{\eta}^i[pN_s+m] \end{aligned}. \tag{4.1}$$

4.2.1 Least Squares Estimator

The estimates of $\bar{c}_{k,p,D}^{i,pN_S+m}$ and $\bar{c}_{k,p,I}^{i,pN_S+m}$ can be obtained by minimizing the sum error squares cost function

$$\xi = \sum_{i=i_1+1}^{i_1+N_T} \left|e^i\left[m\right]\right|^2 \tag{4.2}$$

where N_T+1 is a number of training symbol and the error function $e^i\left[m\right]$ is defined as

$$e^i\left[m\right] = x_p^i\left[m\right] - \left(\sum_{k=0}^{N_U-1} \hat{\bar{c}}_{k,p,D}^{i,pN_S+m} b_{k,p}^i + \sum_{k=0}^{N_U-1} \hat{\bar{c}}_{k,p,I}^{i,pN_S+m} b_{k,p}^{i-1} \right). \tag{4.3}$$

The solution to the above minimization problem is obtained by taking gradient of the cost function (4.2) with respect to the unknown variables:

$$\nabla\xi = 0. \tag{4.4}$$

$\bar{c}_{k,p,D}^{i,pN_S+m}$ and $\bar{c}_{k,p,I}^{i,pN_S+m}$ are assumed to vary at a rate slow enough that they can be regarded as essentially fix during a training period. i.e. $\bar{c}_{k,p,D}^{i,pN_S+m} = \bar{c}_{k,p,D}^{\bar{i},pN_S+m}$ and $\bar{c}_{k,p,I}^{i,pN_S+m} = \bar{c}_{k,p,I}^{\bar{i},pN_S+m}$ for $i_1 \le i \le i_1+N_T$. By direct mathematical calculation, (4.4) is equivalent to the following system of equations:

$$\sum_{\bar{k}=0}^{N_U-1} \hat{\bar{c}}_{\bar{k},p,D}^{\bar{i},pN_S+m} \sum_{i=i_1+1}^{i_1+N_T} \left(b_{k,p}^i\right)^* b_{\bar{k},p}^i + \sum_{\bar{k}=0}^{N_U-1} \hat{\bar{c}}_{\bar{k},p,I}^{\bar{i},pN_S+m} \sum_{i=i_1+1}^{i_1+N_T} \left(b_{k,p}^i\right)^* b_{\bar{k},p}^{i-1} = \sum_{i=i_1+1}^{i_1+N_T} \left(b_{k,p}^i\right)^* x_p^i\left[m\right] \tag{4.5}$$

and

$$\sum_{\bar{k}=0}^{N_U-1} \hat{\bar{c}}_{\bar{k},p,D}^{\bar{i},pN_S+m} \sum_{i=i_1+1}^{i_1+N_T} \left(b_{k,p}^{i-1}\right)^* b_{\bar{k},p}^i + \sum_{\bar{k}=0}^{N_U-1} \hat{\bar{c}}_{\bar{k},p,I}^{\bar{i},pN_S+m} \sum_{i=i_1+1}^{i_1+N_T} \left(b_{k,p}^{i-1}\right)^* b_{\bar{k},p}^{i-1} = \sum_{i=i_1+1}^{i_1+N_T} \left(b_{k,p}^{i-1}\right)^* x_p^i\left[m\right] \tag{4.6}$$

for $0 \leq k \leq N_U - 1$. Equation (4.5) and (4.6) can be rewritten in a compact matrix form as

$$\mathbf{Q}\hat{\mathbf{c}}_{p,m} = \mathbf{p}_{p,m} \tag{4.7}$$

where

$$\hat{\mathbf{c}}_{p,m} = \begin{bmatrix} \hat{c}^{\bar{i},pN_S+m}_{0,p,D} & \cdots & \hat{c}^{\bar{i},pN_S+m}_{N_U-1,p,D} & \hat{c}^{\bar{i},pN_S+m}_{0,p,I} & \cdots & \hat{c}^{\bar{i},pN_S+m}_{N_U-1,p,I} \end{bmatrix}^T, \tag{4.8}$$

$$\mathbf{p}_{p,m} = \begin{bmatrix} \rho_{p,m,0,0} & \cdots & \rho_{p,m,0,N_U-1} & \rho_{p,m,1,0} & \cdots & \rho_{p,m,1,N_U-1} \end{bmatrix}^T, \tag{4.9}$$

$$\mathbf{Q} = \begin{bmatrix} \mathbf{Q}_{0,0} & \mathbf{Q}_{0,1} \\ \mathbf{Q}_{1,0} & \mathbf{Q}_{1,1} \end{bmatrix} \tag{4.10}$$

with

$$\mathbf{Q}_{r,s} = \begin{bmatrix} q_{r,s,0,0} & q_{r,s,0,1} & \cdots & q_{r,s,0,N_U-1} \\ q_{r,s,1,0} & q_{r,s,1,1} & \cdots & q_{r,s,1,N_U-1} \\ \vdots & \vdots & \ddots & \vdots \\ q_{r,s,N_U-1,0} & q_{r,s,N_U-1,1} & \cdots & q_{r,s,N_U-1,N_U-1} \end{bmatrix}, \tag{4.11}$$

$$q_{r,s,k,\bar{k}} = \sum_{i=i_1+1}^{i_1+N_T} \left(b^{i-r}_{k,p}\right)^* b^{i-s}_{k,p}, \tag{4.12}$$

and

$$\rho_{p,m,r,k} = \sum_{i=i_1+1}^{i_1+N_T} \left(b^{i-r}_{k,p}\right)^* x^i_{k,p}[m]. \tag{4.13}$$

Directly followed from (4.7), $\hat{\mathbf{c}}_{p,m}$ can be estimated by

$$\hat{\mathbf{c}}_{p,m} = \mathbf{Q}^{-1}\mathbf{p}_{p,m}. \tag{4.14}$$

4.2.2 Mean Square Error of the Least Squares Estimator

By replacing (4.1) into (4.13) and rearranging the terms, (4.13) can be expressed as

$$\begin{aligned} \rho_{p,m,r,k} &= \sum_{i=i_1+1}^{N_T-1} \left(b^{i-r}_{k,p}\right)^* \left(\sum_{k=0}^{N_U-1} \bar{c}^{i,pN_S+m}_{k,p,D} b^i_{k,p} + \sum_{k=0}^{N_U-1} \bar{c}^{i,pN_S+m}_{k,p,I} b^{i-1}_{k,p} + \bar{\eta}^i[pN_s+m] \right) \\ &= \sum_{k=0}^{N_U-1} \bar{c}^{i,pN_S+m}_{k,p,D} \sum_{i=i_1+1}^{N_T-1} \left(b^{i-r}_{k,p}\right)^* b^i_{k,p} + \sum_{k=0}^{N_U-1} \bar{c}^{i,pN_S+m}_{k,p,I} \sum_{i=i_1+1}^{N_T-1} \left(b^{i-r}_{k,p}\right)^* b^{i-1}_{k,p} + w_{k,m,p,r} \end{aligned} \tag{4.15}$$

where

$$w_{k,m,p,r} = \sum_{i=i_1+1}^{N_T-1} \left(b^{i-r}_{k,p}\right)^* \bar{\eta}^i[pN_s+m]. \tag{4.16}$$

Thus, the vector $\mathbf{p}_{p,m}$ can be written as

$$\mathbf{p}_{p,m} = \mathbf{Q}\mathbf{c}_{p,m} + \mathbf{w}_{p,m} \tag{4.17}$$

where

$$\mathbf{c}_{p,m} = \left[\begin{array}{cccccc} \bar{c}^{\bar{i},pN_S+m}_{0,p,D} & \cdots & \bar{c}^{\bar{i},pN_S+m}_{N_U-1,p,D} & \bar{c}^{\bar{i},pN_S+m}_{0,p,I} & \cdots & \bar{c}^{\bar{i},pN_S+m}_{N_U-1,p,I} \end{array} \right]^T \tag{4.18}$$

and

$$\mathbf{w}_{p,m} = \left[\begin{array}{cccccc} w_{0,m,p,0} & \cdots & w_{N_U-1,m,p,0} & w_{0,m,p,1} & \cdots & w_{N_U-1,m,p,1} \end{array} \right]^T \tag{4.19}$$

with

$$E\left\{\mathbf{w}_{p,m}\left(\mathbf{w}_{p,m}\right)^H\right\} = N_C\left(\sigma_\eta\right)^2\mathbf{Q}. \tag{4.20}$$

Substituting (4.17) into (4.14) yields

$$\begin{aligned} \hat{\mathbf{c}}_{p,m} &= \mathbf{Q}^{-1}\left(\mathbf{Q}\mathbf{c}_{p,m} + \mathbf{w}_{p,m}\right) \\ &= \mathbf{c}_{p,m} + \mathbf{Q}^{-1}\mathbf{w}_{p,m} \end{aligned}. \tag{4.21}$$

The above equation indicates the unbiased property of the proposed estimator. The MSE of the estimator is given by

$$\begin{aligned} MSE &= \frac{1}{2N_U}E\left\{\left\|\hat{\mathbf{c}}_{p,m} - \mathbf{c}_{p,m}\right\|^2\right\} \\ &= \frac{1}{2N_U}Tr\left\{\mathbf{Q}^{-1}E\left\{\mathbf{w}_{p,m}\left(\mathbf{w}_{p,m}\right)^H\right\}\left(\mathbf{Q}^{-1}\right)^H\right\}. \\ &= N_C\left(\sigma_\eta\right)^2 Tr\left\{\mathbf{Q}^{-1}\right\} \end{aligned} \tag{4.22}$$

4.2.3 Criterion for the Optimum Training Sequences

From (4.22), it is seen that the MSE of the estimator is depended on matrix $\mathbf{Q}$. In this section, we consider a condition of matrix $\mathbf{Q}$ to achieve a minimum MSE. If $b^i_{k,p}$ is constant modulus and $\left\|b^i_{k,p}\right\|^2 = 1$, then

$$\begin{aligned} Tr\left\{\mathbf{Q}\right\} &= \sum_{k=0}^{2N_U-1}\lambda_k^2 \\ &= 2N_UN_T \end{aligned} \tag{4.23}$$

where λ_k^2 are the eigenvalues of matrix $\mathbf{Q}$. Equation (4.22) can be expressed based on (4.23) as

$$MSE = \frac{1}{2N_U}N_C\left(\sigma_\eta\right)^2\left(\sum_{k=0}^{2N_U-1}\frac{1}{\lambda_k^2}\right). \tag{4.24}$$

By observing (4.24) and (4.23), the MSE is bounded by

$$MSE \geq \frac{1}{2N_U}N_C\left(\sigma_\eta\right)^2\left(\frac{2N_U}{N_T}\right) = N_C\left(\frac{\left(\sigma_\eta\right)^2}{N_T}\right) \tag{4.25}$$

with equality if and only if $\lambda_0^2 = \lambda_1^2 = \cdots = \lambda_{2N_U-1}^2$. Since $b_{k,p}^i$ is constant modulus, matrix $\mathbf{Q}$ can be decomposed as

$$\mathbf{Q} = N_T \mathbf{I}_{2N_U \times 2N_U} + \tilde{\mathbf{Q}} \tag{4.26}$$

where $\mathbf{I}_{x\times x}$ is a $x \times x$ identity matrix and $\tilde{\mathbf{Q}}$ is a matrix representing off-diagonal elements of matrix $\mathbf{Q}$. By applying matrix inversion lemma, $\mathbf{Q}^{-1}$ can be expressed as

$$\begin{aligned} \mathbf{Q}^{-1} &= \left(N_T \mathbf{I}_{2N_U \times 2N_U} + \tilde{\mathbf{Q}} \right)^{-1} \\ &= \frac{\mathbf{I}_{2N_U \times 2N_U} - \tilde{\mathbf{Q}}\mathbf{Q}^{-1}}{N_T} \end{aligned} . \tag{4.27}$$

Hence,

$$Tr\left\{\mathbf{Q}^{-1}\right\} = \frac{2N_U}{N_T} - \frac{1}{N_T} Tr\left\{\tilde{\mathbf{Q}}\mathbf{Q}^{-1}\right\}. \tag{4.28}$$

By replacing the above equation into (4.22), the minimum MSE is achieved if $\tilde{\mathbf{Q}}$ is a zero matrix or equivalently

$$\mathbf{Q} = N_T \mathbf{I}_{2N_U \times 2N_U}. \tag{4.29}$$

It is interesting that if the training sequence, satisfying (4.29), is used, the estimator in (4.14) becomes

$$\hat{\mathbf{c}}_{p,m} = \frac{1}{N_T} \mathbf{p}_{p,m}, \tag{4.30}$$

which does not require a matrix inversion. Therefore, the optimum training sequences do not only result in the minimum MSE, but they also simplify the estimator.

4.2.4 Optimum Training Sequence Generation

In previous section, a condition for the optimum training sequences has been established. The rest is to show that such sequences exist. This section presents three different methods for generating the optimum training sequences, time division training sequences, odd-even training sequences, and cyclically orthogonal training sequences.

4.2.4.1 Time Division Training Sequences

In this scheme, a training block, consisting of three consecutive time slots, is assigned to each user as shown in figure 4.1. The first time slot and the last time slot of each training block are silent time slots. A MC-CDMA modulated training symbol is transmitted in the middle time slot. Two successive training blocks may share the same null time slot, whereas the middle time slot for each user is essentially non-overlapping.

The time division training sequence can be mathematically described by

$$b_{k,p}^i = \begin{cases} 1 & (i = i_1 + 1 + k) \\ 0 & (otherwise) \end{cases} . \tag{4.31}$$

For the system with N_U users and the common null time slots are shared between the successive training blocks, a number of the training symbol periods including the null periods is $N_T + 1 = 2N_U + 1$.

4.2.4.2 Odd-Even Training Sequences

The arrangement of odd-even training sequence is depicted in figure 4.2. The training symbols in each training period are grouped into 2 sets according to odd and even indices. All the odd sequences, $\mathbf{b}_{k,p}^{Odd} = \begin{bmatrix} b_{k,p}^{i_1+2} & b_{k,p}^{i_1+4} & \cdots & b_{k,p}^{i_1+N_T} \end{bmatrix}$, as well as all the even sequence, $\mathbf{b}_{k,p}^{Even} = \begin{bmatrix} b_{k,p}^{i_1+1} & b_{k,p}^{i_1+3} & \cdots & b_{k,p}^{i_1+N_T-1} \end{bmatrix}$, are mutually orthogonal. Supposed that the training symbols are indexed as shown in figure 4.2, all the odd sequences are orthogonal to all the even sequences, i.e. $\left(\mathbf{b}_{k,p}^{Odd}\right)^H \mathbf{b}_{k,p}^{Even} = 0$ for $0 \leq k \leq N_U - 1$ and $0 \leq p \leq N_P - 1$, and all the even sequence are orthogonal to all the cyclic rotated odd sequences, i.e. $\left(\mathbf{b}_{k,p}^{Even}\right)^H \mathbf{b}_{k,p}^{\overline{Odd}} = 0$ for $0 \leq k \leq N_U - 1$ and $0 \leq p \leq N_P - 1$ where $\mathbf{b}_{k,p}^{\overline{Odd}} = \begin{bmatrix} b_{k,p}^{i_1} & b_{k,p}^{i_1+1} & \cdots & b_{k,p}^{i_1+N_T-2} \end{bmatrix}$ and $b_{k,p}^{i_1} = b_{k,p}^{i_1+N_T}$.

To satisfy these criteria, a possible selection of training sequences is from the standard Hadamard-Walsh matrix. In this case, Hadamard-Walsh matrix size must be a multiple of two and larger than $2N_U$. For the system with N_U users, the number of training symbols is $N_T + 1 = 4N_U + 1$ users (if N_U is a multiple of two).

4.2.4.3 Cyclically Orthogonal Training Sequences

Defining a training sequence matrix as

$$\mathbf{\Gamma} = \begin{bmatrix} \mathbf{\Gamma}_0 & \mathbf{\Gamma}_1 \end{bmatrix} \tag{4.32}$$

where

$$\mathbf{\Gamma}_0 = \begin{bmatrix} b_{0,p}^{i_1+1} & b_{1,p}^{i_1+1} & \cdots & b_{N_U-1,p}^{i_1+1} \\ b_{0,p}^{i_1+2} & b_{1,p}^{i_1+2} & \cdots & b_{N_U-1,p}^{i_1+2} \\ \vdots & \vdots & \ddots & \vdots \\ b_{0,p}^{i_1+N_T} & b_{1,p}^{i_1+N_T} & \cdots & b_{N_U-1,p}^{i_1+N_T} \end{bmatrix} \tag{4.33}$$

and

$$\mathbf{\Gamma}_1 = \begin{bmatrix} b_{0,p}^{i_1} & b_{1,p}^{i_1} & \cdots & b_{N_U-1,p}^{i_1} \\ b_{0,p}^{i_1+1} & b_{1,p}^{i_1+1} & \cdots & b_{N_U-1,p}^{i_1+1} \\ \vdots & \vdots & \ddots & \vdots \\ b_{0,p}^{i_1+N_T-1} & b_{1,p}^{i_1+N_T-1} & \cdots & b_{N_U-1,p}^{i_1+N_T-1} \end{bmatrix}. \tag{4.34}$$

Matrix $\mathbf{Q}$ can be formulated by using the training sequence matrix as

$$\mathbf{Q} = \mathbf{\Gamma}^H \mathbf{\Gamma}. \tag{4.35}$$

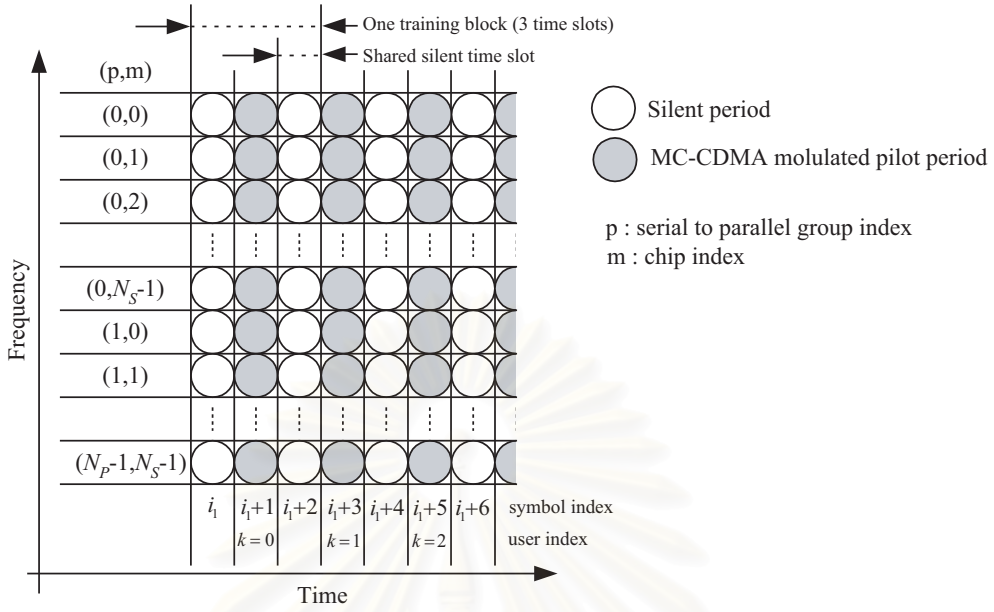

Figure 4.1 Time division training sequence diagram

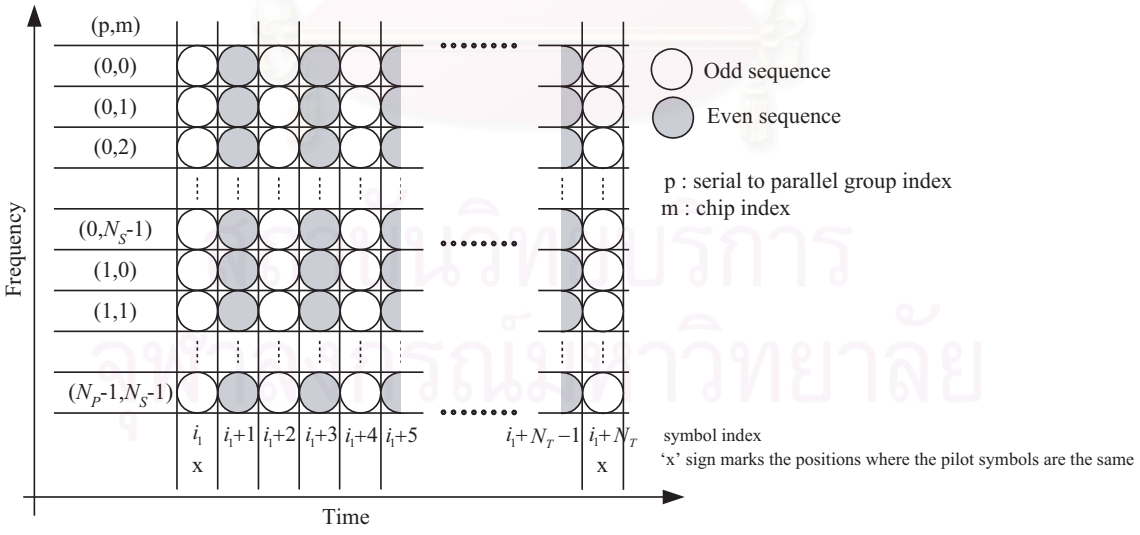

Figure 4.2 Odd-even training sequence diagram

From (4.29), the optimum training sequence matrix must satisfy

$$\mathbf{\Gamma}^H\mathbf{\Gamma} = N_T\mathbf{I}_{2N_U\times 2N_U}, \tag{4.36}$$

or equivalently

$$(\mathbf{\Gamma}_0)^H\,\mathbf{\Gamma}_0 = (\mathbf{\Gamma}_1)^H\,\mathbf{\Gamma}_1 = N_T\mathbf{I}_{N_U\times N_U} \tag{4.37}$$

and

$$(\mathbf{\Gamma}_0)^H\,\mathbf{\Gamma}_1 = (\mathbf{\Gamma}_1)^H\,\mathbf{\Gamma}_0 = \mathbf{0}_{N_U\times N_U} \tag{4.38}$$

where $\mathbf{0}_{x\times x}$ is a $x \times x$ zero matrix.

The above conditions imply that the optimum training sequence matrix must be an orthogonal matrix. If we consider the special case that $b_{k,p}^{i_1} = b_{k,p}^{i_1+N_T}$ for $0 \le k \le N_U - 1$ or, in the other word, the matrix $\mathbf{\Gamma}_1$ is a row-wise cyclic rotation of the matrix $\mathbf{\Gamma}_0$, then the optimum training sequence matrix is an orthogonal matrix having that special structure.

Since $\mathbf{\Gamma}_1$ is a row-wise cyclic rotation of $\mathbf{\Gamma}_0$, $\mathbf{\Gamma}_1$ can be expressed in term of $\mathbf{\Gamma}_0$ by

$$\mathbf{\Gamma}_1 = \tilde{\mathbf{I}}_{2N_U\times 2N_U}\mathbf{\Gamma}_0 \tag{4.39}$$

where

$$\tilde{\mathbf{I}}_{2N_U\times 2N_U} = \begin{bmatrix} 0 & 0 & \cdots & 0 & 1 \\ 1 & 0 & \cdots & 0 & 0 \\ 0 & 1 & \cdots & 0 & 0 \\ \vdots & \vdots & \ddots & \vdots & \vdots \\ 0 & 0 & \cdots & 1 & 0 \end{bmatrix} \tag{4.40}$$

is a row-wise cyclic rotation of an identity matrix. Hence, the optimum training sequence can be written as

$$\mathbf{\Gamma}^{opt} = \begin{bmatrix} \mathbf{\Gamma}_0^{opt} & \tilde{\mathbf{I}}_{2N_U\times 2N_U}\mathbf{\Gamma}_0^{opt} \end{bmatrix}. \tag{4.41}$$

Considering matrix $\mathbf{\Gamma}_0^{opt}$ in the form of

$$\mathbf{\Gamma}_0^{opt} = \mathbf{V}\,[\mathbf{H}_W]_{(0\ldots 2N_U-1)\times(0\ldots N_U-1)} \tag{4.42}$$

where $\mathbf{H}_W$ is a conventional Hadamard-Walsh Matrix, $\mathbf{V}$ is a diagonal matrix that each diagonal element is 1 or -1, and $[\,.\,]_{(r1\ldots r2)\times(c1\ldots c2)}$ denotes a sub matrix, constructed by taking $r1$ to $r2$ rows and $c1$ to $c2$ columns from a matrix inside a square bracket.

Since

$$(\mathbf{H}_W)^H\,\mathbf{H}_W = N_T\mathbf{I}_{2N_U\times 2N_U} \tag{4.43}$$

and

$$(\mathbf{V})^H\,\mathbf{V} = \left(\tilde{\mathbf{I}}_{2N_U\times 2N_U}\right)^H\tilde{\mathbf{I}}_{2N_U\times 2N_U} = \mathbf{I}_{2N_U\times 2N_U} \tag{4.44}$$

using the training sequence in the form of (4.42) fulfills the condition (4.37). The optimum training sequence design problem now becomes a problem of finding matrix $\mathbf{V}$ so that the condition (4.38) is satisfied. Based on (4.43) and (4.44), the condition (4.38) is equivalent to

$$\left([\mathbf{H}_W]_{(0\ldots 2N_U-1)\times(0\ldots N_U-1)}\right)^H(\mathbf{V})^H\,\tilde{\mathbf{I}}_{2N_U\times 2N_U}\mathbf{V}\,[\mathbf{H}_W]_{(0\ldots 2N_U-1)\times(0\ldots N_U-1)} = 0_{N_U\times N_U} \tag{4.45}$$

which is interchangeable to

$$(\mathbf{V})^H \tilde{\mathbf{I}}_{2N_U \times 2N_U} \mathbf{V} [\mathbf{H}_W]_{(0 \ldots 2N_U-1)\times(0 \ldots N_U-1)} = [\mathbf{H}_W]_{(0 \ldots 2N_U-1)\times(N_U \ldots 2N_U-1)} . \quad (4.46)$$

By elaborating on the above equation, the diagonal element of matrix $\mathbf{V}$ is obtained as

$$diag(\mathbf{V}) = [\underbrace{1, \ldots, 1}_{N_U-1}, \underbrace{-1, 1, \ldots, -1, 1}_{N_U}, 1] \quad (4.47)$$

In conclusion, the optimum training sequence matrix is generated by (4.41) and (4.42) with matrix $\mathbf{V}$ given by (4.47).

4.2.4.4 Optimum Training Sequence Comparison

The three different methods for generating the optimum training sequence, time division training sequences, odd-even training sequences, and cyclically orthogonal training sequences, have been presented. All of these training sequence families satisfy the optimum condition (4.29) and easy to construct. The comparison of each training sequence family is briefly summarized in table 4.1.

The time division training sequences have discontinuous signal structure. This structure may lead to large spectrum dispersal. Moreover, the time division training sequences are also susceptible to an impulsive noise because the power for each user training sequence only concentrates on a specific time slot. In general, the high training symbol power can be used for compensating the noise. However, the high peak power impairs the performance of the non-linear amplifier. In addition, transmission of too high power may not comply with the regulation for the out of band interference.

Compared with the time division training sequence scheme, the odd-even training sequences require much more time slots for training sequence transmission. For the system, supporting upto 32 users, the odd-even training sequences occupy 129 time slots, whereas the time division training sequences only require 65 time slots. An inefficient bandwidth utilization of the odd-even training sequences dilutes the attractiveness of this training sequence family.

The quest for a suitable training sequence set arrives at the cyclically orthogonal training sequences, which require the same number of time slots as the time division training sequences but have the continuous signal structure. The cyclically orthogonal training sequences equally spread power of the training sequences over the training time intervals. Therefore, the cyclically orthogonal training sequences can overcome the weakness of the time division training sequences. The derivation of the cyclically orthogonal training sequences may be cumbersome but the result is quite simple. The generation of the cyclically orthogonal training sequences only requires a standard Hadamard-Walsh matrix and a rotation matrix $\mathbf{V}$, which is easy to generate.

Table 4.1 Optimum training sequence comparison

	Time division training sequences	Odd-even training sequences	Cyclically orthogonal training sequences
Number of training time slots	$2N_U + 1$	$4N_U + 1$	$2N_U + 1$
Generation complexity	low	low	low
Out of band emission	high	low	low
Bandwidth utilization efficiency	high	low	high

4.2.5 Adaptive Estimator

Opposed to the conventional LS method, the classical recursive least squares (RLS) algorithm [81] can also be used to adaptively estimate the ISI generation sequences and the transformed signature sequences.

Let

$$\mathbf{\Theta^i_{p,m}} = \left[\begin{array}{cccccc} \hat{c}^{\bar{i},pN_S+m}_{0,p,D} & \cdots & \hat{c}^{i,pN_S+m}_{N_U-1,p,D} & \hat{c}^{i,pN_S+m}_{0,p,I} & \cdots & \hat{c}^{i,pN_S+m}_{N_U-1,p,I} \end{array} \right]^{\mathbf{H}} \tag{4.48}$$

and

$$\mathbf{\Phi^i_p} = \left[\begin{array}{cccccc} b^i_{0,p} & \cdots & b^i_{N_U-1,p} & b^{i-1}_{0,p} & \cdots & b^{i-1}_{N_U-1,p} \end{array} \right]^{\mathbf{T}} \tag{4.49}$$

be a parameter vector corresponding to the m^{th} element of the DFT output vector of the p^{th} parallel symbols during the i^{th} symbol interval and an input vector corresponding to the p^{th} parallel symbols during the i^{th} symbol interval, respectively. From (4.1), the estimate of $x^i_p[m] = x^i\left[pN_S + m\right]$ can be expressed as

$$\hat{x}^i_p[m] = \left(\mathbf{\Theta^i_{p,m}}\right)^H \mathbf{\Phi^i_p}. \tag{4.50}$$

The error function in (4.3) can be rewritten in the matrix form as

$$e^i\left[m\right] = x^i_p\left[m\right] - \left(\mathbf{\Theta^i_{p,m}}\right)^H \mathbf{\Phi^i_p}. \tag{4.51}$$

The RLS algorithm is initialized at $n = 0$ iteration by setting

$$\mathbf{\Theta^0_{p,m}} = \mathbf{0} \tag{4.52}$$

and

$$\mathbf{P}^0 = \delta_{RLS}\mathbf{I}_{2N_U \times 2N_U} \tag{4.53}$$

where δ_{RLS} is a small positive constant. At the n^{th} iteration, the algorithm computes

$$\mathbf{q}^n = \mathbf{P}^{n-1}\mathbf{\Phi^n_p}, \tag{4.54}$$

$$\mathbf{k}^n = \frac{\mathbf{q}^n}{\lambda + \left(\mathbf{\Phi^n_p}\right)^H \mathbf{q}^n}, \tag{4.55}$$

$$\hat{x}^n_p[m] = \left(\mathbf{\Theta^{n-1}_{p,m}}\right)^H \mathbf{\Phi^n_p}, \tag{4.56}$$

$$e^n[m] = x_p^n[m] - \hat{x}_p^n[m], \tag{4.57}$$

$$\mathbf{\Theta_{p,m}^{n}} = \mathbf{\Theta_{p,m}^{n-1}} + \mathbf{k^n}\left(\mathbf{e^n}[\mathbf{m}]\right)^*, \tag{4.58}$$

and

$$\mathbf{P}^n = \lambda^{-1}\mathbf{P}^{n-1} - \lambda^{-1}\mathbf{k}^n\left(\mathbf{\Phi_p^n}\right)^H\mathbf{P}^n \tag{4.59}$$

where λ is the exponential weighting factor which lies in the interval $0 < \lambda \leq 1$.

4.3 Noise Variance Estimation

The estimate of noise variance is required for some multiuser detection techniques, such as the linear MMSE detector. The noise variance can be estimated by considering a variance of the m^{th} entry of the DFT output associated with the p^{th} parallel symbols:

$$\left(\sigma_x\left[pN_S + m\right]\right)^2 = E\left\{x_p^i[m]\left(x_p^i[m]\right)^*\right\}. \tag{4.60}$$

By substituting the term in (4.1) into (4.60) and using the assumption that data and noise are uncorrelated, (4.60) can be elaborated as

$$\left(\sigma_x\left[pN_S + m\right]\right)^2 = \sum_{k=0}^{N_U-1}\left(\bar{c}_{k,p,D}^{i,pN_S+m}\right)^2 + \sum_{k=0}^{N_U-1}\left(\bar{c}_{k,p,I}^{i,pN_S+m}\right)^2 + N_C\left(\sigma_\eta\right)^2. \tag{4.61}$$

As a result, the noise variance can be approximated as

$$\left(\sigma_\eta\right)^2 = \frac{1}{N_C}\left(\left(\sigma_x\left[pN_S + m\right]\right)^2 - \sum_{k=0}^{N_U-1}\left(\bar{c}_{k,p,D}^{i,pN_S+m}\right)^2 - \sum_{k=0}^{N_U-1}\left(\bar{c}_{k,p,I}^{i,pN_S+m}\right)^2\right). \tag{4.62}$$

In the real application, the expectation operation in (4.60) is approximated by the time averaging. The approximated noise variances for each DFT output are averaged to yield the final noise variance estimate.

4.4 Simulation Results and Discussion

This section presents the simulation results on the proposed parameter estimation techniques and the MUD-ISIC, applied the proposed parameter estimation techniques. The key parameters, used in the simulations, are the same as that outlined in the previous chapter (table 3.1). The simulated MC-CDMA systems have processing gain 32. The transmission is carried out using a packet frame consisting of 65 training symbols succeeding by 512 data symbols. Since the cyclically orthogonal training sequences are the best among 3 optimum training sequence families, only the cyclically orthogonal training sequences are used in the simulations. Channel is assumed to vary at a rate slow enough that it can be regarded as essentially fixed during a burst. The time averaging over one packet frame is used for a noise estimation process (section 4.3).

4.4.1 Performance of the Transformed Signature Sequence and ISI Generation Sequence Estimator

Since the development of algorithms in this dissertation are based on the sub-band approach as discussed in the previous chapter, the existence of cross parallel symbol interference is considered as negligible due to the use of CSA scheme. the cross parallel symbol interference is thus omitted from the derivation. In order to show the validity of the theoretical minimum MSE (4.25), the simulated system, having only one active subcarrier group, is considered so that the detection of the active parallel symbols is free from the cross parallel symbol interference. For the serial to parallel conversion size of $N_P = 8$, only one subcarrier group out of the total 8 subcarrier groups carries the training symbols. The other 7 subcarrier groups are left unused, or, in the other word, transmit the null symbols. The MSE of the proposed estimator versus a number of users for such system is plotted in figure 4.3. Signal to noise ratio per bit (Eb/N0) is set at 10 and 20 dB. From figure 4.3, the MSE is independent of channel MIP type. The LS estimator using the optimum training sequences can accomplish the minimum MSE. The MSE of the LS estimator using the optimum training sequences is independent of a number of users. The LS estimator using the random training sequences only gives satisfactory low MSE in a system with small number of users. The MSE difference between the LS estimator using the optimum training sequence and that using the random training sequence is substantial in a system with large number of users. This difference does not linearly increase proportional to a number of users but it is likely to grow in an exponential rate. The performance of the adaptive estimator is similar to the LS estimator. The adaptive estimator using the optimum training sequences also achieves the minimum MSE and it is robust to the system load. The MSE of the adaptive estimator using the random training sequences degrades as a number of users increases. In case of using the random training sequences, the adaptive estimator is more robust to the increasing number of users than the LS estimator. This property is from the inherent capability of the RLS algorithm over the explicit inversion of the near singular matrix of the direct LS method.

Since the LS estimator employing the optimum training sequences has relatively low complexity and the adaptive estimator does not show any superiority over the LS estimator for the case of optimum training sequences, the application of the adaptive estimator during the training period is not much beneficial. However, the adaptive estimator may be useful for the decision direct estimation due to the randomness nature of the data. The decision direct operation will be discussed in more detail later in this chapter.

Figure 4.4 presents the MSE of the estimator for the fully operated system where the cross parallel symbol interference exists. It is seen from the figure that the cross parallel symbol interference results in the error floor from the theoretical minimum MSE for both the LS estimator and the adaptive estimator. However, the advantage of the optimum training sequences over the random training sequences is still obvious. The optimum training sequences provide the robustness against the increasing number of users. The LS estimator and the adaptive estimator, employing the optimum training sequences, yield similar MSE, whereas the adaptive estimator give lower

MSE than the LS estimator for the random training sequences.

The advantages of the optimum training sequence over the random training sequences is emphasized in figure 4.5 where the BER of the MUD-ISIC employing several estimation techniques is plotted as a function of a number of users. The linear MMSE detector is used in the multiuser detection part of the MUD-ISIC. As expected, the optimum training sequences give the lower BER than the random training sequences.

4.4.2 Performance Over the Serial to Parallel Conversion Size - Cyclic Prefix Length Grid

In the previous chapter, the simulation results for the systems, provided the perfect knowledge of all the required parameters, demonstrate that the best performance is achieved in the system with insufficient cyclic prefix regardless of the serial to parallel conversion size. This section will investigate the claim for more realistic systems with parameter estimation. The 8 users system with fully operated subcarrier groups is considered. Eb/N0 = 10 dB, $\left(\sigma_{\Delta_f}\right)^2 = 62.5$ kHz, maximum asynchronous delay is 1 μsec and the linear MMSE detector is used for the multiuser detection part. The simulated system employs cyclically orthogonal training sequences and the transformed signature sequences and the ISI generation sequence are estimated by using the LS estimator. The BER of the receiver as a function of serial to parallel conversion size and cyclic prefix is plotted in figure 4.6. As can be seen, the error in estimation process only raises the BER level from the perfect estimation case. The best performance is still obtained in the insufficient cyclic prefix environment for both the uniform MIP channel and the exponentially decaying MIP channel. The power loss due to the cyclic prefix insertion degrades the BER. Increasing the serial to parallel conversion size may alleviate such power loss but it poses another adverse consequence to the system performance.

4.4.3 Multiuser Detection Techniques Comparison

This section studies an influence of the proposed estimation techniques to the MUD-ISIC employing several multiuser detection techniques. In figure 4.7-4.16, performance of the MUD-ISIC using various multiuser detection techniques is compared in the uniform MIP channel and the exponentially decaying MIP channel. The simulated system uses the LS estimator, provided the cyclically orthogonal training sequences. The MC-CDMA systems without cyclic, having 8, 16, 24, and 32 users, are considered and the serial to parallel conversion size is set at 8. Several configurations of WMIC in table 3.3 are evaluated and compared.

Compare figure 4.7-4.16 with figure 3.16-3.25, it is seen that error from the estimator only slightly degrades the BER. For example, in the 24 users system, using the MUD-ISIC employing MMSE-WMIC.(1) and MMSE-WMIC.(2) under the uniform MIP channel (figure 4.9 and 3.18), the system with parameter estimation only requires 2 dB higher Eb/N0 in order to attain the same

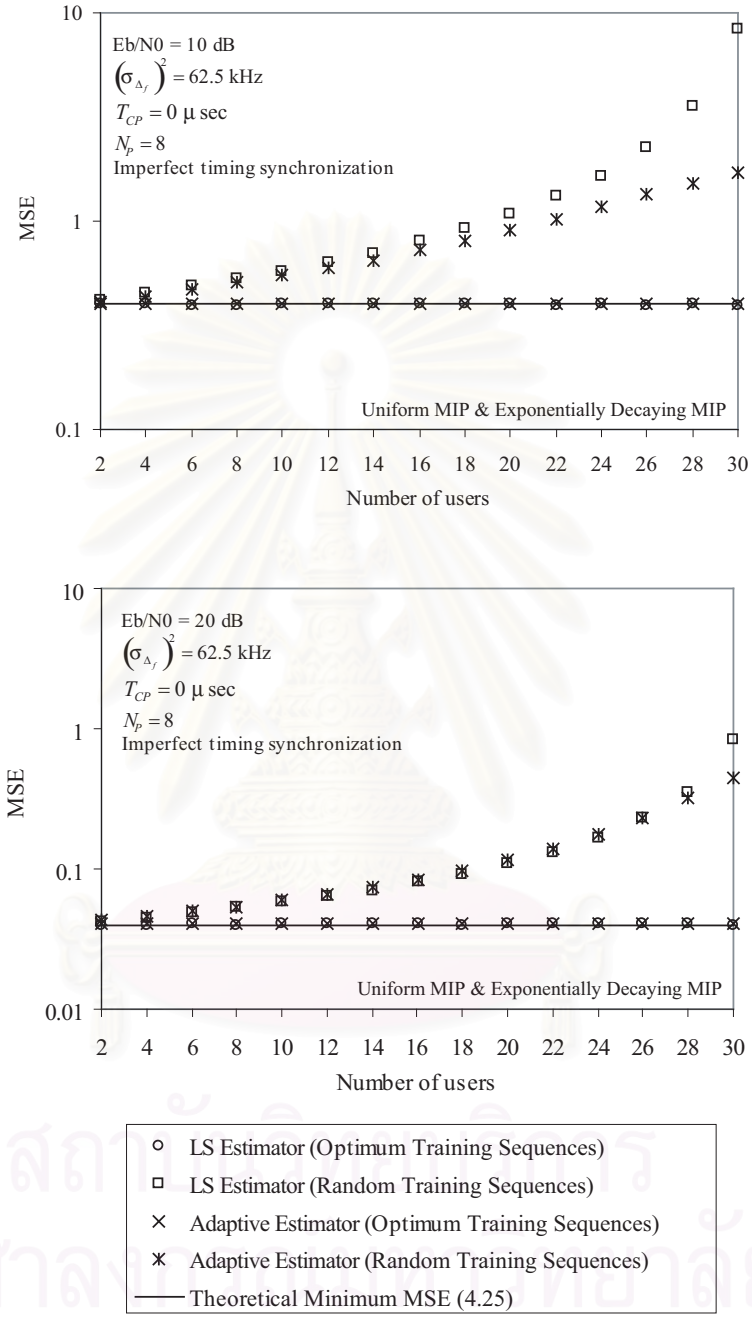

Figure 4.3: MSE of the transformed signature sequences and ISI generation sequence estimator for the system having only one active subcarrier group

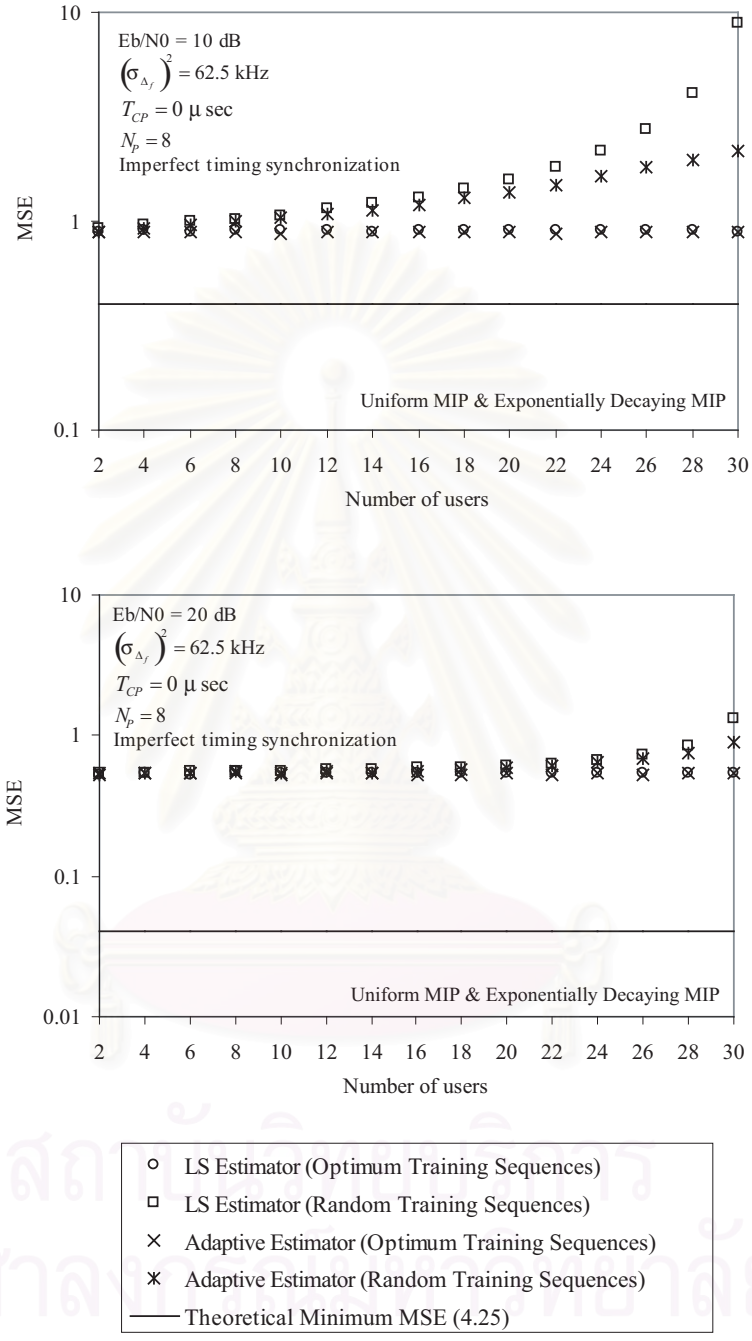

Figure 4.4: MSE of the transformed signature sequences and ISI generation sequence estimator for the system with 8 fully active subcarrier groups

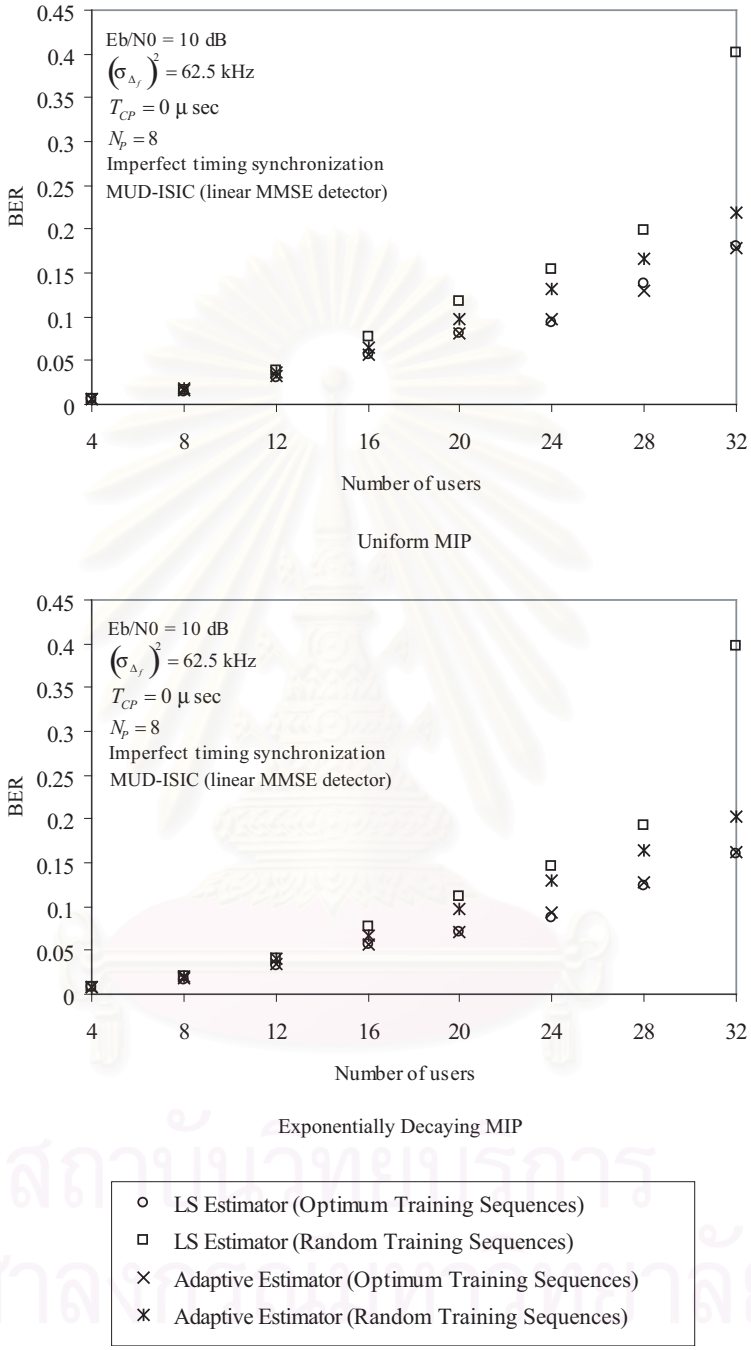

Figure 4.5: BER of MUD-ISIC (linear MMSE detector) employed various parameter estimation techniques

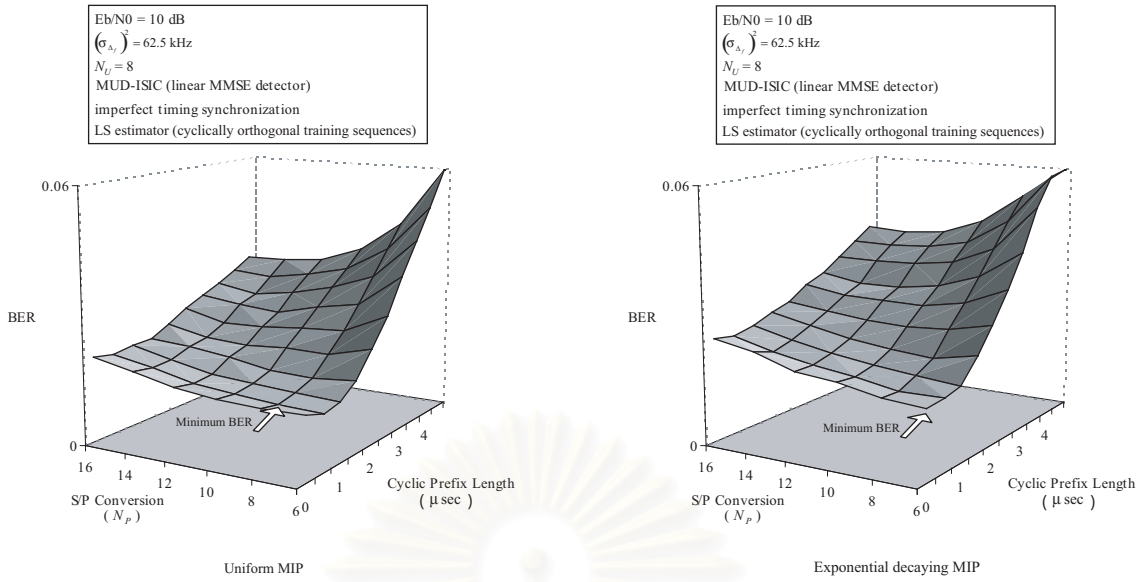

Figure 4.6 BER of MUD-ISIC (linear MMSE detector) using LS estimator

BER at 0.01 as the system with perfect parameter information. This small degradation confirms the effectiveness of the proposed estimation techniques.

Similar to the perfect parameter estimation case, the best multiuser detection technique is also a MMSE-WMIC.(2). The promising performance of the non-linear multiuser detection technique is still obvious in the system with imperfection. The noise variance estimation has a significant contribution to the receiver performance. The linear MMSE detector, provided the noise variance estimate, greatly outperforms the DD, which does not require the noise variance estimation. Without noise variance estimation, the DD can only give satisfactory BER in the high Eb/N0 region of the system with low to moderate number of users. The DD is even unusable in the system with full load. Only few increment in complexity for noise variance estimation allows the linear MMSE detector to operate in the low Eb/N0 region and also in the highly loaded systems.

Figure 4.17 shows the basic improvement by increasing the training symbol transmission power. The simulated system for the figure is the system without cyclic prefix supporting 8 active users, serial to parallel conversion size is 8, and the Eb/N0 is 10 dB.

4.4.4 Performance Comparison with the Other Receivers

The advantage of the MUD-ISIC over the other receivers is obvious for the system, provided perfect parameter information. In this section, the performance comparison in the system with parameter estimation is presented. The performance of the truncated time-domain MMSE multiuser detector [34] and the MMSE-DFE [35] is excluded from consideration because of their inferiority to the frequency offset and their unacceptable requirement of knowledge about actual channel impulse response. The technique for estimating multipath coefficients and delays [78] severely

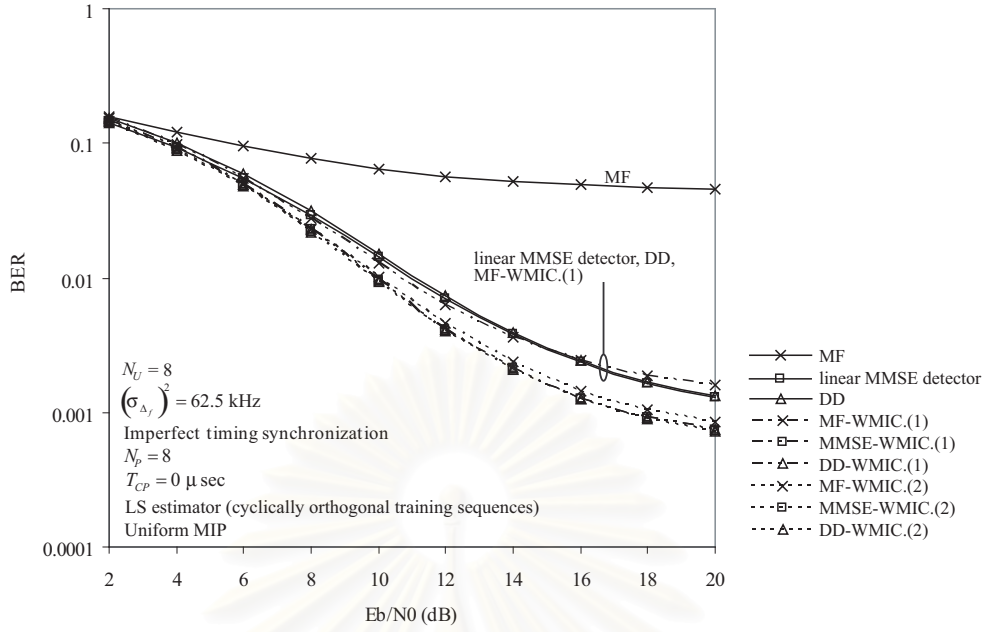

Figure 4.7: BER of the MUD-ISIC, employed various multiuser detection techniques, for 8 users system with LS estimator (cyclically orthogonal training sequences) under the uniform MIP channel

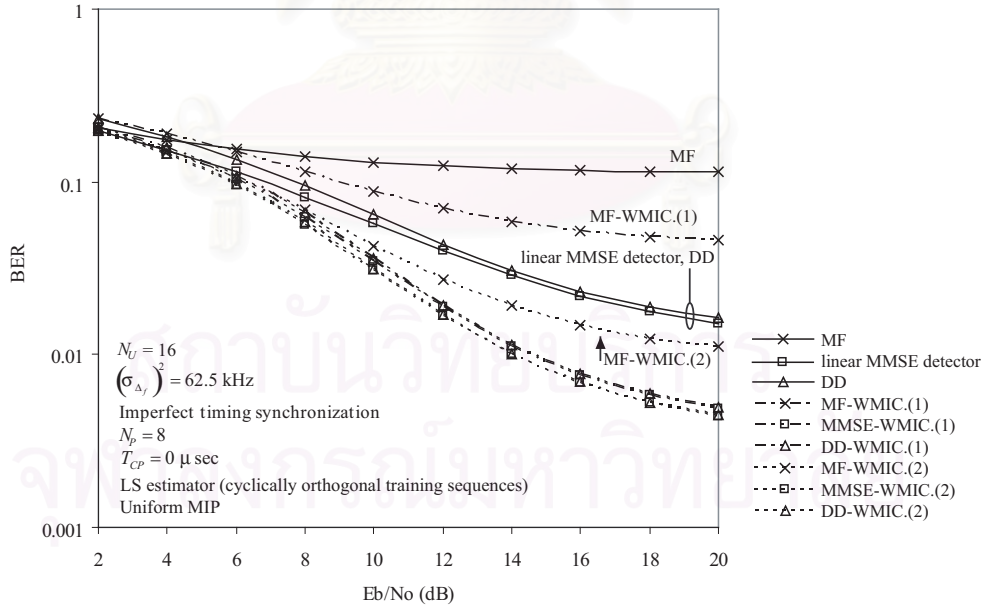

Figure 4.8: BER of the MUD-ISIC, employed various multiuser detection techniques, for 16 users system with LS estimator (cyclically orthogonal training sequences) under the uniform MIP channel

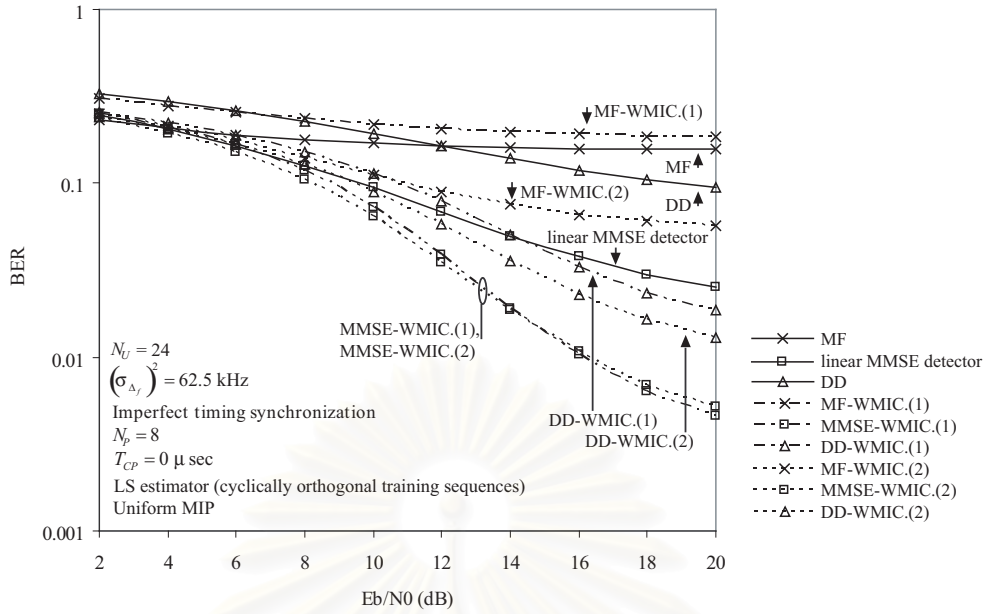

Figure 4.9: BER of the MUD-ISIC, employed various multiuser detection techniques, for 24 users system with LS estimator (cyclically orthogonal training sequences) under the uniform MIP channel

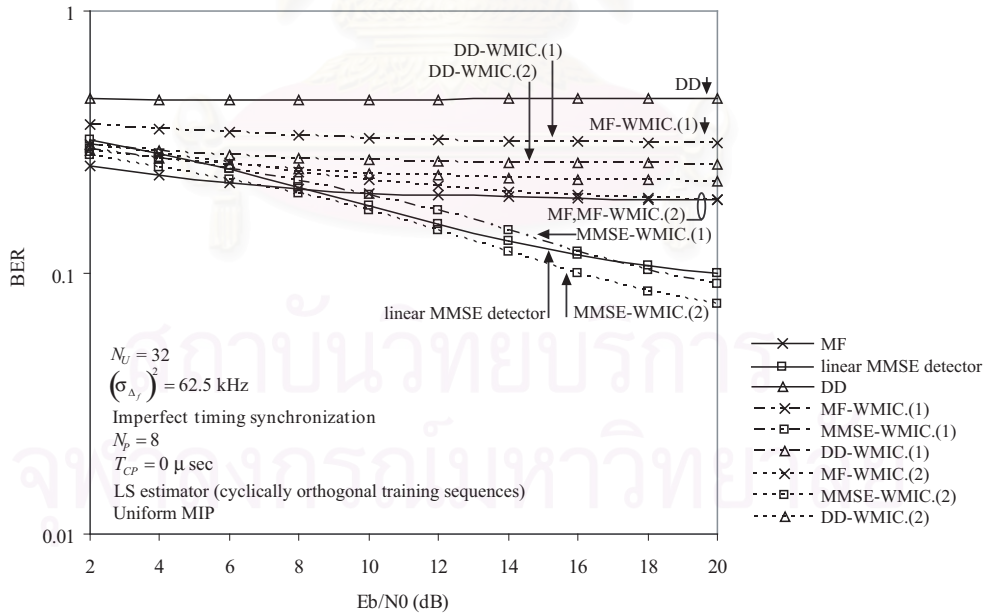

Figure 4.10: BER of the MUD-ISIC, employed various multiuser detection techniques, for 32 users system with LS estimator (cyclically orthogonal training sequences) under the uniform MIP channel

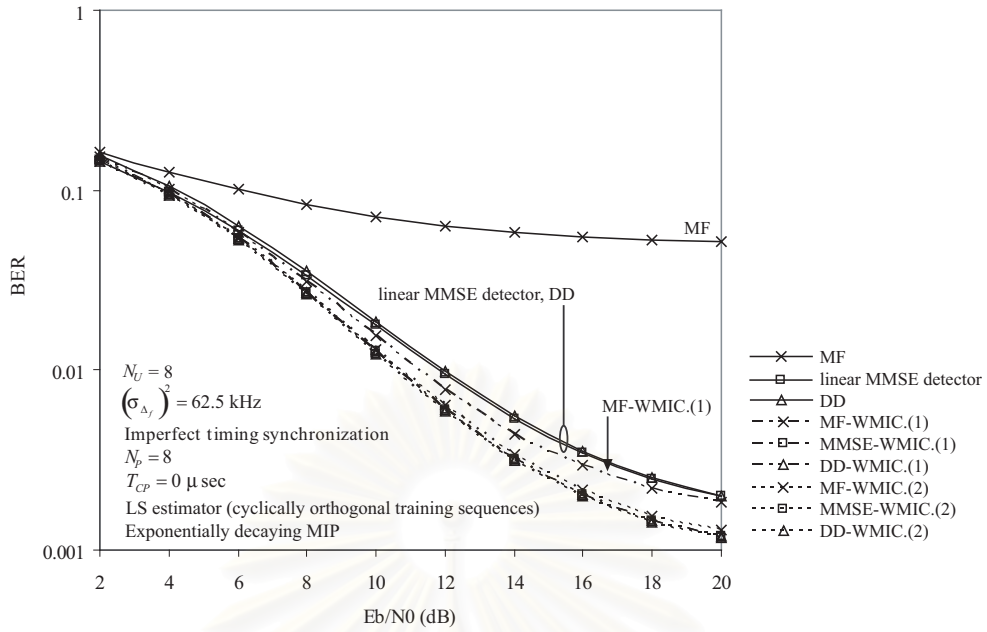

Figure 4.11: BER of the MUD-ISIC, employed various multiuser detection techniques, for 8 users system with LS estimator (cyclically orthogonal training sequences) under the exponentially decaying MIP channel

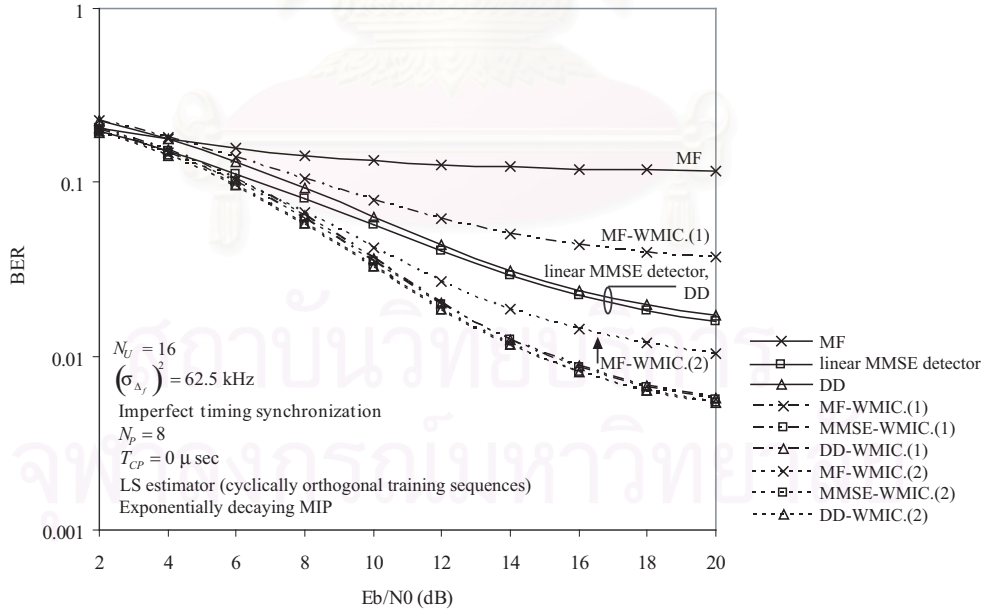

Figure 4.12: BER of the MUD-ISIC, employed various multiuser detection techniques, for 16 users system with LS estimator (cyclically orthogonal training sequences) under the exponentially decaying MIP channel

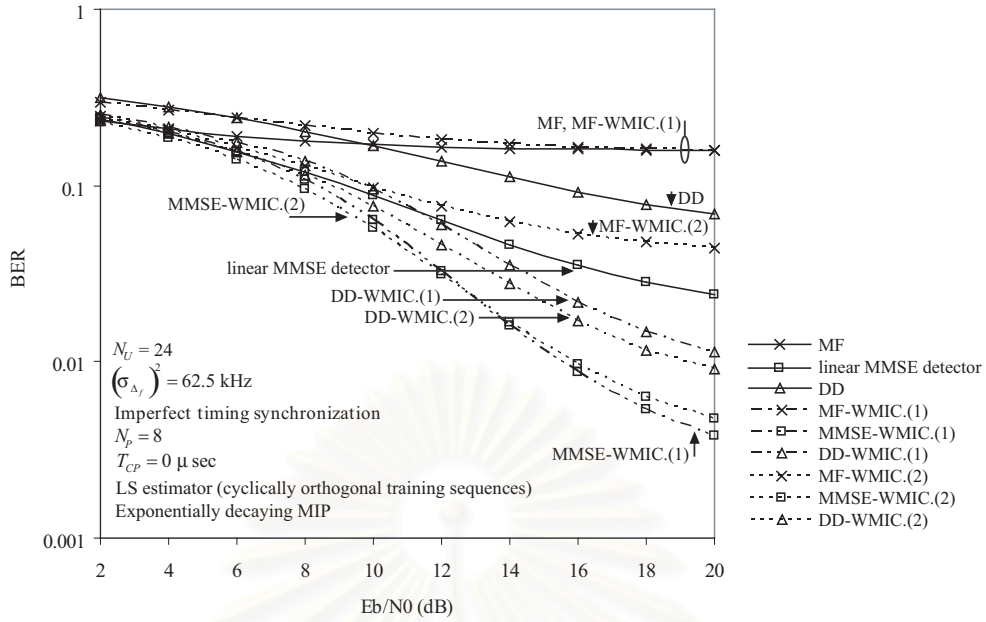

Figure 4.13: BER of the MUD-ISIC, employed various multiuser detection techniques, for 24 users system with LS estimator (cyclically orthogonal training sequences) under the exponentially decaying MIP channel

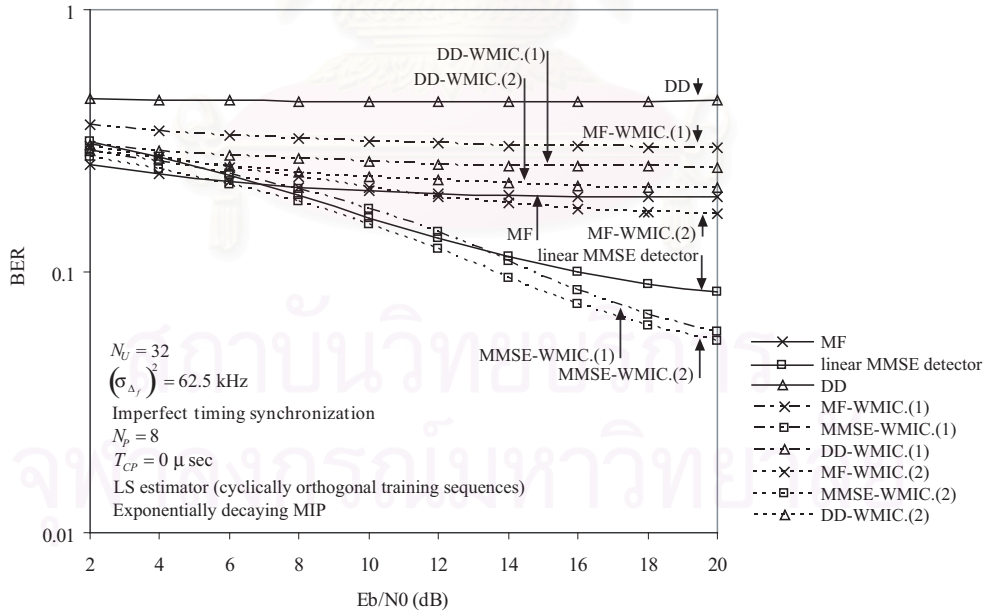

Figure 4.14: BER of the MUD-ISIC, employed various multiuser detection techniques, for 32 users system with LS estimator (cyclically orthogonal training sequences) under the exponentially decaying MIP channel

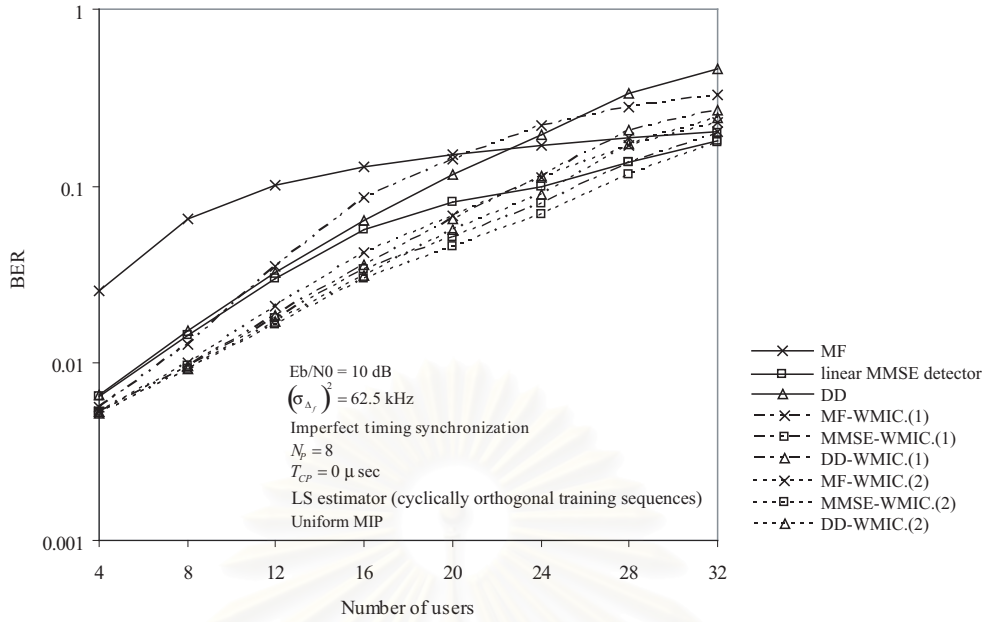

Figure 4.15: BER of the MUD-ISIC, employed various multiuser detection techniques, versus the number of users in the system with LS estimator (cyclically orthogonal training sequences) under the uniform MIP channel

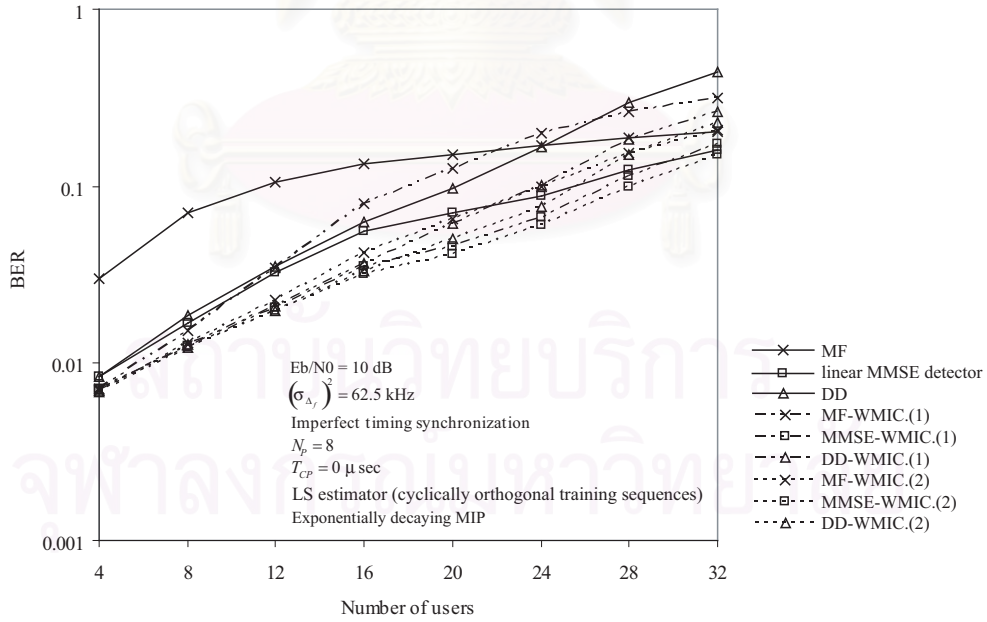

Figure 4.16: BER of the MUD-ISIC, employed various multiuser detection techniques, versus the number of users in the system with LS estimator (cyclically orthogonal training sequences) under the exponentially decaying MIP channel

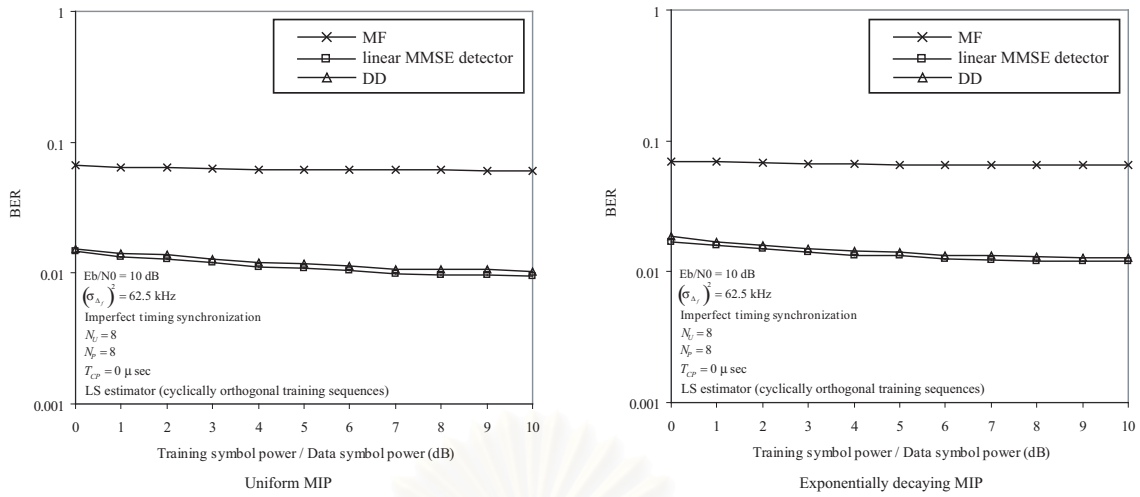

Figure 4.17: BER of the MUD-ISIC (linear MMSE detector) versus the training symbol power in the system with LS estimator using cyclically orthogonal training sequences

suffers from several disadvantages as discussed at the beginning of this chapter. These drawbacks even prohibit the implementation of such estimator in a real system. Furthermore, the algorithm in [78] only supports a forward link case. Thus, it cannot be operated in the target reverse link. In addition, this channel impulse response estimation technique as well as the receivers themselves is not capable to work under the presence of the frequency offset.

Two estimators, which were designed for sufficient cyclic prefix presumed reverse link multicarrier systems, provide estimates of the multiplicative subcarrier coefficients to the frequency offset compensated MMSE detector. Both estimators deliver the estimates of subcarrier coefficients to the detector, but only the recursive estimator based on the EKF additionally give the estimates of frequency offset to the detector. The noise variance estimation algorithm, proposed in this dissertation, is used for both the MUD-ISIC employing the linear MMSE detector and the frequency offset compensated MMSE detector.

For a conventional sufficient cyclic prefix presumed approach, a transmitter adds 2 μ sec cyclic prefix to each multicarrier symbol in order to compensate for the maximum effective channel delay. In this case, the cyclic prefix is approximately 23.8 % of the total symbol power (for bandwidth=40MHz, $N_P = 8$, $N_S = 32$, $N_C = 256$, $T_B = 6.4\mu\,\text{sec}$, $T_S = T_{CP} + T_B = 2 + 6.4 = 8.4\mu\,\text{sec}$). For the system, supporting upto 32 users, the sufficient cyclic prefix presumed reverse link estimator requires 32 training symbols, whereas the proposed estimator requires 65 training symbols (for the cyclically orthogonal training sequences). This larger number of training symbols may mislead the system designer that the proposed technique has lower bandwidth efficiency than the sufficient cyclic prefix approach. However, in fact, the proposed technique gains much more bandwidth efficiency due to the capability to neglect the cyclic prefix. Figure 4.18 shows the achievable symbol rate versus a number of data symbols in a packet frame for the system without cyclic prefix and the sufficient cyclic prefix presumed system. From the figure, the sufficient cyclic prefix presumed system offers better bandwidth utilization efficiency

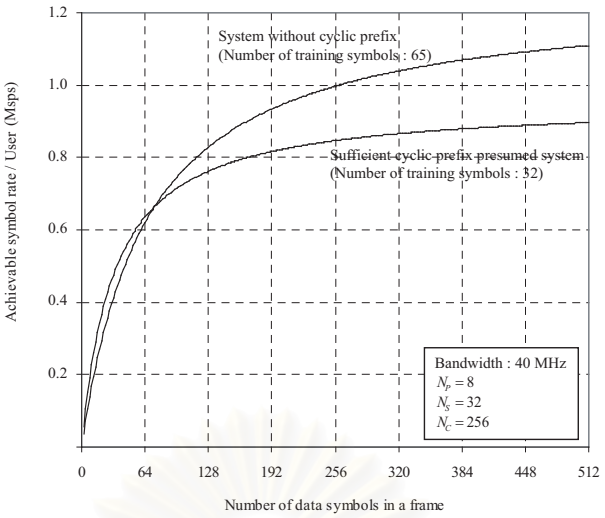

Figure 4.18 Achievable symbol rate as a function of number of data symbol in a packet frame

only in the case that a number of data symbols within a frame are less than 74. A small ratio between number of data symbols and number of training symbols results in a low total achievable symbol rate. It is seen from the figure that the symbol rate of the sufficient cyclic prefix presumed system never reaches the 1 mega symbols per second (Msps) level. In addition to the better bandwidth efficiency, a higher number of training sequences also gives a more accurate estimation.

In the following, the comparison on the systems using the same number of training sequences and the same cyclic prefix length will be presented. Each packet frame contains 65 training symbols. BER versus the cyclic prefix length in the perfect frequency synchronized system is depicted in figure 4.19. The frequency offset compensated MMSE detector acquires the subcarrier coefficients by using the conventional reverse link estimator. Similar to the case of having perfect knowledge about channel parameters, the MUD-ISIC is more robust to the cyclic prefix length than the frequency offset compensated MMSE detector. The frequency offset compensated MMSE detector requires large amount of cyclic prefix to attain the same BER level as the MUD-ISIC. By comparing figure 4.19 and figure 3.28, it can be observed that error in parameter estimation process widens the performance gap between 2 receivers in the insufficient cyclic prefix environment. The frequency offset compensated MMSE detector slightly outperforms the MUD-ISIC in the system with sufficient cyclic prefix. This result is due to an error in the ISI generation sequences estimation process. In fact, the ISI generation sequence matrix should be a zero matrix if the cyclic prefix is longer than the maximum effective channel delay. However, due to the error in the estimation process, probably from a background noise, the estimated ISI generation sequence matrix is close to but not a zero matrix. Thus, in this case, the performance of MUD-ISIC is slightly inferior to that of the frequency offset compensated MMSE detector which does not have ISI cancellation part. However, from the practical standpoint, the system having such large cyclic prefix would never employ the proposed MUD-ISIC.

Figure 4.20 depicts the performance of the receivers in the system with imperfect frequency

synchronization. In this case, the conventional reverse link subcarrier coefficients estimator, which cannot be operated in the presence of frequency offsets and is certainly unable to estimate the frequency offsets, is replaced by the EKF estimator. The frequency offset compensated MMSE detector, using the EKF estimator, is examined in the system with 4 and 8 users. Figure 4.20 clearly confirms the effectiveness of the proposed parameter estimation technique in the system with frequency offsets. The MUD-ISIC outperforms the frequency offset compensated MMSE detector regardless of the cyclic prefix length.

4.5 Sequences Estimation During a Data Period

The ISI generation sequences and the transformed signature sequences have already been successfully estimated by using the proposed estimator. The proposed estimator uses the information of the known transmitted symbols (training sequences) to acquire the parameter estimates. For a data period, the parameter estimates, obtained during a training period, are used. Unfortunately, channel is naturally time-varying. The necessary parameters, which are the functions of channel impulse response, also vary in time. This section presents techniques for tracking the parameters variation.

The parameter estimation during a data period can be accomplished by 2 schemes. The first method is the decision-direct estimation, which uses the detected symbols as the known transmitted symbols. The LS estimator, which requires matrix inversion, is inferior to the adaptive estimator for the decision-direct estimation. For a training period, the matrix inversion is only calculated once and may possibly be calculated off-line. Therefore, the receiver does not need to calculate matrix inversion. As a consequence, the use of random training sequences in the training period is feasible. For the decision-direct estimation, the matrix inversion has to be frequently recalculated due to the randomness of data. Moreover, according to the simulation results, the adaptive estimator outperforms the LS estimator in case of the random training sequences. Therefore, only the adaptive estimator is considered for decision-direct estimation in this dissertation.

The other method is simple and does not depend on the detected symbols. The parameter estimates during a data period is determined by interpolating two set of parameter estimates obtained from training period at the beginning of the current packet frame and at the beginning of the next packet frame. The interpolation can be carried out by averaging method or linear interpolation method. The averaging method regards a channel as time invariant during a data period. The parameter estimates from two training periods are averaged. The resulting parameter estimates are used through out the entire data period. Linear interpolation method models the time variation by a linear function. For the linear interpolation method, the estimates of parameters during a data period is given by

$$\hat{x}^{i_D} = \left(\frac{x^{\langle 2 \rangle} - x^{\langle 1 \rangle}}{N_D} \right) i_D + x^{\langle 1 \rangle}. \tag{4.63}$$

where $x^{\langle 1 \rangle}$ is a parameter estimated from the beginning of the current packet frame, $x^{\langle 2 \rangle}$ is a

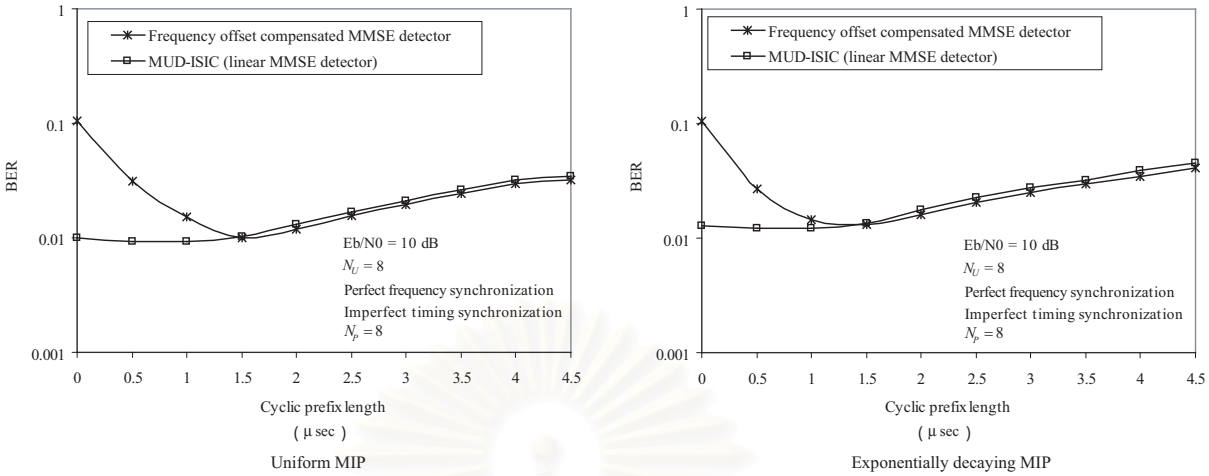

Figure 4.19: Performance of the frequency offset compensated MMSE detector using conventional reverse link subcarrier coefficient estimator and the MUD-ISIC (linear MMSE detector) using the LS estimator with cyclically orthogonal training sequences under the perfect frequency synchronization situation

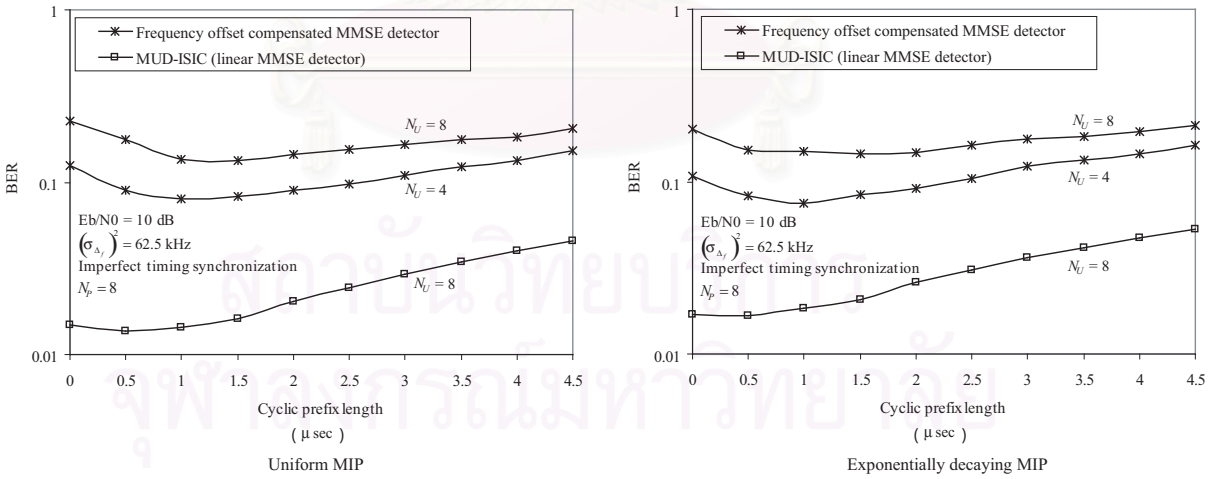

Figure 4.20: Performance of the frequency offset compensated MMSE detector using EKF estimator and the MUD-ISIC (linear MMSE detector) using the LS estimator with cyclically orthogonal training sequences under the imperfect frequency synchronization situation

parameter estimated from the beginning of the next packet frame, N_D is a number of data symbol in a packet frame, i_D is a data symbol index in a packet frame; $0 \leq i_D < N_D$, and $\hat{x}^{i_D}$ is an interpolated parameter at the $(i_D)^{th}$ data symbol.

Figure 4.21 compares the performance of each tracking techniques applied to the LS estimator using the cyclically orthogonal training sequences. The linear MMSE detector is used in the multiuser detection part of the MUD-ISIC. A packet frame consists of 65 training symbols and 512 QPSK modulated data symbols. The channel, having Jakes' Doppler power spectral density, is generated by using the L_p-Norm method [65]. For adaptive estimator, the forgetting factor is set at 0.9999, 0.99, and 0.9. The simulated symbol does not use cyclic prefix. From figure 4.21, the best BER is obtained by using the linear interpolation method. The linear interpolation method performs mostly better than the averaging method. However, the averaging method can slightly outperform the linear interpolation method in the system with very slow variation. This is because the averaging method gains from the virtually double number of training symbols. The performance of the adaptive estimator is not good and strongly depended on the forgetting factor value. For the channel with doppler frequency 0 Hz, BER of the detected symbols assisted adaptive estimator is inferior to the methods, which are independent of the detected symbols. It should be recalled that the adaptive estimator without decision direct operation can perform in the same level as the LS estimator in the time-invariant channel. This means that the errors in symbol detection pose significant adverse impact on the decision direct estimator.

Figure 4.22 shows the performance in the system having only 260 data symbols in each packet frame. According to figure 4.18, a packet frame, consisting of 260 data symbols, results in a 1 Msps effective symbol rate per user. Compared figure 4.22 with figure 4.21, the obvious performance improvement can be observed with loss of approximately 100 Ksps effective symbol rate per user.

4.6 Summary

In this chapter, the parameter estimation techniques for the MUD-ISIC have been presented. The proposed estimators avoid the obstacles in explicitly estimating the channel impulse response by directly estimating the necessary sequences, transformed signature sequences and ISI generation sequences. Following from the estimator MSE analyses, the conditions for training sequences to achieve the minimum MSE and the systematic generation of the optimum training sequences have been presented. The sequence estimation is derived by the traditional LS approach and the recursive implementation is also investigated.

Simulation results have clearly demonstrated the advantages of the optimum training sequences over the random training sequences. Compared with the simulation results in the previous chapter where the perfect information of the necessary parameter is available at the receivers, the simulation results in the system with parameter estimation show the similar characteristics. In summary, the best performance is still obtained in the system with insufficient

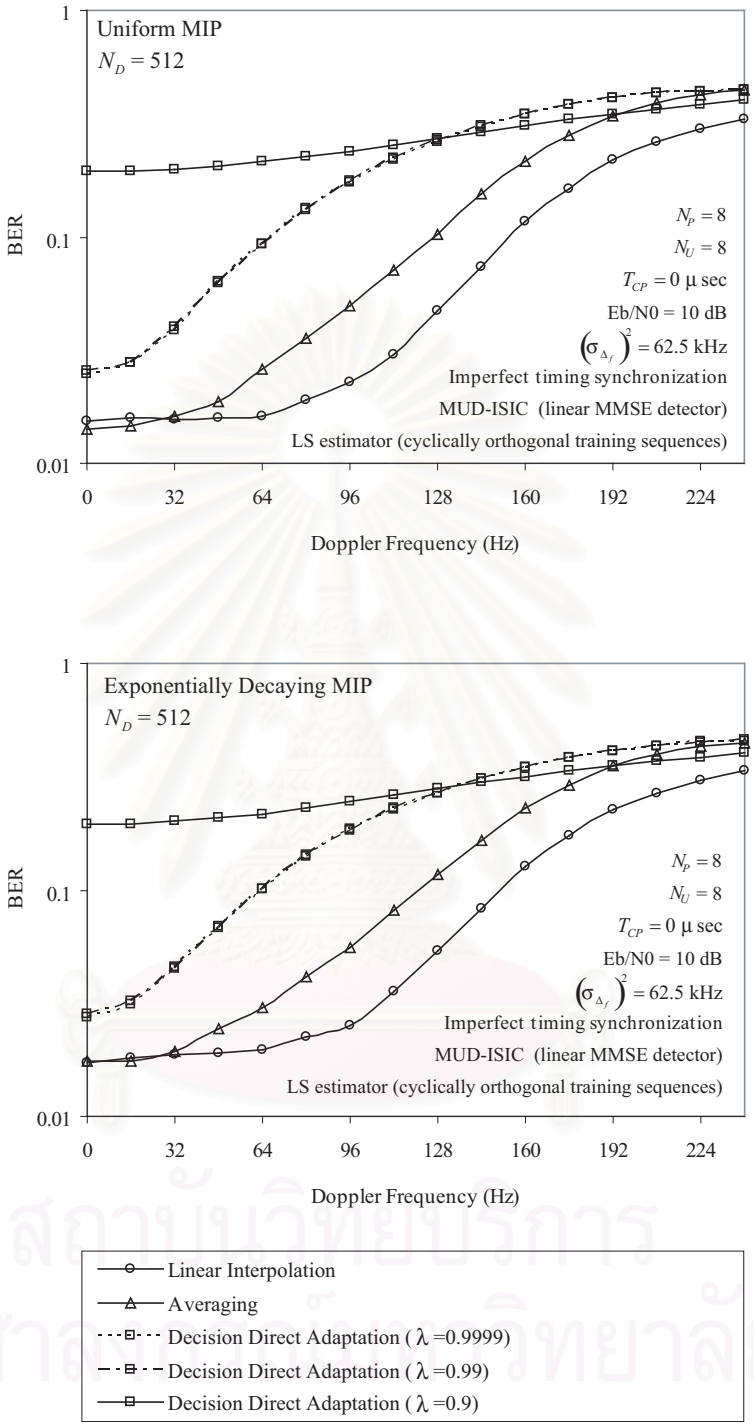

Figure 4.21: Performance of the MUD-ISIC (linear MMSE detector) using various parameter estimation techniques during a data period for the system having 512 data symbols in each packet frame

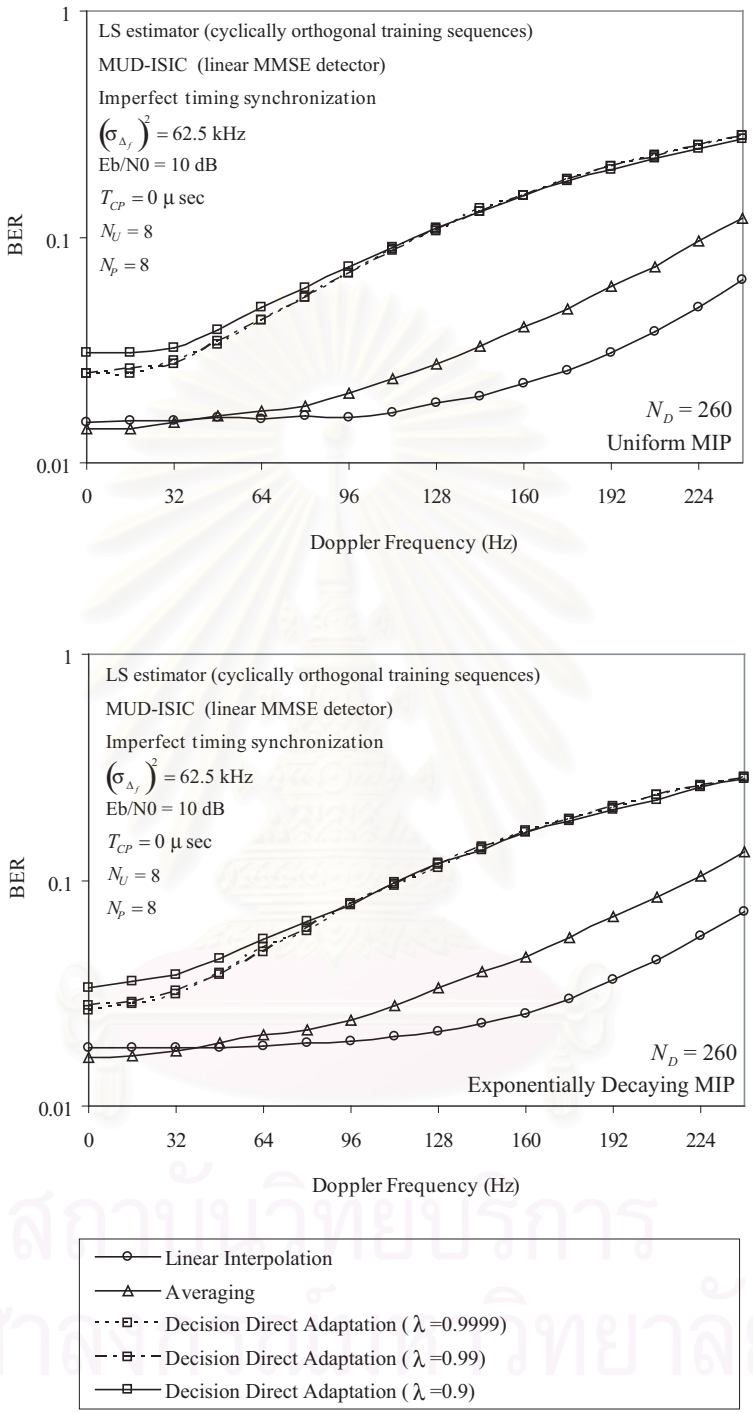

Figure 4.22: Performance of the MUD-ISIC (linear MMSE detector) using various parameter estimation techniques during a data period for the system having 260 data symbols in each packet frame

cyclic prefix and the best multiuser detection technique remains the WMIC employing the linear MMSE detector. These results further insist the merits of the proposed receiver.

This chapter also presents the noise variance estimation technique. The proposed noise variance estimation technique significantly helps improving the BER because this technique enables the linear MMSE detector which is much better than the DD.

The algorithms for tracking variation of the estimated parameters during a data period have also been studied. According to the simulation results, the decision direct adaptation is susceptible to the error in symbol detection. The linear interpolation method is the best technique in most cases except in the very slow varying channel that the averaging method is slightly better.

CHAPTER V

CONCLUSIONS

A MC-CDMA system has received considerable attention as a potential air-interface technique for the future wireless communication. However, its performance, especially in a reverse link, suffers from ISI, ICI, and MAI. In order to attain good communication quality, such interference has to be carefully handled.

This dissertation has proposed a new technique to jointly overcome an insufficient cyclic prefix problem, a frequency offset problem, and a multiple access interference problem in a quasi-synchronous reverse link MC-CDMA system. The receiving techniques for a reverse link are much more complicated than the techniques for a forward link owing to the fact that each user experiences different channels and different frequency offsets in the reverse link. Since the forward link is a special case of the reverse link where channels and frequency offsets are common for all the users, the proposed technique can be simplified to work in the forward link as well. From the models, analyzed in chapter 2, the original signature sequences are distorted by channel fading, insufficient cyclic prefix situation, and frequency offsets. The insufficient cyclic prefix condition incurs additional ISI, of which amount is determined by channels, cyclic prefix length, and frequency offsets.

The proposed technique, namely MUD-ISIC, is composed of 2 parts. The first part performs ISI cancellation and the other part performs MAI suppression by using multiuser detection techniques. The equalization of frequency offsets and insufficient cyclic prefix problem are integrated along with the MAI suppression in the multiuser detection part. The proposed MUD-ISIC can support a number of multiuser detection techniques, available in the literatures. This flexibility benefits the system designer in compromising cost and performance. In addition, compared with the existing receivers which only consider the linear MMSE approach, the non-linear detection techniques can offer relatively good performance. According to the simulation results, the best multiuser detection technique is a WMIC using linear MMSE detector in the initial stage. The potential of the alternative non-linear multiuser detection brings the attractiveness to the proposed MUD-ISIC.

Simulation results have demonstrated merits of the proposed MUD-ISIC in various aspects. It can outperform the truncated time-domain MMSE multiuser detector in the system with perfect frequency synchronization and insufficient cyclic prefix. In such system condition, the MUD-ISIC is equivalent to the MMSE-DFE. For the system with imperfect frequency synchronization, performance of both the truncated time-domain MMSE multiuser detector and the MMSE-DFE is rapidly deteriorated. Even small frequency offsets can severely affect both receivers. On the other hand, the MUD-ISIC shows satisfactory robustness against the frequency offsets. The frequency offset compensated MMSE detector is also robust to the frequency offsets. However,

its performance is obviously inferior to the performance of the MUD-ISIC in the system with insufficient cyclic prefix.

One of the major advantages of the MUD-ISIC is that it enables the implementation of MC-CDMA system without cyclic prefix or with small amount of cyclic prefix. Without cyclic prefix, the system can utilize bandwidth more efficiently. The sufficient cyclic prefix condition helps simplifying the receiver in the forward link. This property is very desirable since a receiver in the forward link is a mobile unit, which has a limited complexity allowance. For the reverse link, the sufficient cyclic prefix condition does not contribute much on the receiver complexity. In addition, a complexity constraint for base station is quite relaxed. Therefore, a system without cyclic prefix for reverse link is practically interesting. According to the simulation results, the power loss due to the introduction of cyclic prefix substantially degrades the BER. This power loss may be alleviated by using the serial to parallel conversion process to prolong symbol duration. Unfortunately, high serial to parallel conversion introduces other disadvantages which also degrade the BER. Simulation results show that the best performance is achieved in the system with insufficient cyclic prefix. These results together with the success in implementing the MUD-ISIC encourage a new system design that the cyclic prefix should be less important.

In order to realize the proposed MUD-ISIC, the parameter estimation techniques for acquiring the necessary parameters have also been proposed in this dissertation. The necessary parameters include the transformed signature sequences, the ISI generation sequences, and the noise variance. The transformed signature sequences and the ISI generation sequences are directly estimated rather than indirect calculation from channel impulse response to avoid several limitations in channel impulse response estimation such as complexity burden, requirement of large number of training symbols, etc. With feasible sequences estimation technique, the advantage of the proposed MUD-ISIC over the existing techniques in term of implementation becomes more obvious. The proposed sequence estimation technique is based on the classical least squares method. The MSE of the estimator has been analyzed, the expression for the minimum MSE has been obtained, and the criteria for training sequences to achieve the minimum MSE has been revealed. Following from the analyses, three techniques for generating the optimum training sequences have been presented. Among the three optimum training sequence families, the cyclically orthogonal training sequences gain the most attention because it uses as low number of training symbols in each sequence as the time division training sequence family and it has continuous signal structure, which provides robustness against noise and low out of band emission, as the odd-even training sequence family. Surprisingly, the optimum training sequences also help simplifying the LS estimator as they replace a matrix inversion by a basic scalar division. Simulation results confirm the validity of the LS estimator and the benefits of the optimum training sequences over the random training sequences. The performance of the LS estimator using the optimum training is independent of a number of users whereas the LS estimator using the random training sequences suffers severe degradation in the highly loaded system. Since this dissertation considers the sub-band detection approach, the cross parallel symbol interference is neglected from consideration. The MSE of the LS estimator using the optimum training sequence reaches the minimum MSE in a case that only

one subcarrier group out of N_P parallel subcarrier groups is active. The residual cross parallel symbol interference results in an error floor of MSE in the system with fully operated subcarriers. The adaptive estimator based on the well-known recursive least squares algorithm has also been proposed. The performance of the adaptive estimator is similar to that of the LS estimator in the system employing the optimum training sequences. For the system using the random training sequences, the adaptive estimator shows significant gain over the LS estimator because it does not have to deal with a singular or a near singular matrix as the LS estimator.

The existing receivers for the MC-CDMA system with insufficient cyclic prefix does not only suffer from frequency offsets but they also face implementation obstacles due to the requirement of the knowledge about actual channel impulse response. The necessity of sufficient cyclic prefix condition for the frequency offset compensated MMSE detector is obvious in both the system with zero frequency offset and the system with non-zero frequency offset. In contrast, the performance of MUD-ISIC does not much rely on the cyclic prefix. For the system with perfect frequency synchronization, the conventional reverse link subcarrier coefficients estimation can give substantially good subcarrier coefficient estimates to the frequency offset compensated MMSE detector. For such system, the MUD-ISIC only outperform the frequency offset compensated MMSE detector in the insufficient cyclic prefix scenario. For the system with frequency offset, the estimation error of the EKF estimator further deteriorates the performance of the frequency offset compensated MMSE detector. In this case, the MUD-ISIC employed the proposed estimator is better than the frequency offset compensated MMSE detector employed the EKF estimator for all the cyclic prefix length.

From the simulation results, as expected, the parameter estimation error raises the BER of the MUD-ISIC. However, the BER characteristics are the same as in the system, provided perfect parameter information. The lowest BER is still achieved in the system with insufficient cyclic prefix and the best multiuser detection technique is a WMIC using linear MMSE detector in the initial stage. An improvement can basically be obtained by increasing the training symbols' transmitted power. The noise variance estimation algorithm significantly contributes to the multiuser detection. It enables an implementation of the linear MMSE detector which is far better than the DD.

The techniques for obtaining parameter estimates during the data period have also been studied in this dissertation. Three basic approaches have been evaluated in the system with various rate of variation. The tracking based on the decision direct adaptation shows disappointing performance. On the other hand, a basic linear interpolation can track the variation quite well. An averaging approach, which regards a physical channel as static, is also not appropriate for the channel with Doppler. The only drawback of the linear interpolation method is the requirement of one packet frame delay. The shorter packet frame improves the tracking capability and relaxes the delay requirement. However, the loss in achievable symbol rate has to be compromised with the improvement. With a packet frame of 65 training symbols and 260 data symbols, the total symbol rate for the system without cyclic prefix employing cyclically orthogonal training sequences is 1 Msps / user. The higher symbol rate can be accomplished by using the multicode scheme where one user is a virtual multiple users, or, in the other word, one user is assigned more than one signature sequence.

5.1 Future Works

Although the concepts of MUD-ISIC and its parameter estimation have been developed and they have been extensively studied, there are some interesting issues worth of investigations.

First, the multiuser detection technology is currently developing toward the joint MAI suppression and channel decoding detector. This class of multiuser detection, usually referred as iterative (turbo) multiuser detection, may offer the potential for further performance improvement to the MUD-ISIC.

Second, in some scenario such as low signal to noise ratio, large number of users, etc., the receiver cannot deliver sufficiently accurate decisions. The ISI cancellation structure may propagate this error to the following symbols which would worsen the detector performance. To alleviate the error propagation, weighted (soft or partial) cancellation approach may be applied to the ISI cancellation process.

Third, the spatial diversity is currently being exploited in order to attain higher quality links. Such diversity may be used as supplementary to the frequency diversity. In the simulation results, it is demonstrated that the uniform MIP channel, which has higher degree of diversity, can offer better BER than the exponential decaying MIP channel. Similarly, we can expect that any additional forms of diversity would result in the better BER. In this point of views, the received signals from different antennas may be coherently combined before processing by the MUD-ISIC.

Several other issues have to be further explored in order to realize the next generation wireless communication systems. These topics include wireless networking protocols, channelization strategies, more advanced parameter tracking techniques, etc. For example, there are some reports on subspace tracking algorithms, exploiting the delay subspace which is considered as slow variation part. These algorithms may be able to apply to the proposed estimation technique. The networking protocols are the other important parts of the wireless communication. Some forms of automatic repeat request protocol have shown good potential over the erroneous scenario. In conclusion, the continuous researches and efforts in various aspects are very necessary and important to the success of the next generation wireless communication systems. The mission cannot be reached without the advanced physical layer techniques, but at the same time only the development of physical layer technique cannot fulfill the utmost goal.

References

1. Lee W. C. Y. Mobile communications engineering. Singapore : McGraw-Hill, 1997.

2. Adachi, F., Sawahashi, M., and Suda, H. Wideband DS-CDMA for next-generation mobile communications systems. IEEE Communication Magazine Vol. 36 No. 9 (September 1998): 56–69.

3. Dahlman, E., Beming, P., Ovesjo, F., Persson, M., and Roobol, C. WCDMA-the radio interface for future mobile multimedia communications. IEEE Transaction on Vehicular Technology Vol. 47 No. 4 (November 1998): 1105–1118.

4. Knisely, D., Kumar, S., Laha, S., and Nanda, S. Evolution of wireless data services: IS-95 to cdma2000. IEEE Communication Magazine Vol. 36 No. 10 (October 1998): 140–149.

5. Dinis, M. and Fernandes, J. Provision of sufficient transmission capacity for broadband mobile multimedia: a step toward 4G. IEEE Communication Magazine Vol. 39 No. 8 (August 2001): 46–54.

6. Yamao, Y., Suda, H., Umeda, N., and Nakajima, N. Radio access network design concept for the fourth generation mobile communication system. Proceeding of IEEE Vehicular Technologies Conference 2000 Spring Vol. 3 (May 2000): 2285–2289.

7. Huang, V. and Zhuang, W. QoS-oriented access control for 4G mobile multimedia CDMA communications. IEEE Communication Magazine Vol. 40 No. 3 (March 2002): 118–125.

8. Raivio, Y. 4G-hype or reality. Proceeding of 2nd International Conference on 3G Mobile Communication Technologies (March 2001): 346–350.

9. Wang, Z. and Giannakis, G. B. Wireless multicarrier communications: where Fourier meets Shannon. IEEE Signal Processing Magazine Vol. 17 No. 3 (May 2000): 29–48.

10. Nee, R. V. and Prasad, R. OFDM for Wireless Multimedia Communications. London : Artech House, 2002.

11. Zou, W. Y. and Yiyan, W. COFDM: an overview. IEEE Transactions on Broadcasting Vol. 41 No. 1 (March 1995): 1–8.

12. Maeda, N., Atarashi, H., Abeta, S., and Sawahashi, M. Pilot channel assisted MMSE combining in forward link for broadband OFCDM packet wireless access. IEICE Transaction on Fundamentals of Electronics, Communications and Computer Sciences Vol. E85-A No. 7 (July 2002): 1635–1645.

13. Zong, P., Novel Multiuser Detection and Multi-Rate Schemes for Multi-Carrier CDMA. Ph.D. dissertation New Jersey Institute of Technology, 2001.

14. Yee, N., Linnartz, J. P., and Fettweis, G. Multi-Carrier CDMA in indoor wireless radio networks. Proceeding of IEEE International Symposium on Personal, Indoor and Mobile Radio Communications 1993 (September 1993): 109–113.

15. DaSilva, V. and Sousa, E. Performance of orthogonal CDMA codes for quasi-synchronous communication systems. Proceeding of 2nd International Conference on Universal Personal Communications 1993 Vol. 2 (October 1993): 995–999.

16. Vandendorpe, L. Multitone spread spectrum multiple access communications system in a multipath Rician fading channel. Proceeding of IEEE International Conference on Communications 1994 Vol. 3 (May 1994): 1638–1642.

17. Hara, S. and Prasad, R. Overview of multicarrier CDMA. IEEE Communication Magazine Vol. 35 No. 12 (December 1997): 126–133.

18. Tsumura, S. and Hara, S. Design and performance of quasi-synchronous multi-carrier CDMA system. Proceeding of IEEE Vehicular Technologies Conference 2001 Fall Vol. 2 (October 2001): 843–847.

19. DaSilva, V. and Sousa, E. Multicarrier orthogonal CDMA signals for quasi-synchronous communication systems. IEEE Journal on Selected Areas in Communications Vol. 12 No. 5 (June 1994): 842–852.

20. Iltis, R. Decorrelator detection for quasi-synchronous multicarrier CDMA. Proceeding of Military Communications Conference 1997 Vol. 2 (November 1997): 862–866.

21. Kleer, F., Hara, S., and Prasad, R. Performance evaluation of a successive interference cancellation scheme in a quasi-synchronous MC-CDMA system. Proceeding of IEEE International Conference on Communications 1998 Vol. 1 (June 1998): 370–374.

22. Kunaruttanapruk, S. and Jitapunkul, S. Partial weight multistage interference cancellation for reverse link MC-CDMA system using pilot assisted channel estimation. Proceeding of Communication Networks and Systems Research Conference 2004 (May 2004): 39–45.

23. Petre, F., Vandenameele, P., Bourdoux, A., Gyselinckx, B., Engels, M., Moonen, M., and De, M. H. Combined MMSE/pcPIC multiuser detection for MC-CDMA. Proceeding of IEEE Vehicular Technologies Conference 2000 Fall Vol. 2 (May 2004): 770–774.

24. Luan, Y.Z., Yang, J. W., Sun, Y. C., and Li, J. D. Performance analysis of the multi-user receiver exploited in MC-CDMA system. Proceeding of 2nd International Conference on 3G Mobile Communication Technologies (March 2001): 346–350.

25. Miller, S. and Rainbolt, B. MMSE detection of multicarrier CDMA. IEEE Journal on Selected Areas in Communications Vol. 18 No. 11 (November 2000): 2356–2362.

26. Melsa, P. J. W., Younce, R. C., and Rohrs, C. E. Impulse response shortening for discrete multitone transceivers. IEEE Transaction on Communications Vol. 44 No. 12 (December 1996): 1662–1672.

27. Sun, Y. and Tong, LE. Channel equalization for wireless OFDM systems with ICI and ISI. Proceeding of IEEE International Conference on Communications 1999 Vol. 1 (June 1999): 182–186.

28. Sun, Y. Bandwidth-efficient wireless OFDM. IEEE Journal on Selected Areas in Communications Vol. 19 No. 11 (November 2001): 2267–2278.

29. Zhu, J., Ser, W., and Nehorai, A. Channel equalization for DMT with insufficient cyclic prefix. Proceeding of IEEE Asilomar Conference on Signals, Systems, and Computers 2000 Vol. 2 (October 2000): 951–955.

30. Suyama, S., Ito, M., and Suzuki, H. A scattered pilot OFDM receiver with equalization for multipath environments with delay difference greater than guard interval. IEICE Transaction on Communications Vol. E86-B No. 1 (January 2003): 275–282.

31. Dukhyun, K. and Stuber, G. L. Residual ISI cancellation for OFDM with applications to HDTV broadcasting. IEEE Journal on Selected Areas in Communications Vol. 16 No. 8 (October 1998): 1590–1599.

32. Kunaruttanapruk, S. and Jitapunkul, S. The novel decision feedback equalizer for OFDM system with insufficient cyclic prefix. Proceeding of Communication Networks and Systems Research Conference 2004 (May 2004): 19–24.

33. Kunaruttanapruk, S. and Jitapunkul, S. Parameter acquisition techniques for multiuser detection with ISI cancellation in a quasi-synchronous reverse link MC-CDMA system. IEICE Transaction on Communications Vol. E88-B No. 1 (January 2005): 93–105.

34. Xiaojun, W., Qinye, Y., Hanguo, Z., and Ke, D. Time-domain multiuser detection for MC-CDMA systems without cyclic prefix. Proceeding of IEEE International Conference on Communications 2002 Vol. 2 (May 2002): 921–925.

35. Ikonomou, D. and Vandendorpe, L. A fractionally spaced DF equalisation scheme performing joint detection for MC-CDMA transmissions. Proceeding of IEEE Vehicular Technologies Conference 1999 Fall Vol. 2 (September 1999): 1150–1154.

36. van de Beek, J.-J., Edfors, O., Sandell, M., Wilson, S. K., and Börjesson, P. O. On channel estimation in OFDM systems. Proceeding of IEEE Vehicular Technologies Conference 1995 Vol. 2 (July 1995): 815–819.

37. Moose, P. H. A technique for orthogonal frequency division multiplexing frequency offset correction. IEEE Transaction on Communications Vol. 42 No. 10 (October 1994): 2908–2914.

38. Luise, M. and Reggiannini, R. Carrier frequency acquisition and tracking for OFDM systems. IEEE Transaction on Communications Vol. 44 No. 11 (November 1996): 1590–1598.

39. van de Beek, J.-J., Sandell, and Börjesson, P. O. ML estimation of time and frequency offset in OFDM systems. IEEE Transactions on Signal Processing Vol. 45 No. 7 (July 1997): 1800–1805.

40. Songping, W. and Bar-Ness, Y. OFDM channel estimation in the presence of frequency offset and phase noise. Proceeding of IEEE International Conference on Communications 2003 Vol. 5 (May 2003): 3366–3370.

41. Tansongcharoen, P., Lee, W., Kunaruttanapruk, S., and Jitapunkul, S. Improved maximum likelihood frequency offset estimation for multi-carrier CDMA systems over multipath fading channel. Proceeding of IEEE Internation Symposium on Communications and Information Technologies 2004 Vol. 1 (October 2004): 159–162.

42. Liu, H. and Tureli, U. A high efficiency carrier estimator for OFDM communications. IEEE Communication Letters Vol. 2 No. 4 (April 1998): 104–106.

43. Tureli, U., Liu, H., and Zoltowski, M. A high efficiency carrier estimator for OFDM communications. Proceeding of IEEE Asilomar Conference on Signals, Systems, and Computers 1997 Vol. 1 (November 1997): 505–509.

44. Tureli, U., Liu, H., and Zoltowski, M. OFDM blind carrier offset estimation: ESPRIT. IEEE Transactions on Communications Vol. 48 No. 9 (September 2000): 1459–1461.

45. van de Beek, J. -J., Börjesson, P. O., Boucheret, M. -L., Landstrom, D., Arenas, J. M., Odling, P., Ostberg, C., Wahlqvist, M., and Wilson, S. K. A time and frequency synchronization scheme for multiuser ofdm. IEEE Journal on Selected Areas in Communications Vol. 17 No. 11 (November 1999): 1900–1914.

46. Barbarossa, S., Pompili, M., and Giannakis, G. B. Channel-independent synchronization of orthogonal frequency division multiple access systems. IEEE Journal on Selected Areas in Communications Vol. 20 No. 2 (February 2002): 474–486.

47. Songthanasak, J., Parallel Interference Cancellation Receiver with Adaptive Frequency Offset Correction for Multi-Carrier CDMA System. Master's thesis Chulalongkorn University, 2003.

48. Songthanasak, J., Kunaruttanapruk, S., Tangsangiumvisai, N., and Jitapunkul, S. Parallel interference cancellation receiver with maximum likelihood frequency offset estimation for

uplink MC-CDMA system. Proceeding of the 3rd IEEE International Symposium on Signal Processing and Information Technology 2003 (December 2003): 387–390.

49. Takyu, O., Otsuki, T., and Nakagawa, M. Frequency offset compensation with MMSE-MUD for multi-carrier CDMA in quasi-synchronous uplink. Proceeding of IEEE International Conference on Communications 2003 Vol. 4 (May 2003): 2485–2489.

50. Takyu, O., Otsuki, T., and Nakagawa, M. Frequency offset compensation with MMSE-MUD for multi-carrier CDMA in quasi-synchronous uplink. IEICE Transaction on Communications Vol. W87-B No. 6 (June 2004): 1495–1504.

51. Tureli, U., Kivanc, D., and Liu, H. MC-CDMA uplink-blind carrier frequency offset estimation. Proceeding of IEEE Asilomar Conference on Signals, Systems, and Computers 2000 Vol. 1 (October 2000): 241–245.

52. Roman, T., Enescu, M., and Koivunen, V. Recursive estimation of time-varying channel and frequency offset in MIMO OFDM systems. Proceeding of IEEE International Symposium on Personal, Indoor and Mobile Radio Communications 2003 Vol. 2 (September 2003): 1934–1938.

53. Verdu, S. Minimum probability of error for asynchronous gaussian multiple access channels. IEEE Transaction on Information Theory Vol. 32 No. 1 (January 1986): 85-99.

54. Fazel, K. and Papke, L. On the performance of convolutionally-coded CDMA/OFDM for mobile communication system. Proceeding of IEEE International Symposium on Personal, Indoor and Mobile Radio Communications 1993 (September 1993): 468–472.

55. Verdu, S. Multiuser Detection. U.K. : Cambridge University Press, 1998.

56. Ojanpera, K. and Papke, L. Overview of multiuser detection/interference cancellation for DS-CDMA. Proceeding of IEEE International Symposium on Personal, Indoor and Mobile Radio Communications 1997 (December 1997): 115–119.

57. Duel-Hallen, S., Holtzman, J., and Zvonar, Z. Multiuser detection for CDMA systems. IEEE Personal Communications Vol. 2 No. 2 (April 1995): 46–58.

58. Xie, Z., Short, R., and Rushforth, C. A family of suboptimum detectors for coherent multiuser communications. IEEE Journal on Selected Areas in Communications Vol. 8 No. 4 (May 1990): 683–690.

59. Buehrer, R., Correal, N., and Woener, B. A comparison of multiuser receivers for cellular CDMA. Proceeding of IEEE Global Telecommunications Conference 1996 Vol. 3 (November 1996): 1571–1577.

60. Woodward, G. and Vucetic, B. Adaptive detection for DS-CDMA. Proceedings of the IEEE Vol. 86 No. 7 (July 1998): 1413–1434.

61. Divsalar, D., Simon, M.K., and Raphaeli, D. Improved parallel interference cancellation for CDMA. IEEE Transaction on Communications Vol. 46 No. 2 (February 1998): 258–268.

62. Shan, P. and Rappaport, T. S. Parallel interference cancellation (PIC) improvements for CDMA multiuser receivers using partial cancellation of MAI estimates. Proceeding of IEEE Global Telecommunications Conference 1998 Vol. 6 (November 1998): 3282–3287.

63. Visser, M., Adaptive Interference Cancelation Techniques for Multicarrier Modulated Systems. Ph.D. dissertation New Jersey Institute of Technology, 1999.

64. Proakis, J. Digital Communications. New York : McGraw-Hill, 1989.

65. Patzold, M. Mobile Fading Channels. U.K. : John Wiley & Sons, 2002.

66. Hoeher, P., Kaiser, S., and Robertson, P. Two-dimensional pilot-symbol-aided channel estimation by Wiener filtering. Proceeding of IEEE International Conference on Acoustics, Speech, and Signal Processing 1997 (April 1997): 1845–1848.

67. Li, Y. Pilot-symbol-aided channel estimation for OFDM in wireless systems. IEEE Transaction on Vehicular Technology Vol. 49 No. 4 (July 2000): 1207–1215.

68. Fujii, M., Shimizu, R., Itami, M., and Itoh, K. The optimum channel estimation for coherent receivers in multicarrier CDMA system with antenna array. IEICE Transaction on Communications Vol. E86-B No. 1 (January 2003): 365–374.

69. Li, Y., Seshadri, N., and Ariyavisitakul, S. Channel estimation for OFDM systems with transmitter diversity in mobile wireless channels. Journal on Selected Areas in Communications Vol. 17 No. 3 (March 1999): 461–471.

70. Chen, B. S., and Tsai, C. L. Frequency offset estimation in an ofdm ststem. Proceeding of IEEE Signal Processing Workshop on Signal Processing Advances in Wireless Communications 2001 (March 2001): 150–153.

71. Sinthusak, J., Improvement of hybrid interference cancellation using partial cancellation PIC technique in rayleigh-fading channels in DS-CDMA system. Master's thesis Chulalongkorn University, 2000.

72. Suwa, S., Atarashi, H., and Sawahashi, M. Radio link capacity comparison between mc/ds-cdma and mc-cdma in reverse link broadband wireless access. IEICE Transaction on Fundamentals of Electronics, Communications and Computer Sciences Vol. W86-A No. 7 (July 2003): 1645–1655.

73. IEEE, IEEE Std 802.11g-2003, 2003.

74. Iltis, R.A. and Mailaender, L. Multiuser detection of quasisynchronous CDMA signals using linear decorrelators. IEEE Transaction on Communications Vol. 44 No. 11 (November 1996): 1561–1571.

75. Available from: http://www.absolutetime.com (october 2004).

76. Available from: http://www.lowrance.com (october 2004).

77. Hong, E., Hwang, S., Kim, K., and Whang, K. Synchronous transmission technique for the reverse link in DS-CDMA terrestrial mobile systems. IEEE Transaction on Communications Vol. 47 No. 11 (November 1999): 1632–1635.

78. Yang, B., Letaief, K.B., Cheng, R.S., and Cao, Z. Channel estimation for OFDM transmission in multipath fading channels based on parametric channel modeling. IEEE Transaction on Communications Vol. 49 No. 3 (March 2001): 467–478.

79. Simeone, O., Bar-Ness, Y., and Spagnolini, U. Pilot-based channel estimation for OFDM systems by tracking the delay-subspace. IEEE Transaction on Wireless Communications Vol. 3 No. 1 (January 2004): 315–325.

80. Du, J. and Li, Y. MIMO-OFDM channel estimation based on subspace tracking. Proceeding of IEEE Vehicular Technologies Conference 2003 Vol. 2 (April 2003): 1084–1088.

81. Haykin, S. Adaptive Filter Theory. U.S.A. : Prentice Hall, 2002.

Appendices

Appendix A
List of Abbreviations

A/D	analog-to-digital
BER	bit error rate
CDMA	code division multiple access
CE	controlled equalization
CSA	continuous subcarrier assignment
DAB	digital audio broadcasting
DD	decorrelating detector
DFE	decision feedback equalization
DFT	discrete Fourier transform
dTTb	digital terrestrial television broadcasting
DS-CDMA	direct sequence code division multiple access
Eb/N0	signal to noise ratio per bit
EGC	equal gain combining
EKF	extended Kalman filter
FDMA	frequency division multiple access
FIR	finite impulse response
FFT	fast Fourier transform
GPS	global positioning system
IDFT	inverse discrete Fourier transform
IFFT	inverse fast Fourier transform
ICI	intercarrier interference
i.i.d.	independent and identically distributed
ISA	interleaved subcarrier assignment
ISI	intersymbol interference
LS	least squares
MAI	multiple access interference
MC-DS-CDMA	multicarrier direct sequence code division multiple access
MC-CDMA	multicarrier code division multiple access
MF	matched filter
MIP	multipath intensity profile
MLSE	maximum likelihood sequence estimator
MMSE	minimum mean square error

MMSEC	minimum mean square error combining
MMSE-DFE	minimum mean square error decision feedback equalizer
MRC	maximum ratio combining
MSE	mean square error
Msps	mega symbol per second
MT-CDMA	multitone code division multiple access
MUD-ISIC	multiuser detection with intersymbol interference cancellation
OFDM	orthogonal frequency division multiplexing
OFDMA	orthogonal frequency division multiple access
ORC	orthogonal restore combining
PAPR	peak-to-average power ratio
RLS	recursive least squares
SINR	signal to interference plus noise ratio
SIRF	shortened impulse response filter
SNR	signal to noise ratio
TDMA	time division multiple access
WLAN	wireless local area network
WMIC	weighted multistage interference cancellation
WSSUS	wide sense stationary uncorrelated scattering

Appendix B
Publications and Presentations

Kunaruttanapruk, S. and Jitapunkul, S.

"Parameter acquisition techniques for multiuser detection with ISI cancellation in a quasi-synchronous reverse link MC-CDMA system," IEICE Transaction on Communications, vol. E88-B, no. 1, pp. 93–105, January 2005.

Kunaruttanapruk, S. and Jitapunkul, S.

"The novel decision feedback equalizer for OFDM system with insufficient cyclic prefix," Proceeding of Communication Networks and Systems Research Conference 2004 (Fredericton, Canada), pp. 19–24, May 2004.

Kunaruttanapruk, S. and Jitapunkul, S.

"Partial weight multistage interference cancellation for reverse link MC-CDMA system using pilot assisted channel estimation," Proceeding of Communication Networks and Systems Research Conference 2004 (Fredericton, Canada), pp. 39–45, May 2004.

Kunaruttanapruk, S., Jitapunkul, S., Archawanichakul, C.

"Code selection scheme for Multi-Carrier CDMA in correlated fading channel", Proceeding of 9th International Workshop on Systems (Manchester, UK), Signals and Image Signal Processing, pp.147-153, Nov. 2002.

Vitae

Suwich Kunaruttanapruk was born in Bangkok, Thailand, in 1978. He received the B.Eng. (Hons. I) degree in electrical engineering from Dept. of Electronics Engineering, King Mongkut's Institute of Technologies Ladkrabang, Thailand, in 1998 and the M.Eng. degree in electrical engineering from Dept. of Electrical Engineering, Chulalongkorn University, Thailand, in 2001. He is now working toward the Ph.D. degree in electrical engineering from Chulalongkorn University, Thailand. His research areas are digital signal processing in wireless communication systems including DS-CDMA, OFDM, MC-CDMA, etc.